University of Strathclyde

Department of Electronic & Electrical Engineering

Inductive interconnecting solutions for airworthiness standards and power-quality requirements compliance for more-electric aircraft/engine power networks

by

Theodoros Kostakis

2018

A thesis presented in fulfilment of the requirements for the degree of

Doctor of Philosophy

Declaration of Authenticity and Author's Rights

This thesis is the result of the author's original research. It has been composed by the author and has not been previously submitted for examination which has led to the award of a degree.

Signed:

Date:

Acknowledgements

I would like to offer sincere thanks to Dr Stuart Galloway for the opportunity to undertake this research work and the trust shown in me from the beginning of this project. I would like to express my enormous gratitude to Dr Patrick Norman for his technical guidance, endless support and patience. Thank you for your efforts and motivation throughout the duration of this project.

Thanks to all my colleagues within the UTC research team for their help and input, in particular Steven Fletcher, Puran Rakhra and Chung Man Fong. I would also like to extend my gratitude to Rolls-Royce plc. for their technical and financial support over the duration of this project.

I would also like to thank my friends and family for their continuous support and encouragement over the years. Special thanks go to my partner Ina. Thank you so much for your understanding and support, especially during the write up period, and your attempts to understand this project.

Abstract

Driven by efficiency benefits, performance optimization and reduced fuel-burn, the aviation industry has witnessed a technological shift towards the broader electrification of on-board systems, known as the More-Electric Aircraft (MEA) concept. Electrical systems are now responsible for functions that previously required mechanical, hydraulic or pneumatic power sources, with a subset of these functions being critical or essential to the continuity and safety of the flight. This trend of incremental electrification has brought along benefits such as reductions in weight and volume, performance optimization and reduced life-cycle costs for the aircraft operator. It has however also increased the necessary engine power offtake and has made the electrical networks of modern MEA larger and more complex. In pursuit of new, more efficient electrical architectures, paralleled or interconnected generation is thought to be one platform towards improved performance and fuel savings.

However, the paralleling of multiple generation sources across the aircraft can breach current design and certification rules under fault conditions. This thesis proposes and evaluates candidate interconnecting solutions to minimize the propagation of transients across the interconnected network and demonstrates their effectiveness with reference to current airworthiness standards and MIL-STD-704F power quality requirements. It demonstrates that inductive interconnections may achieve compliance with these requirements and quantifies the estimated mass penalty incurred on the electrical architecture, highlighting how architectural and operating strategies can influence design options at a systems level. By examining the impact of protection operation speed on the electrical network, it determines that fast fault protection is a key enabling technology towards implementing lightweight and compliant interconnected architectures. Lastly, this thesis addresses potential implications arising from alternate standards interpretations within the framework of interconnected networks and demonstrates the impact of regulatory changes on the electrical architecture and interconnecting solutions.

Contents

List of Figures

List of Tables

List of Abbreviations

AEA	All Electric Aircraft
APU	Auxiliary power unit
ATRU	Auto-transformer rectifier unit
BTB	Bus tie breaker
CB	Circuit breaker
CF	Constant frequency
CLD	Current limiting diode
CSD	Constant Speed Drive
DAB	Dual active bridge
EASA	European Aviation Safety Agency
ECS	Environmental control system
EMCB	Electro-magnetic circuit breaker
ETOPS	Extended Operations
FAA	Federal Aviation Administration
FADEC	Full authority digital engine controls
FBW	Fly-By-Wire
GCB	Generator circuit breaker
HP	High pressure
HVDC	High voltage direct current
IDG	Integrated drive generator

ILS	Intelligent load controller
IP	Intermediate pressure
LP	Low pressure
MEA	More-Electric Aircraft
MEE	More-Electric Engine
MIL-STD	Military Standard
PDU	Power distribution unit
RAT	Ram air turbine
SSPC	Solid state power controller
SYNC	Synchronising
TRU	Transformer rectifier unit
VF	Variable frequency
VFG	Variable frequency generator
VSC	Voltage source converter
VSCF	Variable speed constant frequency

Chapter 1

Introduction

Conventional civil-aviation aircraft incorporate a series of systems that require mechanical, pneumatic, hydraulic and electrical power sources. Given that the only main source of power on an aircraft is from its gas turbine engines, the majority of generated power is used to provide thrust whilst the remaining power is used for non-propulsive functions. For example, pneumatic power is required for cabin pressurisation, air-conditioning and anti-ice wing protection, hydraulic power is required for the actuation of flight surfaces and landing gear, and mechanical power drives the engine fuel and oil pumps [1]. On conventional jetliners, electrical power is mainly limited to avionics, fans, cabin and exterior lights [2].

This variety of power sources however comes at a cost as it reduces efficiency, increases the complexity of the aircraft systems and makes maintenance and servicing more difficult and expensive [3]. To power pneumatic loads, bleed-air is off-taken from the engine, reducing the amount of air contributing to thrust and therefore reducing engine efficiency, and mechanical power is extracted via a heavy gearbox connected to the engine shaft. The hydraulic system comprises of a network of heavy pipes and ducts which is demanding to maintain and prone to leaks [1].

The More-Electric Aircraft (MEA) concept is a technological shift in the aviation industry that seeks to replace hydraulic, pneumatic and mechanical systems with their electrical equivalents. The underpinning assumption is that having a single type of power source taken from the engine is more effective [4], and electrical power was chosen as that single source due to flexibility advantages and application range [5]. This incremental electrification trend is thought to introduce a small mass penalty to the overall weight of the aircraft [3], but is a necessary step towards the ultimate goal of achieving the All Electric Aircraft (AEA) [6, 7]. The adoption of the AEA concept could completely eliminate bleed-air systems and replace traditional hydraulic

systems with electro-mechanical equivalents, reducing aircraft weight and therefore fuel consumption by up to 4.5% [3].

However, the ever-increasing electrification of MEA imposes the need for new technologies and novel electrical architectures [8], without adversely affecting the pre-existing levels of reliability of today's systems. New power-system design options that could reduce fuel consumption and improve engine operability are needed, with one possible choice being the interconnection of generation sources to produce a single combined power source.

The paralleling of power sources can facilitate optimised power sharing based on the individual operating characteristics of these sources, thus providing the opportunity to increase the efficiency of power generation [9]. For many years, this principle has been applied on AC and DC land-based power grids to increase the security of supply, offer multiple routes for power flow, and to control the output of power stations through the use of economic dispatch [10].

A key technological driver for the implementation of more interconnected electrical architectures is the potential for multi-shaft power off-takes. Advances in the mechanical design of the aircraft engines, more specifically in the number of spools, have opened up the possibility of having multiple generators been driven from different shafts on the jet engine. Multi-spool engines can allow different parts of the engine to rotate at different, more optimum speeds, thus improving engine performance and efficiency [11]. Therefore particularly for aircraft applications, the interconnection of power sources may provide a more feasible route for the facilitation of more efficient power sharing between multiple engine-driven generators [12, 13].

From the above points, it is clear that significant efficiency and operability benefits can be realised through the adoption of interconnected generation in aircraft electrical networks. However, there are several key factors and challenges that need to be overcome, or complied with, for the feasible implementation of such network topologies on MEA/E. The first main factor that must be addressed is how the interconnection of generation sources can be achieved, in other words, by which

implementation method or approach. As will be illustrated within this thesis, a direct connection between MEA/E AC generation sources is not applicable, subsequently novel interconnecting design approaches and mechanisms have to be considered.

Moreover, these mechanisms face additional operational and size requirements, as they must be able to function properly in the harsh operating conditions of the aviation environment. In applications where weight and volume come at a premium, such as in aviation installations, there are constraints on the mass and size of components, as the operating cost of platforms is highly dependent on their weight and volume [14]. Consequently, any candidate interconnecting solution must be compact and lightweight in order to be viable.

The second set of challenges are the regulatory requirements governing aircraft and systems design, known as airworthiness standards. Regulatory bodies, such as the European Aviation Safety Agency, oversee a wide variety of aviation-related activities, including design, operation and maintenance of airborne systems and platforms, and also make provisions for the electrical power system architecture. Additionally, power-quality requirements for normal and abnormal operating conditions of the electrical system are set out in Military Standard 704F. Therefore, any interconnecting solution option installed on-board must conform to established airworthiness standards and power-quality requirements.

Moreover, the greater electrification of MEA/E brings with it a new set of protection challenges. To supply the ever-growing demand for electrical power, MEA/E networks have become larger and more complex, with state-of-the-art models capable of nominal electrical-power outputs of around 1 MW. The increased complexity of such electrical networks requires significant design undertaking to ensure proper and reliable systems operation. This, paired with novel paralleled-generation schemes that result in an even greater electrical unification of aircraft platforms, introduces significant protection and power-quality challenges in comparison with isolated topologies.

Parallel generation systems reduce the isolation of the electrical network, therefore advanced, fact-acting protection strategies are required, with higher rated protection

devices in comparison to radial systems. As the degree of interconnection increases, a greater portion of aircraft systems is exposed to transients and single-point faults that may occur in the network. This can create significant issues on a sub-set of electrical systems on-board MEA/E that are critical to the safety and continuity of flight. In order to function properly, these 'essential loads' require higher levels of reliability and redundancy in comparison with the rest of the power network. Consequently, to safeguard the unobstructed operation of these systems, protection equipment will need to detect and clear faults before network conditions breach the power quality requirements.

Arguably, technological advances in the field of civil aviation and passenger aircraft, such as the MEA and AEA concepts, have created considerable step changes in technology and design philosophy. However, current airworthiness standards and requirements do not feature dedicated rules specifically for interconnected systems. Consequently, the exploitation and implementation of such innovative design concepts, paired with novel paralleled-generation schemes, could risk having to be based on standards or requirements that may potentially be unsuitable or antiquated.

Based on the challenges mentioned above, four key research questions can be posed.

- How can the interconnection of generation sources be feasibly implemented on MEA/E with regards to size and weight penalty?
- Are current protection systems sufficiently fast to safeguard the unobstructed operation of essential loads and unified electrical system?
- Do the established airworthiness standards permit the implementation of candidate interconnecting solutions and do these solutions meet the power-quality requirements of the aviation sector?
- Are the current power-quality requirements suitable or strict enough for the proper function of interconnected MEA/E?

1.1 Summary of key contributions

In addressing the research questions outlined in the previous section, a number of contributions are made within this thesis.

- The implementation challenges and barriers to paralleled generation in future MEA/E are identified and categorized, and key enabling technologies that will facilitate commercially feasible interconnected MEA/E systems are proposed.
- It is shown that protection methods and certification implications of interconnected systems are not sufficiently addressed in the relevant research literature and patents for future MEA/E applications with higher power flight-critical electrical loads. As a result, the systems-level impact of abnormal operation of interconnected power systems is not yet well documented.
- The behaviour of an interconnected MEA/E power system during fault conditions is analysed, showing that some configurations can breach power-quality requirements under fault conditions.
- The effectiveness of three potential technology-based solutions to provide power-quality compliance of interconnected MEA/E power systems under fault conditions is analysed. These are: current limiting diodes, solid-state power controllers and inductive coupling.
- Of these, only inductive coupling solutions are shown to provide the necessary power-quality compliance. This is achieved by ‘transforming’ the short-circuit into a normal voltage transient, permissible by the power-quality requirements, for the non-faulted parts of the network.
- The three most important factors that enable the minimisation of the mass of the inductive coupling are shown to be:
    - Fast acting fault clearance.
    - The level of power quality compliance.
    - Power offtake mix and architecture channel configuration.
- Novel interpretations of existing airworthiness standards are derived which accommodate the fault-to-transient transformation realised by inductive

coupling solutions. These focus on the requirement to redefine independent generation sources and segregation of essential loads in an interconnected network.

- Three new power quality standards for interconnected MEA/E systems are proposed. The impact on the technological solutions required for compliance to each is examined.
- It is shown that the adoption of the '5ms ride-through' power quality standard, if practically permissible, coupled with very fast acting protection, can facilitate the implementation of standards-compliant interconnected power networks with no added weight penalty or unacceptable risk to the aircraft operation.

1.2 Publications

- T. Kostakis, P.J Norman, S.J. Galloway, "Assessing Network Architectures for the More Electric Aircraft", presented at 49th International Universities Power Engineering Conference (UPEC), pp. 1-6, Romania, 2014 doi:10.1109/UPEC.2014.6934680
- T. Kostakis, P.J. Norman, S.J. Galloway, G.M. Burt, "Investigations into Standards Compliant Paralleled Generation in Civil Aircraft", presented at 2015 International Conference on Electrical Systems for Aircraft, Railway, Ship Propulsion and Road Vehicles (ESARS15), pp. 1-5, Germany, doi:10.1109/ESARS.2015.7101484
- T. Kostakis, P.J. Norman, S.A. Fletcher, S.J. Galloway, G.M Burt, "Evaluation of Paralleled Generation Architectures for Civil Aircraft Applications", presented at SAE 2015 AeroTech Congress, pp. 1-8, USA, doi:10.4271/2015-01-2407
- T. Kostakis, P.J. Norman, S.J. Galloway, G.M. Burt, "Demonstration of Fast-acting Protection as a Key Enabler for More-Electric Aircraft Interconnected Architectures", *IET Electrical Systems in Transportation*, vol. 7, is. 2, pp. 170-178, doi:10.1049/iet-est.2016.0065

1.3 Thesis structure

An outline of the work presented in this thesis is presented in this section. Chapter 2 introduces the MEA/E concept in more detail and outlines the key differences between MEA and conventional aircraft. It addresses the technological challenges and breakthroughs of this more-electric shift, and presents novel power generation and distribution systems. To provide some context in this area of research, this chapter summarizes the evolution of aircraft electrical networks and gas turbine engine developments.

Chapter 3 reviews the state of interconnected generation in the current and past aviation industry and presents the challenges associated with paralleled architectures. It also identifies key technological drivers that may provide a more feasible route for the implementation of such architectures. Finally, it outlines the benefits and drawbacks of proposed approaches in the relevant literature.

Chapter 4 presents the interconnected DC architectures that will be simulated and examined within this thesis, and investigates the behaviour of each interconnected system under fault conditions. It also presents the tools and methods used to examine the viability of several potential solution approaches to mitigate the breaching of power-quality requirements set out in MIL-STD-704F for paralleled power networks. This chapter concludes by demonstrating that smoothing filtering solutions comprised of reactors have the potential to provide voltage compliance for interconnected systems under fault conditions.

Chapter 5 demonstrates that purely inductive interconnecting components appear to be sufficient in achieving normal and steady-state voltage compliance, thus focuses on the design and implementation of suitable inductive-connection options for the candidate DC architectures. It will also highlight the two main variables which impact the size of inductance required to achieve bus-voltage compliance, and present the apparent trade-off between the size of inductance against these variables. Additionally, a weight-penalty estimation analysis of the interconnecting solutions

will enable the depiction of the influence of these solutions on the selection of generation source type and architectural design at a systems level.

Lastly, chapter 6 debates alternate airworthiness-standards and power-quality interpretations that may be afforded by the implementation of inductors as interconnecting mechanisms. This requires the re-evaluation of the requirement for independent power sources within the framework of interconnected networks, and the subsequent implications of this on generation sources and essential loads. This chapter also addresses several key factors that distinguish MEA/E from other airborne platforms in the commercial transport sector, and subsequently argues the need for a dedicated set of requirements for interconnected MEA/E systems. To this end, several candidate voltage envelopes are presented to evaluate the impact of potential regulatory changes on the ratings and mass on given inductive interconnecting solutions.

Chapter 2

More-Electric Aircraft concept

This chapter will briefly present the More-Electric Aircraft concept and outline the differences between MEA and conventional aircraft. The technological challenges and breakthroughs of this more-electric shift are addressed, and novel power generation and distribution systems are presented. To provide some context for the area of research, the evolution of aircraft electrical networks and gas turbine engines is summarised.

2.1 A typical MEA

The concept of the MEA has brought many technological breakthroughs compared to conventional aircraft architectures and has changes the way on-board systems are designed and utilised. This change has brought along benefits such as sub-system weight reductions, optimized performance and reductions in the life-cycle costs for the aircraft operator [15]. More specifically, this incremental electrification has improved aircraft maintainability as better fault-diagnosis can be afforded through build-in components [16] and fewer tools and spares are required, therefore achieving faster aircraft turnarounds [17]. Additionally, system availability and reliability is improved as electrical distribution is more practical and allows for greater reconfiguration flexibility compared to hydraulics [18].

Arguably, the three main differences between MEA and conventional aircraft are minimisation of bleed-air off-take, engine electric self-start and superior power generation and distribution capabilities [19]. Minimising the amount of air that would

Figure 1. Comparison of a conventional jet engine (left) and a bleed-less (right) [19].

have been bypassed away from the engine to power pneumatic loads means more of the air-intake is transformed into thrust. This, in combination with the engine's ability to electrically self-start consequently makes the respective pipework and valves obsolete, as illustrated in Fig. 1, providing further improvements in engine reliability [20]. However, the previously pneumatically-powered loads now have to be powered electrically.

Overall, this more-electric architectural shift demands greater on-board power generation and distribution capabilities as, inevitably, the electrical substitution of a plethora of pneumatic, hydraulic and mechanical loads significantly increases the on-board electrical demand. To address this issue, aircraft designers have implemented novel electrical architectures and distribution topologies, capable of delivering more power to ever-more loads, implementing hybrid AC and DC systems and utilising up to four voltage types, as will be explained in the next section.

The Boeing 787 represents the state-of-the-art in MEA as it is the first civil aircraft to substitute most of the pneumatic systems with electric equivalents [19, 21]. It is a wide-body, twin-engine jetliner which first flew in 2009 and is thought to be 20% more fuel-efficient than the Boeing 767 it was intended to replace [22], with around 8% of that efficiency gain coming from the engines [23]. It is capable of producing almost 1.4 MW of electrical power from two variable-frequency 250 kW generators per engine and two 225 kW Auxiliary Power Units (APUs) [24].

Airbus have also built their most electric aircraft, the A380, a double-decker, wide-body, four-engine airplane which first flew in 2005. Although it does not have the power generation capabilities of the B787, it too features variable-frequency

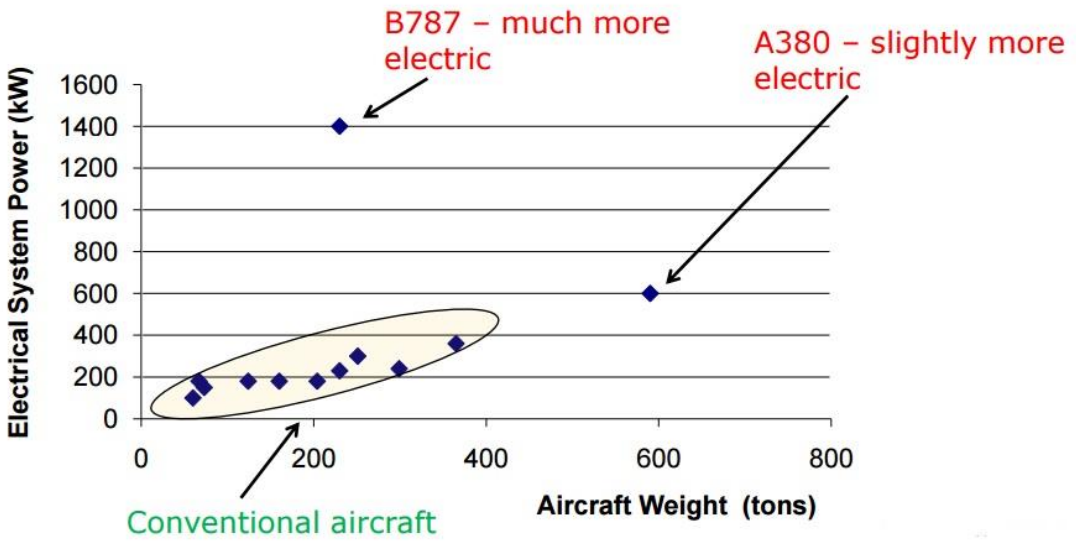

Figure 2. Electrical power generation capabilities of passenger aircraft [25].

generators and incorporates electrically-assisted actuation on all flight-control surfaces [26]. It features one 150 kW generator per engine and two 120 kW APUs, capable of producing a maximum of 0.84 MW of power [27]. The on-board power generation capabilities of the abovementioned aircraft are depicted in Fig. 2. It should be noted that the power generation capability of the B787 in this figure includes the electrical power the APU can deliver.

2.2 Electrical power generation and distribution

In conventional aircraft, the electrical distribution system is typically centralized. Primary and secondary power distribution units located in the electrical/electronics (E/E) bay at the front of the aircraft regulate power to loads spread out across the entire aircraft. In this topology, electrical cables have to go from the E/E bay to every electrical consumer throughout the body of the aircraft. This topology would have been inefficiently heavy for the multitude of new loads a MEA would introduce to the electrical network.

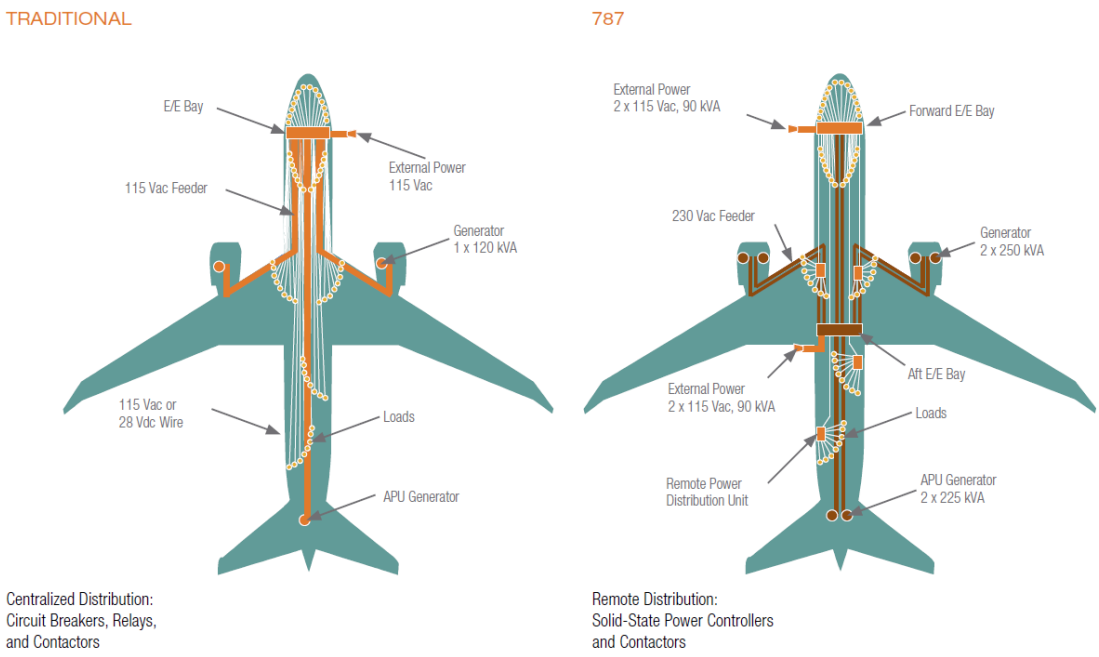

Figure 3. A comparison between a traditional centralized power distribution system and a de-centralized MEA ditribution system [19].

In an effort to reduce the weight and volume implications of the distribution system, aircraft designers adopted a de-centralized or remote-distribution system, illustrated in Fig. 3. The aircraft is divided into several zones where primary and secondary power distribution units regulate power in their respective zones. In this manner, the weight and length of power cables is significantly reduced. Boeing estimates that this topology reduces wiring on the B787 by 32 km [28]. At the same time, novel power generation systems had to be adopted for the MEA/E power supply requirements, as technology and solutions applied previously on traditional aircraft were not capable of meeting these requirements [29].

Traditionally, aircraft use a gearbox to produce a fixed-speed shaft from the variable-speed engine shaft. The fixed speed shaft, known as Constant Speed Drive (CSD), is linked to an Integrated Drive Generator (IDG) which produces a constant-frequency 400 Hz power supply. However, this approach has the disadvantage that the mechanical gearbox is heavy, expensive and difficult to maintain due to its complexity in design [4]. Even though the IDG has been the predominant generator technology for civil aircraft, new MEA/E are turning towards the more efficient

Variable Frequency Generator (VFG). A comparison of the two different generation systems is shown in Fig. 4.

By removing the need for constant frequency of supply, it is possible to remove the CSD and connect the generator to the engine via an accessory gearbox. In this manner, the generator will output 230 V AC power of variable frequency, typically in the range of 320 Hz to 800 Hz [30], depending on the rotational speed of the gas turbine. This direct approach allows for the elimination of the heavy gearbox that would otherwise be used to couple the IDG to the engine shaft, supports the electric engine starting ability and makes for a simpler, more reliable generation option [31]. However, given that electrical supply of variable frequency cannot be used directly for most on-board applications, the drawback of this approach is that now almost all loads will require power converters for control. Nonetheless, several applications such as flight-control actuators and the Environmental Control System (ECS) still require a power conversion stage [4], so the weight penalty is to some extent mitigated.

Overall, the growing electrification of passenger aircraft has increased the on-board power generation and distribution requirements, which in turn has increased the size and complexity of a MEA/E electrical network, as will be analysed in the following section. The B787 for example, has a main AC architecture, features four voltage types, 230 V and 115 V AC, 270 V and 28 V DC, and has approximately 1055 circuits, shown in Fig. 5 [32]. The generated power is fed directly onto the 230 V AC bus to power large loads, such as the ECS and wing anti-ice, before being converted to other voltage types. ±270 V DC is obtained through Auto-Transformer Rectifier Units (ATRUs) to power adjustable speed motors, 28 V DC is obtained through Transformer Rectifier Units (TRUs), and finally 115 V AC is obtained via Auto-Transformer Units (ATUs).

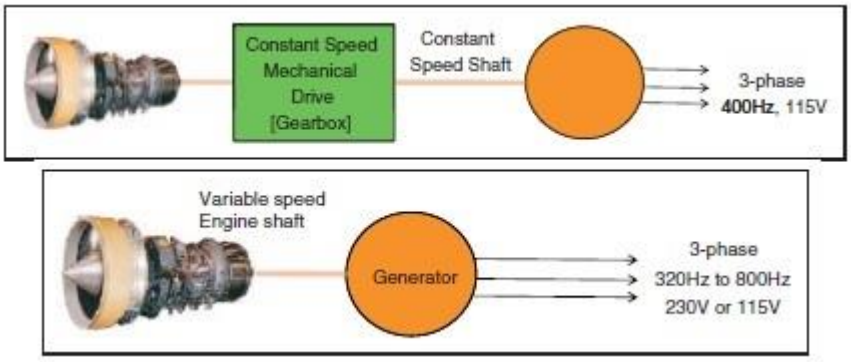

Figure 4. A comparison between a fixed frequency generation system (top) and a variable frequency generation system (bottom) [4].

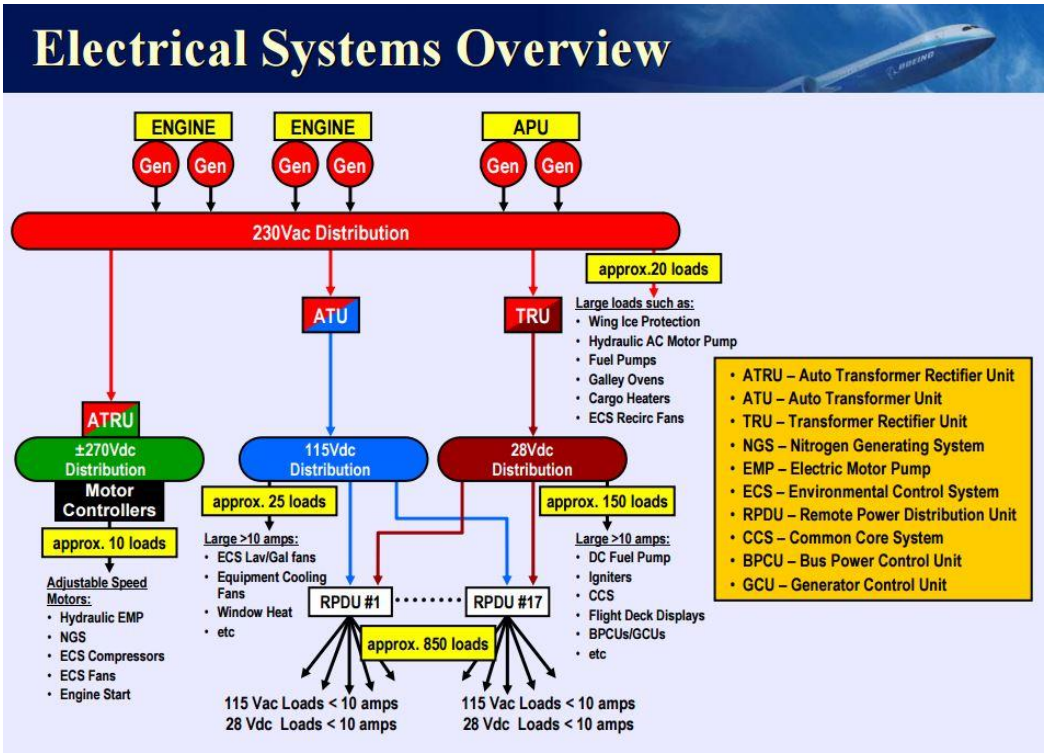

Figure 5. Electrical system of the Boeing 787 [32].

2.3 Evolution of airplane electrical networks

To fully comprehend the complexity of today's MEA power networks, it would be beneficial to briefly review several milestones in the evolution of aircraft networks in time. Most if not all were trialled and implemented on board military platforms. In

twin-engine airplanes of the 1940s, each engine powered a 28 V DC generator and an inverter was fitted to supply 115 V AC to the flight instruments [21]. The advent of the Second World War significantly increased the on-board power requirements of military planes as electronic warfare equipment, radio and radar was installed [33].

During development of the four-engine Vickers Valiant, it was decided to design the airplane as electrical as possible, featuring electric actuators for landing gear, flight surfaces, flaps and air brake [34, 35], due to hydraulics being heavier that electrical cabling at that time [36]. The Valiant was fitted with one 115 V AC generator per engine, and all four generators were paralleled to provide no-break power and an increased level of control and circuitry protection [37]. Applications that required large amounts of power were connected to the 112 V DC generators. The flight surfaces were controlled by AC motors, therefore in the event of a total electrical failure, the crew would fly the plane manually, something that required considerable effort [38].

The more advanced Avro Vulcan B.1 featured a primary 112 V DC electrical system supplied by four 22.5 kW engine-driven generators, and a secondary system consisting of 28 V DC, three-phase 115 V AC at 400 Hz and single-phase 115 V AC at 1600 Hz, driven by inverters and transformers from the primary system [39]. The voltage level of the primary system was later increased in the B.2 variant to 200 V AC at 400 Hz for higher reliability and greater efficiency [40]. All variants of the Vulcan featured hydraulically-actuated flight controls but the hydraulic pumps were driven by electric motors [41]. A complete electrical failure would result in loss of control, as there was no manual reversion, which inevitably led to two aircraft crashing due to this [42]. What sets the B.2 apart however, is its then-revolutionary four channel AC electrical system featuring TRUs and frequency converters [41], an architectural philosophy that can still be found in many airplanes today.

High power AC generation systems were installed in military fighter aircraft such as the McDonnel Douglas F-4 in the 1960s and the General Dynamics F-16 in the 1970s. More powerful radar systems, radios, advanced weapon systems and avionics meant higher power requirements. To cope with the increased energy demand, the F-16 was fitted with 40/60 kVA generators, driven by a constant speed drive from the

engine [43]. The F-16 was also the first fighter jet to introduce a Fly-By-Wire (FBW) system [44], a system which eliminates the mechanical linkages between the control stick and rudder pedals, and the flight-control surfaces. Consequently, electrical systems relayed flight commands to control surfaces through an analogue control system in A/B variants, and via a digital computer in later C/D versions [45]. However, the FBW system was vulnerable to static electricity, with up to 80% of C/D models' electronics suffering from electrostatic discharge [46]. To prevent a single point electrical failure from rendering the aircraft uncontrollable, the FBW system was designed with quadruple backup [47], so in case of a fault in one or even two channels, the remaining channels would prevent the loss of signals to control surfaces. This was a big leap in system redundancy compared to World War II fighter aircraft.

In the 1990s, the McDonnel Douglas F-18 featured even higher levels of redundancy in its electrical system. Its electrical system consisted of two 40/65 kVA AC generators, two TRUs and two batteries [48]. During normal operation, its two AC generators would independently power their respective, isolated AC buses, however in the case of one generator dropping offline, power from the operating generator would be transferred to the bus of the offline generator via a bus tie breaker, shown in Fig. 6. This was made possible as either generator was capable of supplying power to the entire electrical system [49]. Additionally, the terminals of the TRUs were connected in parallel, with the manufacturer's manual stating that a short-circuit in one of the TRU buses does not affect the operation of the other, as adequate protection was in place. Similarly to the generators, one TRU could power the entire DC network in case the other failed [49]. Overall, the F-18 would not lose any system functionality in the case of a single generator or TRU shutting down.

Arguably, the last technological milestone in airplane networks today is the advent of ±270 V DC systems. Again, these systems were first trialled and fitted in state of the art military jets, such as the Lockheed Martin F-22 and F-35 [50], for increased power density and weight reductions in conductors. The F-22's electrical system consists of two 65 kVA generators, a 27 kVA APU, two 270 V DC/115 V AC and

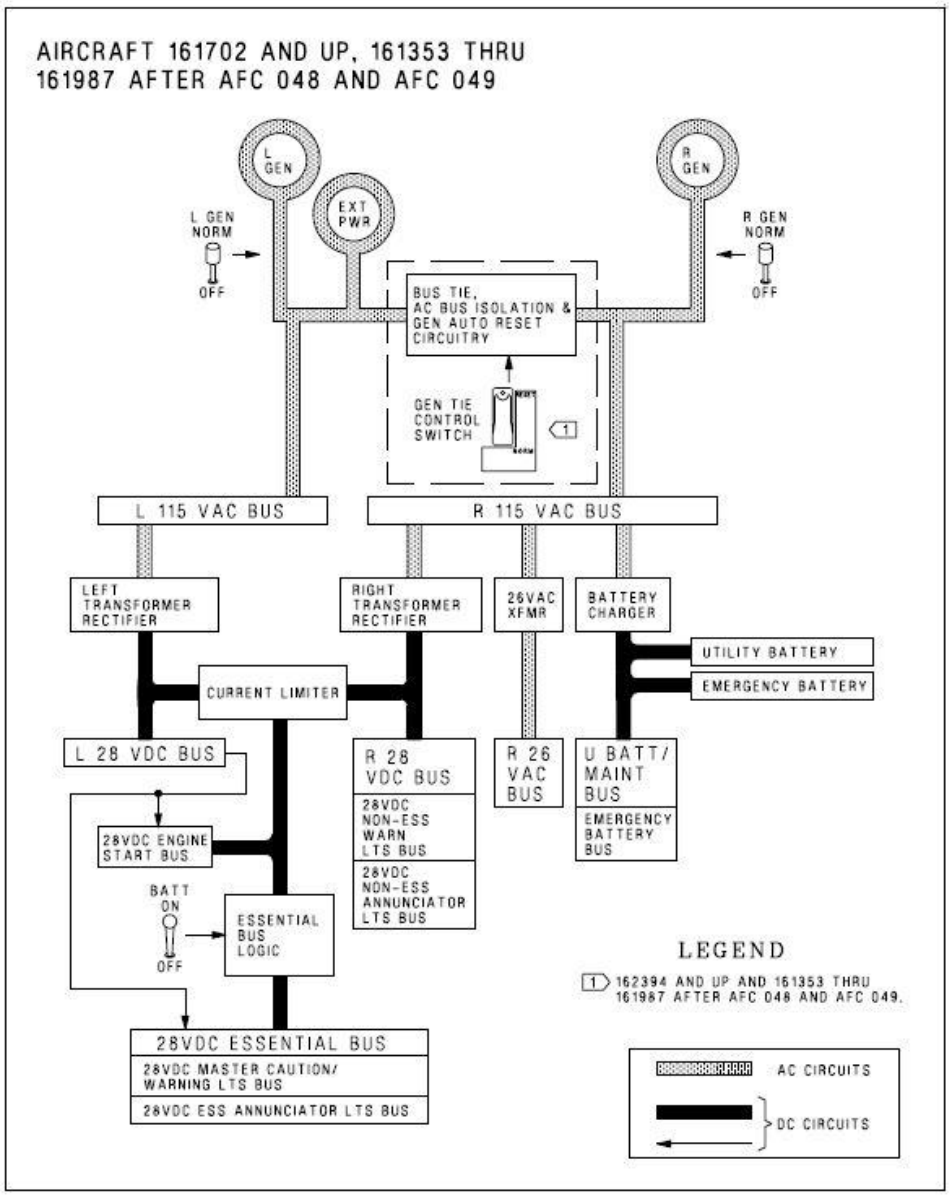

Figure 6. Electrical system of the F/A-18 [49].

two 270 V DC/ 28 V DC converters [51]. Both fighter aircraft have huge power demands due to even more powerful radars, avionics suites and electrically-driven hydraulic actuators. This requires the electrical system to respond to rapid load changes while maintaining a constant voltage. Another interesting reason into the substitution of a main AC architecture with a DC system is for stealth concerns [52], with one possible explanation being that design changes were needed for better heat dissipation, which in turn improves the aircraft's protection against heat-seeking missiles, however limited information on this topic is available due to its nature.

Overall, the transition to a main DC architecture was not without issues, as several prototypes of both models suffered electrical failures that led to crashes and fleet groundings [53]. On one occasion, a short-circuit disabled the flight controls of the horizontal stabiliser on a F-35 [54] and a feeder arc resulted in the total aircraft loss of a F-22 [55]. In today's MEA/E, only the B 787 features a 270 V DC system, as the A380 only utilises a 28 V DC generation [56]. The historic evolution of aircraft electrical systems is summarized in Fig. 7.

The technological breakthroughs, and more importantly, the lessons learned from military aircraft design have been passed-on down to passenger airplanes, given that civil aviation aircraft have to adhere to stricter redundancy requirements and safety regulations, explained in greater detail in the next chapter. These requirements have shaped the design, development and certification of on-board systems, and have imposed a multiple-redundancy philosophy for hydraulic and electrical systems. As these systems have been traditionally powered by the aircraft's engine, any shift in aircraft- or system-design philosophy will inevitably be reflected in the engine design approach as well. The next section briefly analyses advances in aircraft engines and how the MEA/E has changed the gas turbine.

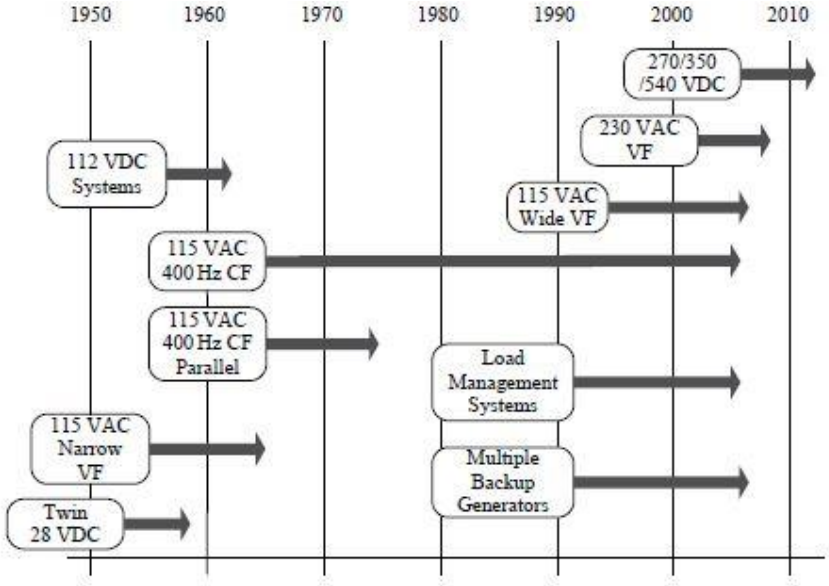

Figure 7. Evolution of aircraft electrical networks [21].

2.4 Evolution of aircraft engines

A turbofan jet engine produces thrust by igniting pressurized air in its high-pressure (HP) turbine (or combustion chamber) which exits the back of the engine as very hot, high-velocity exhaust gas, and in the process, spins a low-pressure (LP) shaft which turns a fan in the front of the engine. Most of the air pushed rearwards by this fan bypasses the turbine. The ratio of air mass-flow that bypasses the turbine compared to the air mass-flow that enters the turbine is known as the bypass ratio. Most civil-aviation aircraft in use today are fitted with high-bypass type engines [57, 58]. High-bypass engines offer many benefits compared to turbojets or low-bypass jet engines of the past. As moving large volumes of air at slower speeds is more energy-efficient than moving small amounts of air at large speeds [59], high-bypass engines are therefore quieter and more fuel-efficient [60].

Additional advances have been made in the mechanical design of the engine, more specifically in the number of spools. Early designs featured a single shaft connecting the turbine to the fan, therefore both components rotated at the same speed. This was inefficient, as the bigger blades of the fan cannot be rotated as fast as the smaller turbine blades due to stress limitations [61]. Multi-spool engines allow the HP and LP shafts to rotate at their optimum speeds, further improving performance and efficiency [11]. To date, engine manufacturer Rolls-Royce produces the only three-spool, high-bypass ratio jet engines available, the Trent series. Besides the HP and LP shaft, this family of engines features an Intermediate Pressure (IP) shaft, shown in Fig. 8, from which electrical power can also be off-taken to aid with the greater power requirements of MEA/E [62].

Digital technology and data transmission systems have made the integration of digital control systems with aircraft flight control systems and avionics possible [21]. Systems like Full Authority Digital Engine Controls (FADEC) control and monitor all aspects of the engine's performance, allowing it to operate at maximum efficiency for a given flight condition. This system allows for optimum fuel management, and also provides the engine manufacturer with engine prognostics and diagnostics, potentially aiding in the reduction of maintenance costs [63]. To monitor the engine

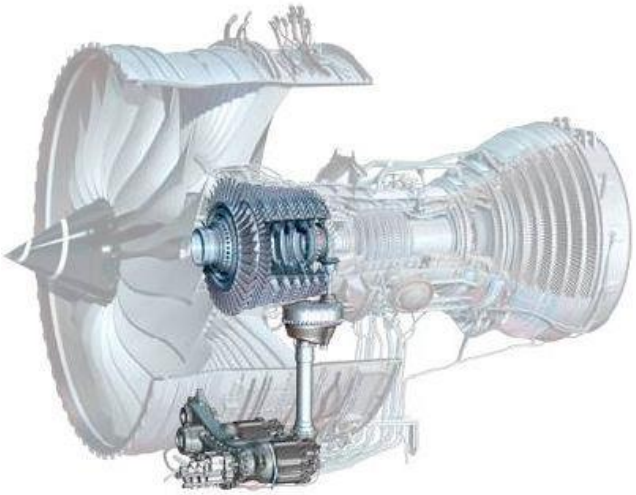

Figure 8. A Trent 1000 engine with Intermediate Pressure (IP) shaft off-take [11].

status and performance requires mounting electronic control-units on to the engine itself, however, this can be a challenging undertaking not only due to thermal and vibration concerns, but also in terms of electrical power provision for these units and sensors. An adequate engine electrification network is therefore necessary in order for FADEC systems to operate properly.

The MEA/E has undoubtedly changed aircraft engine design, as the minimisation of hydraulic and mechanical engine off-takes led to a greater electrification of engine accessories [8]. Hydraulic pumps and mechanically-driven fuel and oil pumps for example are replaced with electric motor-driven equivalents, reducing complexity and increasing reliability [64]. The electrical self-start of the engine eliminates the accessory gearbox and shaft, and improves starting performance in cold conditions [65]. Active magnetic bearings have showed promising results as an alternate way of supporting rotating engine assemblies, and could potentially eliminate the complex oil system and its accessories of pumps, coolers and filters [66]. These technological advances are associated the More-Electric Engine (MEE) concept, the engine-equivalent to the more-electric airplane philosophy [67, 68].

Apart from the MEE, advances have also been made at a mechanical level. Super-alloys and new blade/vane cooling techniques enable the HP turbine to operate at a higher overall pressure ratio and temperature [69]. This raises the core's thermal

efficiency, which in turn increases the fuel efficiency of the turbofan [70]. However, by increasing the overall pressure ratio of an engine cycle, it becomes more difficult to operate the engine at low power/rpm without encountering compression surge, a violent and damaging reversal of airflow through the compressor [71]. This phenomenon will be analysed in more detail in Chapter 3 (section 3.3.1).

The ever-increasing electrification of MEA/E imposes the need for new technologies and novel electrical architectures [8], without adversely affecting the pre-existing levels of reliability of today's systems. New power-system design options that could reduce fuel consumption and improve engine operability are needed, with one possible choice being the interconnection of generators to produce a single combined power source.

2.5 Chapter summary

This chapter reviewed the MEA and MEE concepts and outlined the key differences between MEA and conventional aircraft. It addressed the technological challenges and breakthroughs of this more-electric shift, and presented novel power generation and distribution systems. Arguably, the latest technological milestone in military and commercial airplane networks today is the advent of ±270 V DC generation and distribution systems. The ever-increasing electrification of MEA/E systems imposes the need for new technologies and novel electrical architectures. To satisfy the need for reduced fuel consumption and improved engine operability, this chapter identified that new power-system design options are needed, with one possible choice being the interconnection of generators to produce a single combined power source.

Chapter 3

Interconnected Generation

This chapter will briefly review the state of interconnected generation in the current and past aviation industry and present the challenges associated with paralleled architectures. It will also identify the key technological drivers that may provide a more feasible route for the implementation of such architectures. Finally, it will summarize the benefits and drawbacks of proposed approaches in the relevant literature.

3.1 Historical review

Up until the 1950s, interconnected generation was the design approach in military bombers, such as the Vickers Valliant. In 1951, there was a regulatory attempt in the United States to standardize the civil-aircraft power supply requirements, as to that date, 36 different varieties of electrical-power requirements for accessories existed [72]. It was typical for the electrical system to be comprised of different equipment from various sources, and put together and operated for the first time after the installation on-board the aircraft [73]. This was detrimental for the integrity of the electrical system and unacceptable for civil aviation standards.

In 1952, the very first commercial airliner was launched, the De Havilland Comet 1. The Comet 1 featured four 2.5 kVA generators which were linked, via individual rectifiers, to a common 28 V DC bus [74]. It was soon realized however that an interconnected system brings with it significant protection challenges. AC faults had the tendency to trip the transformer's relay, shutting down the system, whilst DC busbar short-circuits would "kill the supply to all connected sets" [75]. For safety purposes, split busbar systems with at least two busbars per aircraft were advocated.

Significant changes were carried out on the Comet 2E variant due to the installation of the autopilot/autoland system. This system requires the autopilot and flight director functions to be powered from separate power supplies, so no common failure can affect both systems. This was due to the assumption that a complete loss of electrical power occurring in close proximity to the ground could cause disaster during low/bad visibility automatic landings [76]. To provide a high standard of safety, it was required that no single fault condition could cause the loss of more than one power supply to the flight control system. Consequently, the power system was redesigned with no paralleling of generation, in order to provide the triplex flight control system with three separate sources of AC power.

Within the first year, several Comets experienced a series of in-flight breakups and catastrophic failures in well-publicized accidents [77]. Following the grounding of the Comet fleet, valuable lessons were learned regarding metal fatigue and aircraft design, and significant changes were made to later variants. As a result, the electrical distribution system of the Comet 4 was re-designed, with more powerful alternators and separate busbars backed-up with separate emergency busbars [78].

In 1957, the first Boeing jet airliner, the four-engine B707, was designed with an interconnected generation architecture [79]. It featured a primary three-phase 115 V, 400 Hz AC system, where the generated power from its four 30 kVA generators could be supplied to any load bus via a synchronising bus tie loop [80]. In this manner, any combination of generation sources could be paralleled to aid with the total power demand. Finally, TRUs derived 28 V DC power from the main AC system.

The same interconnected power-generation architecture was adopted for the four-engine B720 and the three-engine B727 that followed [79, 81]. This provided a means for powering all buses in case one or two generators were inoperable [82]. When power of acceptable quality was achieved, the respective generator buses would be connected to the synchronisation bus via bus tie breakers. The maximum continuous load for a generator operating separately was 36 kW, however when the generators were paralleled, the power output was not linear, with the output of two paralleled generators being limited to 54 kW, and three paralleled generators being

limited to 102.5 kW [83]. In the B 727, the two TRUs were also connected in parallel via a current limiter as a backup measure in case of a loss of one of the units, as either unit was capable of powering the loads on both DC buses [83].

In Boeing's first two-engine aircraft, the B737, the interconnected architecture was replaced by a fully isolated, three-phase, 115 V, 400 Hz two-channel AC system [84]. The electrical system would not allow any paralleling of generation sources, and the connection of a new power source to an already power bus would cause the disconnection of the existing source [85]. In normal operations, each generator would power its respective AC bus, but in the case of a generator failure, a bus transfer relay would provide power to the opposite bus. Under one-generator operations, the system was designed to perform incremental load sheading, based upon actual load sensing [86]. The B737 featured three TRUs to derive 28 V DC, two main and one backup, with either two being able to power all DC loads. In the event of a double engine or generator failure, a nickel-cadmium battery would provide emergency DC and AC (via a static inverter) power for approximately 30 minutes of flight time [87].

In 1969, when the four-engine B747 came out, Boeing opted again for a 115 V, 400 Hz AC interconnected generation architecture, similar to its previous three- and four-engine models [88]. The electrical system of the B747 features paralleled generation both on an AC and DC level, and is depicted in Fig. 9. Each engine-driven IDG is connected to its respective AC bus via a Generator Circuit Breaker (GCB). To interconnect the generators, each AC bus is then connected to the synchronising (SYNC) bus through Bus Tie Breakers (BTBs). 28 V DC power is derived from four TRUs, each connected to its respective AC bus, and all four TRUs are paralleled via DC Isolation Relays (DCIRs) on to the DC Tie Bus.

For such a broadly interconnected system however, there had to be operational limitations to ensure safe operation of electrical subsystems [89]. Any combination of AC-generator paralleling on the SYNC bus was possible, as long as the voltage and frequency were within limits. Load controllers ensured that the output of

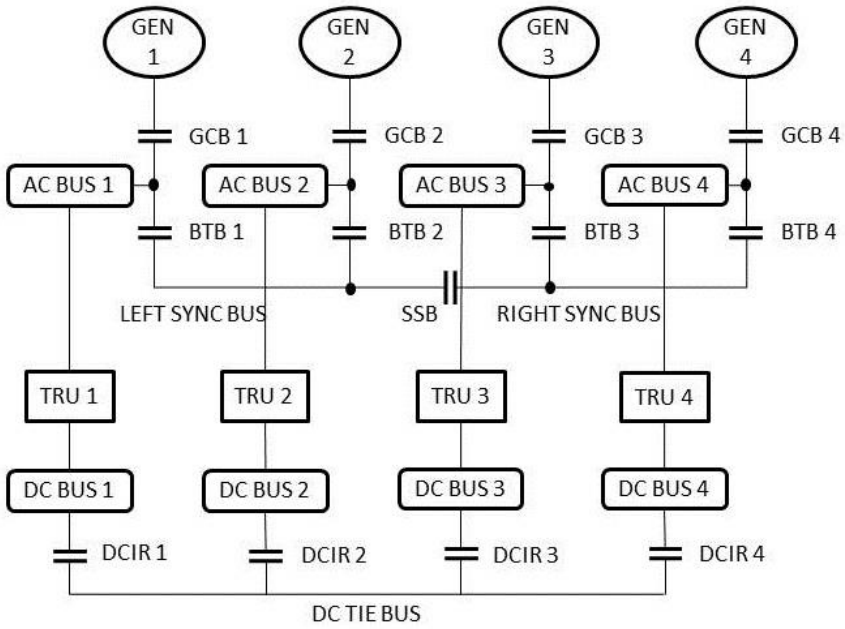

Figure 9. Boeing 747 electrical power generation system (adapted from [88]).

generators was balanced, consequently if a generator was contributing more than its equal share of loading, it would be isolated to supply only its own bus load. As in the B727, when more than one generator is paralleled, the contribution per-generator would reduce. In early variants, each generator was rated at 57 kW (60 kVA) but limited to 54 kW in isolated mode, the output of two interconnected generators was limited to 81 kW, and when three and four generators were paralleled, the total output was limited to 51 kW [89]. One possible explanation for this could be because of protection equipment tripping ratings and limitations. If the electrical demand exceeded the available power, the system was designed to automatically shed galley loads first, followed by utility loads, such as passenger lights and entertainment systems, air-conditioning and lavatory equipment. In the -400 version, the generator rating increased to 90 kVA, but in all variants, if the IDG is mechanically disconnected from the engine accessory gearbox, it may not be reconnected in flight [90].

In normal operating conditions, power from all four AC generators is synchronised and interconnected, however during automatic instrument-landing approaches below 1,500 ft, AC and DC buses are respectively isolated [91]. In this manner, each of the

three autopilot's flight control computer is powered by an independent electrical source, thus achieving higher levels of redundancy and reliability for the autoland system. AC bus 4 will keep powering the SYNC bus, and via automatic system reconfiguration, any other AC bus in case of a generator failure above 200 ft. Below 200 ft., a generator failure may result in the loss of an autopilot channel as the system will not reconfigure itself.

After the B747, Boeing appear to have shifted again to isolated, two-channel electrical systems for its future twin-engine aircraft, such as the 757, 767, 777 and 787 [92-95]. The most recent variant of the 'jumbo' family however, the B747-800 which was launched in 2010, still maintains the interconnected generation architecture of its predecessors, both in the passenger and cargo version [96]. Airbus on the other hand, does not appear to have implemented any interconnected generation scheme on any of its civil-aviation aircraft, including the four-engine A340 and A380 models [97-99].

Overall, interconnected generation is relatively rare in the current aviation industry, as most aircraft power networks feature isolated radial architectures. One reason for this can be attributed to protection issues as in an isolated network, transients and faults do not propagate through the entire network, but remain confined to a specific channel and do not affect the operation of other flight-critical loads and buses outside the faulted area. Isolated generation sources also help in constraining the fault current, as in an interconnected network the fault contribution would be considerably greater. In turn, this requires smaller-rated and lighter protection equipment, further minimising the weight penalty of the electrical system.

3.2 Implementation challenges

The key challenges associated with interconnected-generation architectures can be broadly divided into three categories: electrical generation technology, airworthiness

standards and protection equipment. This section will briefly present the difficulties incurred by each category.

3.2.1 Generation technology

For several decades, the predominant civil-aircraft generation system has been the constant-frequency IDG. In 2006, it was estimated that 95% of all in-service civil aircraft at one point employed mechanically-regulated constant-frequency generation systems [100]. As described in Chapter 1, the IDG produces AC power of constant 400 Hz frequency, regardless of the rotational speed of the engine, therefore AC interconnection options such as on the B 747 could be readily implemented. However, this generation system was complex and had a relatively low power conversion efficiency. As many AC loads, such as motors, require adjustable-frequency control to arrive at the preferred operating torque or speed, constant-frequency power is not optimal for their operation.

Advances in high-power solid-state switching devices have enabled an alternative method for constant-frequency generation to be obtained, through Variable Speed Constant Frequency (VSCF) systems [21]. In such systems, the generator is connected directly on to the engine and produces variable-frequency AC power, the frequency of which depends on the engine's rotational speed. The generator output is then processed by a power converter and filter to produce constant-speed AC power. Typical implementations achieve power conversion via a cycloconverter, matrix converter or DC-link systems [66, 101, 102]. A VSCF system removes the unreliable constant-speed drive of the IDG and VSCF cycloconverters are more efficient than constant-frequency or DC-link systems [31], however there is a reliability issue as all generated power passes through that converter, therefore it remains a rarely chosen option [4]. Although VSCF systems were originally designed to be more reliable than IDGs, in practice they proved to be problematic on the MD-90 [103, 104] and B737 [105]. Particularly for the latter, up until 2001 before modifications where introduced, VSCF system reliability was approximately a third than of constant-speed drives, and models equipped with such systems were limited by the UK Civil

Aviation Authority to be within 45 minutes of flight-time from a suitable airport. Despite these issues, an improved VSCF system serves as backup for AC generation on the B777 [106].

In recent years, the aviation industry has shifted to the more reliable and efficient VFG. Compared to the IDG, this technology increases the overall power system reliability, and has the potential to reduce operating costs by up to $16 per flight hour [107]. The AC power produced by the VFG is of variable (or 'wild') frequency in the range of 320 Hz to 800 Hz, depending on the engine spool speed. This variable-frequency characteristic does not allow for a direct connection of the generation sources [108]. Consequently, AC interconnection options for MEA/E equipped with VFGs, like the B787 and the A380, would require additional frequency-regulating equipment and converters. For the required power ratings/levels however, new converter-design topologies and conversion topologies are needed, as existing frequency converters are not designed for aviation use, and are therefore heavy and bulky [100, 109]. The incurred weight and volume penalties seem to render this approach unfeasible.

In an effort to reduce weight and deliver efficiency benefits, more advanced electrical systems feature DC distribution, with a smaller subset of airborne platforms making use of DC for primary generation. The feasibility and advantages of this design approach will be presented in more detail in Section 3.3.2.

3.2.2 Airworthiness standards and power quality requirements

A wide variety of aviation-related activities, including aircraft design and maintenance, are regulated, to promote safe aviation and protect crew, passengers and the greater public from unnecessary risk. In the U.S., the Federal Aviation Administration (FAA) sets the airworthiness requirements for aircraft and systems design, maintained in Title 14 of the Code of Federal Regulations [110]. In Europe, the European Aviation Safety Agency (EASA) maintains its "Certification Specifications for Large Aeroplanes CS-25" [111]. Both of these codes set out rules

governing aircraft design and certification, and also make provisions for the electrical power system architecture.

To avoid a single point-of-failure in the electrical supply network, CS-25 requires that aircraft have two or more independent sources of electrical energy. The power sources are required to "function properly when independent and when connected in combination". This suggests that to some degree, that interconnection is compatible with the standards, however, "no failure or malfunction of any power source can create a hazard or impair the ability of remaining sources to supply essential loads". In turn, this requires considerable design effort and fast-acting protection equipment to achieve the desired reliability on an interconnected system [112].

CS-25 defines essential loads to be "each installation whose functioning is required for type certification or by operating rules and that requires a power supply". The power system as a whole is required to continue to supply essential loads after "failure of any one prime mover, power converter or energy storage device", and after failure of any one engine on twin-engine aircraft, and any two engines on three or four-engine aircraft. Essential loads that require an alternative power source must continue to operate after "any failure or malfunction" in any one power supply system, distribution system, or other utilisation system". Furthermore, duplicate systems or equipment installed to satisfy the above requirements must be sufficiently segregated, to "minimize the risk of a single occurrence causing multiple failures of circuits or power supplies of the system concerned". These requirements and provisions necessary for essential loads have shaped modern aircraft architectures into having multiple isolated supplies.

In modern commercial aviation, jet aircraft are designed to be flown by a two-man crew, with captain and first officer having two separate flying stations with duplicate instruments and flight controls. Electrically powered liquid-crystal displays have replaced traditional analogue gauges, dials and switches, transferring more information to the flight crew whilst reducing space requirements inside the cockpit. Electronic flight displays have realised the 'glass cockpit' concept, enabling aircraft manufacturers to customise their cockpits, and at the same time improve flight safety

by augmenting pilot understanding of the airplane's status relative to its environment (situational awareness) [113].

CS-25 stipulates that a failure of one power source must not affect the same instrument of both pilot stations, which seems to imply that multiple isolated supplies are required. An additional requirement is that two supplies are provided to each instrument, which can be manually or automatically inter-switched in the event of loss of power on the primary supply. These requirements are satisfied on the B747 by providing the captain's and first officer's instruments from AC Bus 2 and 3 respectively, whilst AC Bus 1 provides the automatic switchover option in case of loss of power on either of these buses [90]. It can therefore be assumed that when the B747 electrical network is in parallel generation mode, a temporary loss of power is acceptable to facilitate switchover of power sources and/or breaking of the bus tie breaker to isolate the power supplies.

Power quality requirements for AC and DC systems are defined in the U.S. Navy Military Standard MIL-STD-704 (currently in revision 'F w/Change 1', discussed herein) [114], which establishes the requirements and characteristics of electrical power provided at the input terminals of all electric utilisation equipment. The on-board electrical system is required to provide satisfactory quality electrical power (as defined for each system) during all operations of the power system, and provisions are made for abnormal operation, to which the systems is expected to conform to during faults or malfunctions of the electrical network.

Normal operation is defined as the intended operation of the power system in the absence of faults or malfunctions that degrade performance beyond the established requirements. It includes prime mover speed changes, switching of utilisation equipment, and synchronising and paralleling of power sources. On the other hand, abnormal operation occurs when "a malfunction or failure in the electric system has taken place and the protective devices of the system are operating to remove the malfunction or failure from the remainder of the system before the limits of abnormal operation are exceeded". The limits set out in MIL-STD-704F for normal and abnormal operation include quantitative restrictions on voltage, frequency and

transients, however, as the primary focus of this thesis is a 270 V DC platform, detailed requirements following will be limited to 270 V DC systems.

Normal operation (or steady state) 270 V DC characteristics define the steady state voltage range to be between 250 V and 280 V, with a permissible voltage ripple of 6 V. The normal voltage transient limits, or normal voltage envelope, for 270 V DC systems is shown in Fig. 10, whilst the overvoltage and undervoltage values during abnormal operation "shall be within the limits" of Fig. 11 [114]. A transient can occur as a result of "normal disturbances such as electric load change and engine speed change" or "of a momentary power interruption or an abnormal disturbance such as fault clearing". Normal transients are defined as transients that exceed the steady state limits (250V to 280V) but remain within the specified normal transient limits, whilst transients that "exceed normal transient limits as a result of an abnormal disturbance and eventually return to steady state limits are defined as abnormal transients". It is therefore evident that the transient fault response caused by an electrical fault is considered by the standards to be an abnormal voltage transient.

Overall, the restrictions imposed by the standards would need to be satisfied by any new architecture. To date, there is no specific standard dedicated exclusively to parallel generation systems, and there are no provisions for an interconnected system functioning under abnormal operation conditions. Although it is permissible by the standards for the voltage level to collapse for a duration of seven seconds under 'abnormal operation' rules, however a loss of power of such magnitude can potentially have a detrimental impact on flight-critical and essential loads in the greatly electrified network of MEA/E. Logically therefore, it would seem necessary that in any interconnected system, a fault on one supply channel should not cause the power quality on the remaining channels to deviate from acceptable levels as defined by MIL-STD-704F, i.e. the normal transient limits. Essentially, this work will not assume that the 'abnormal' voltage performance can be adhered to across all inter-connected channels in the event of a fault, even if an MEA would allow for interconnected generation. This interpretation will be used as the basis for simulation studies in the following chapter.

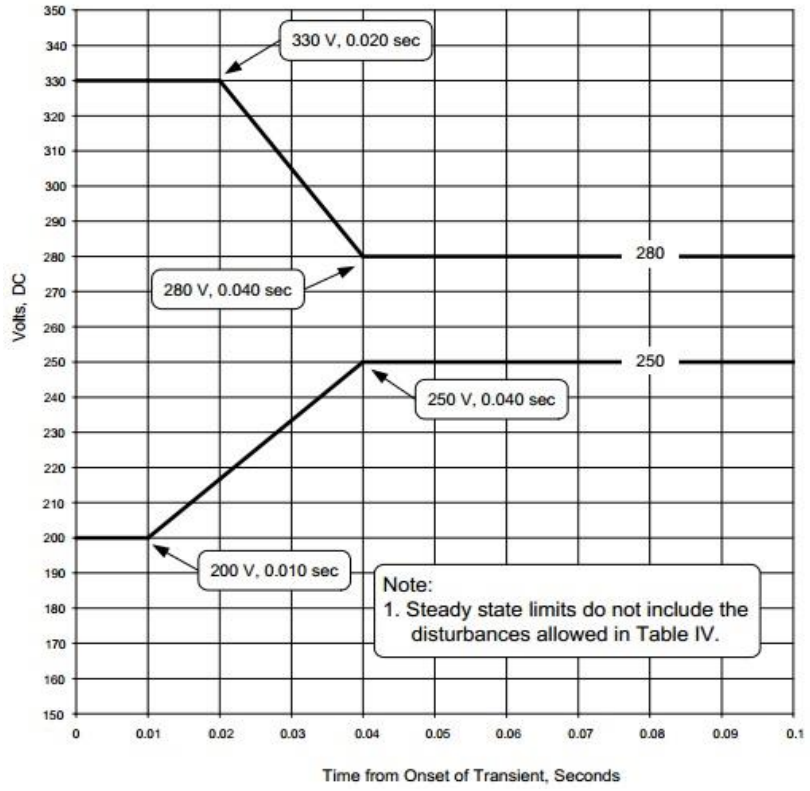

Figure 10. Envelope of normal 270 V DC voltage transient [114].

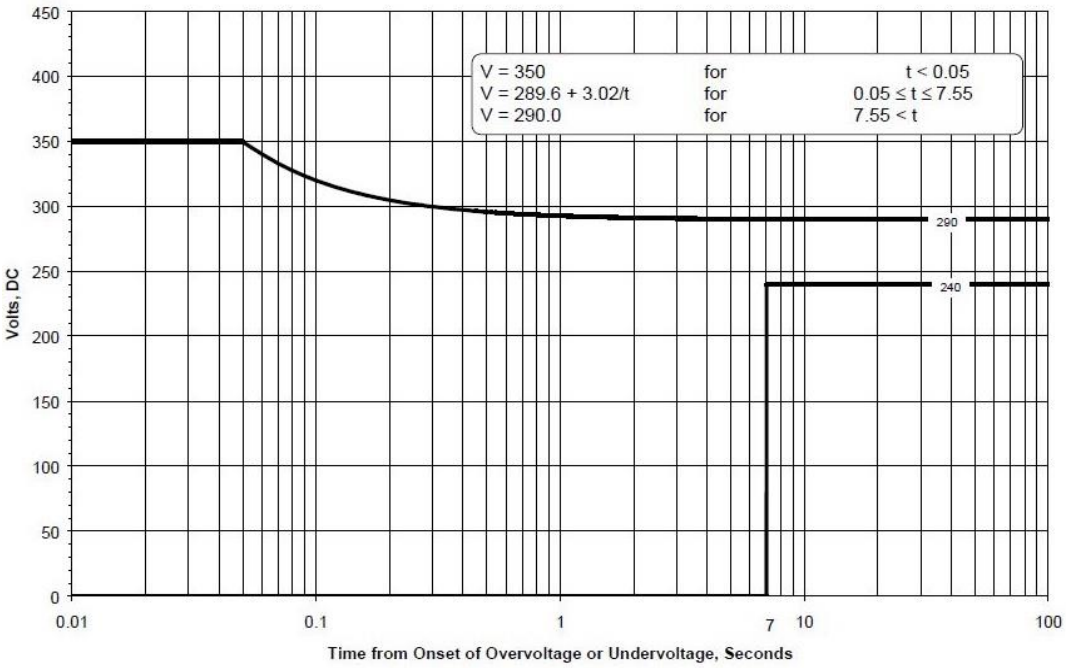

Figure 11. Envelope of abnormal 270 V DC voltage transient [114].

3.2.3 Protection equipment

The greater electrification in MEA/E brings with it new power distribution architectures, with a greater number of on-board systems depending on power electronics. The increase in electric power demand has provoked an increase in the voltage levels both in AC and DC systems. Traditional 115 V AC systems have been replaced with 230 V AC, and novel ±270 V DC-voltage buses have been incorporated in aircraft power networks [115, 116]. The implementation of such complex architectures significantly increases the protection burden for isolated networks, let alone interconnected systems.

Parallel generation systems reduce the isolation of the electrical network, therefore advanced, fact-acting protection strategies are required. As the degree of interconnection increases, a greater portion of aircraft systems is exposed to transients and single-point faults that may occur in the network. Consequently, protection equipment need to detect and clear faults before network characteristics breach the power quality requirements set out by the standards.

Traditionally, circuit breakers are the most common protection devices for 28 V DC and 115 V AC systems [117]. Their functionality is limited however, as they cannot detect and isolate arc faults, require monitoring due to aging and exhibit poor performance at high DC voltage [118]. One of the challenges associated with DC protection is that the fault-current waveform does not have a zero crossing, therefore electromagnetic DC circuit breakers are heavier and larger compared to an equivalent AC device [119]. In the aviation environment, where weight and volume come at a premium/cost, the increased size of electromagnetic circuit breakers (EMCBs) for the ±270 V DC distribution system, paired with their relatively large tripping time of approximately 10 ms, makes them undesirable for such applications [9].

Recent advancements in DC protection devices may enable such protection capabilities to be realized. Solid State Power Controllers (SSPCs) and Fault Isolation Devices (FIDs) [117, 120, 121] offer improved functionality which could potentially enable a larger degree of interconnection in the power network. SSPCs in particular, can detect and isolate arc faults, have very fast operation times (3 μs - 25 μs [117,

122]) and no moving parts, making them ideal candidates for the harsh operating environment of aviation. Component advancements have allowed the addition of new functions and capabilities on SSPCs, such as enabling the control of loads in variable frequency AC [123, 124]. Although there has been encouraging research in the field of protection devices, few commercial devices exist which can operate either at the voltage level or the current level required for 270 V DC distribution on MEA/E [125]. Devices that can simultaneously meet the greater voltage and current requirements of an interconnected MEA/E system do not appear to be commercially available yet [117, 126].

3.3 Drivers for change

In a typical land-based electrical network, interconnection of numerous power sources allows for multiple power paths, better frequency control and greater system inertia. Aircraft power networks however are inherently different, as the compact nature of system does not encapsulate large amounts of inertia and the electrical frequency on MEA/E is variable by design [127].

The benefits of generation-source paralleling in aircraft electrical networks include multiple power flows and increased security of supply to flight-critical loads. From an electrical standpoint, these factors could potentially reduce the need for backup-generation infrastructure, although this infrastructure could be called upon in case of a hazardous mechanical failure condition, such as the remote event of an all-engine failure. Additionally, interconnected generation could also support power transferring and power sharing from the aircraft engine if dual/plural offtakes from independent shafts are employed [128]. The key drivers for revisiting interconnected generation schemes, including but not limited to multi-shaft power offtakes and DC distribution schemes, along with their benefits, will be analysed in the next sessions.

3.3.1 Efficiency gains through multi-shaft offtakes

In Chapter 2, it was briefly mentioned that advances in material technology and cooling techniques have allowed the operation of the turbofan engine at a higher overall pressure ratio and temperature, thus improving the core's thermal efficiency, and consequently the fuel efficiency of the engine. However, by increasing the overall pressure ratio, engine stability becomes more difficult to retain at low power/rpm, and could potentially lead to a disruption of airflow in the compressor, known as compressor stall. Stalls range in severity from a momentary drop in power to compression surge, the catastrophic complete loss of compression. For a safe and stable operation therefore, the engine should be operated at a safe margin away from the surge point under idle or low thrust conditions.

At the same time, engine operation closer to its surge point makes it more fuel-efficient, and potential fuel savings could be realisable during the portion of flight spent under these conditions [112]. However, traditional engine designs that extract all required power from the HP shaft negatively affect engine-stability control [129]. The high and relatively constant operating speed of the HP spool renders it an ideal candidate as a source of mechanical power to drive the generator, but the higher load placed on the HP core can have a detrimental effect on engine performance at low power settings, for example when idly descending.

In an effort to obtain engine operability/performance benefits and reduce the necessary surge margin, and thus fuel consumption, researchers have explored the use of multiple shaft off-takes and power transfers between shafts [129-133]. As the option of installing larger generators is not always possible due to space and design constraints, drawing power from the LP or IP spool shaft could be an alternative approach in extracting power in a more fuel-efficient manner. Benefits in engine performance can be realized by selectively controlling electrical power extraction between the HP and LP (or IP) shafts [130]. As engine operation varies throughout the flight cycle, with high rotational speeds during take-off and climb and low rotational speeds during taxiing and decent, one portion of the engine may be capable of producing more power than is required at a specific operating point compared to

another portion of the engine [134]. Therefore multi-shaft power-extraction optimisation is necessary to ensure engine excess capacity is not left unused.

Derouineau in [135] proposes a multi-shaft offtake configuration where generator control units (GCUs) regulate the output of each AC or DC generator in relation to a wide variety of operational parameters, such as engine thrust setting, turbine rotational speed, aircraft speed and altitude, power network configuration and electrical system load. The complicated control of the LP and HP power mix is thought to improve the surge margin and engine operability during high-power extraction demands.

Colin *et al* propose a twin-rotor electrical machine driven concentrically by both the LP and HP spools of the engine [136]. In one configuration, electrical power can be extracted from both spools using speed-reducing gearboxes, and in another embodiment, the rotors are mounted directly onto the engine without the need of a gearbox, which would have a negative impact on the mass of the engine.

Additionally, transferring power between shafts could aid in engine starting and could allow for better stability control without the use of traditional techniques such as air bleed and variable stator vanes [136-138]. Lastly, an LP-mounted generator appropriately designed could have the potential to generate power in case of an engine failure by exploiting the windmill effect [68, 139], and consequently replace the high-maintenance Ram Air Turbine (RAT) system used today [140].

3.3.2 Growing use of DC distribution

Since the 1940s, aircraft electrical networks have employed DC distribution of up to 28 V for avionics, low-voltage DC loads, battery-driven services and emergency generation. In recent years, modern passenger aircraft like the B787 make use of an additional ±270 V DC distribution system for large DC loads, such as Environmental Control System (ECS) compressors and fans, electric motor pumps and engine starting. The use of higher-voltage DC contributed to the reduction in size the of

current-carrying conductors, which in turn reduces voltage drop, power dissipation and weight [21].

The initiative for main 270 V DC generation was first implemented in state-of-the-art military jets, such as the Lockheed Martin F-22 Raptor and the F-35 Lighting [50], and the Boeing-Sikorsky RAH-66 Comanche helicopter [141]. The F-22 does not power any flight-critical loads from its main DC system, therefore it maintains both 28 V DC and 115 V AC distribution systems [142]. The F-35 that followed features a greater 270 V DC architecture, with critical loads being powered from the 270 V DC system, and 270 V DC batteries, actuators, and emergency generation systems [142, 143]. The vaster utilisation of a higher-voltage DC architecture for all load types, flight-critical or not, was attributed to technology maturation and risk reduction processes [144]. As with any new technology however there were teething problems, with several test planes experiencing electrical faults, ranging from electrical shorts disabling flight controls [145], to a fleet-wide grounding after an in-flight dual generator failure [146, 147].

In civil aviation, the state-of-the-art in all-DC aircraft is represented by the Dassault Falcon 7X, a three-engine business jet which first flew in 2005 [148]. Its electrical system consists of three engine-driven 28 V DC brushless generators, two 24 V DC batteries, two permanent magnet alternators and a RAT, resulting in a total of eight potential DC power sources [149]. Granted that a relatively small passenger aircraft such as a business jet has low electrical demands, this permits the use of low-voltage DC distribution and SSPCs for electrical protection, without a significant increase in weight [150]. To further aid the electrical protection of the system, the left and right buses are segregated throughout the flight, and the generators are automatically disconnected from the network in case of under/over-voltage conditions.

The implementation of multi-shaft power offtakes and power transfer between shafts requires paralleling generators operating at different fundamental frequencies [151, 152]. The generation sources could be more feasibly interconnected within a DC system architecture in a more efficient and lightweight manner [153-155]. Higher voltage DC distribution may provide a more feasible route for paralleled generation,

the use of which is growing within MEA and MEE systems for a number of reasons [67].

DC distribution eliminates the need for frequency and phase synchronisation, therefore the paralleling of non-synchronous power sources can be better facilitated, and also promotes a reduction in cable size and weight [156]. Research has shown that in comparison with an AC system, a DC architecture may provide a more efficient electrical network [31, 157], partly by allowing the generators to run at more efficient operating points [9], and by reducing the number of power conversion stages between source and load [156]. Granted the potential benefits offered by DC distribution for parallel systems, an interconnected DC electrical architecture will be the main platform studied within this thesis.

3.4 Review of relevant literature

To date, the academic literature on parallel generation has mainly focused on three key topics, the benefits afforded by interconnected generation architectures, novel converter and load-grouping topologies, and relevant power/generator control strategies, all examined under normal operating conditions. However, the system-level impact paralleled generation may have under abnormal operation conditions is not well documented and the proposed designs do not address the certification implications of airworthiness standards and requirements. In particular, the voltage disturbance during an electrical fault could potentially propagate throughout the entire network and lead to a breach of the power quality requirements, as Chapter 4 will illustrate.

Chang and Wang in [100] propose a power distribution architecture, shown in Fig. 12, with two parallel conversion subsystems, implemented via bi-directional VF-CF power converters. A portion of the generated variable-frequency AC power is fed through the bi-directional converters and the outputted constant-frequency power is

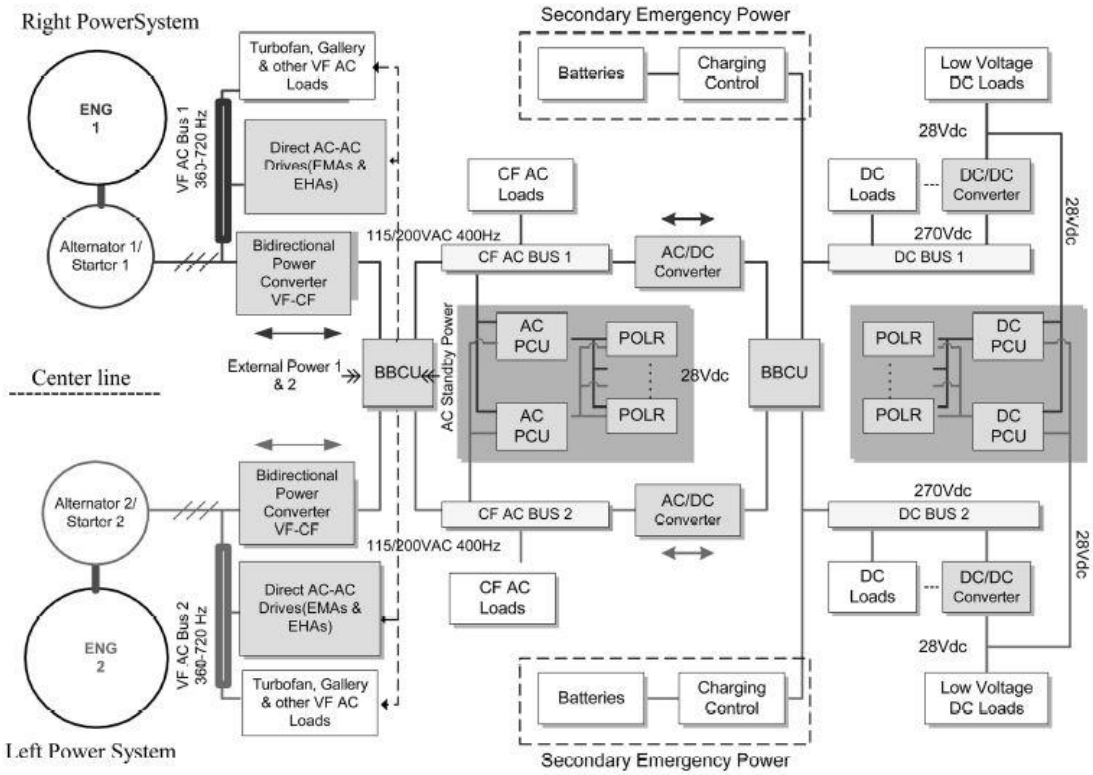

Figure 12. Power distribution architecture utilising bi-directional power converters [100].

distributed to loads grouped according to their voltage and frequency requirements, before being rectified to power the 270 V and 28 V DC buses. Although there is mention of the power quality requirements in this research, it is carried out with respect to input current harmonics and total harmonic distortion. Additionally, one of the candidates studied to act as a bi-directional converter includes the cycloconverter, a device that was shown to be unreliable in previous aircraft models (MD-80, B737).

Reference [158] relates to a 230 V AC aircraft supply system comprising of different generators, where the combined generator output is rectified to ±270 V DC by an AC/DC converter and then distributed to distinct load zones via paralleled power modules. Electrical protection is implemented via switching matrices which reconfigure the contactors in the event of a power module failure. In this implementation however, having all the generated power passing through a single converter creates a big reliability issue, and additionally, a disruption or fault in the AC supply will disrupt the entire power network.

In reference [159], Michalko proposes a multi-shaft off-take method in which the outputs of the engine-driven LP and HP generators are paralleled onto a common DC bus. The power mix is then managed by control of the terminal voltage of each machine. Although this is potentially the simplest multi-shaft offtake arrangement, its most significant drawback is that a fault on the DC bus will result in the loss of supply to all generators.

In a similar approach, Yue e*t al.* [160] propose the paralleling of all generators onto a common DC bus, illustrated in Fig. 13, where each GCU controls the power share of each generator. A supervisory controller responsible for power allocation amongst generators then controls each GCU in accordance with electrical loading/demands. Although contactors or other protection devices may provide some fault isolation capabilities, a fault on the common DC bus will disrupt all generation sources across the network. The same disadvantage can be seen in [161], where the left and right primary HVDC buses are interconnected.

For the DC distribution system in [162], SSPCs are installed as bus-ties between HVDC segments of the power network. In this embodiment, the bus-ties are usually open, however they are activated under emergency operating conditions, i.e. loss of power source, thus allowing power from one HVDC bus to flow to the adjacent HVDC bus. As this implementation is designed for emergency-mode operation and not for normal operating conditions, it does not address the 'normal' certification requirements.

Other offtake methods which seek to achieve power transfer between shafts, such as [163, 164], although differ in their implementation approach, assume normal engine operating conditions and do not consider an on-engine electrical fault. Overall in the literature, relevant patents seem to offer significant gains with respect to engine operability and fuel-burn reduction, however they do not address the certification implementations regarding protection methods and the interconnection of power sources.

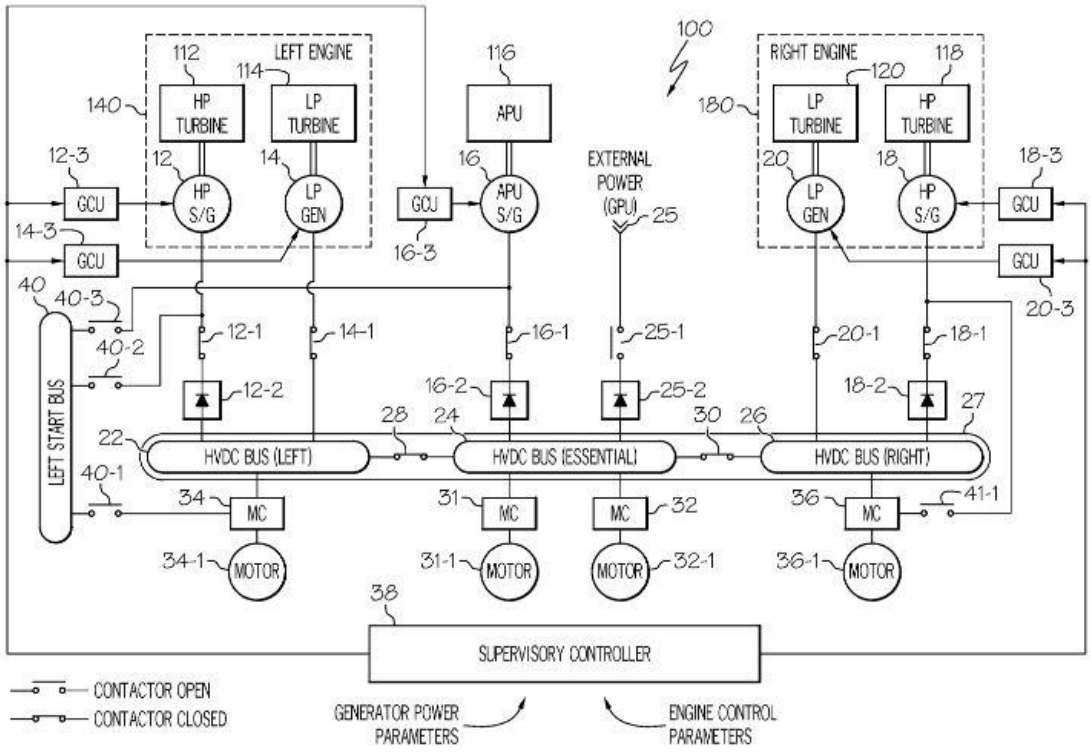

Figure 13. Paralleled HVDC bus electrical power system [160].

Research into novel distribution systems [165] and generator control strategies [151] address the MIL-STD-704F power quality requirements, however they do so on a component level under normal operating conditions. Although Muehlbauer and Gerling [151] do consider three different fault types, loss of generator current control, loss of a generator and current mismatch between generator and load, they are not indicative of abnormal operation conditions as defined in the power quality requirements.

Abdel-Hafez in [31] reviews four ‘fault-tolerant’ distribution system topologies for MEA, two of which implement an interconnected generation approach to some degree, as all generated power is either connected and supplied through the ‘primary power distribution system’ or via switch/load matrices. However, in all but one of the topologies reviewed, a fault in the distribution system may interrupt power supply across the entire network.

Reference [166] investigates control, power management and stability in a multi-generator power system, where generation sources are paralleled onto a common DC

bus. Herein, the performance of droop, voltage and current control modes are assessed in terms of power/load sharing, under a fault scenario which consists of a single power-source outage. This research addresses the steady state AC voltage limits of MIL-STD-704F in its fault scenario, however these are by definition the normal operating condition AC voltage requirements.

In contrast, DC abnormal operation condition limits are more challenging to adhere to for several reasons. DC system faults can present very demanding protection challenges with regards to fault-current magnitude and propagation speed, compared to faults within AC systems [167, 168]. To mitigate these issues, converter designs have evolved to provide more fault ride-through capabilities and current limiting to supress fault magnitude [169-171]. However, the use of current limiting could disrupt the coordination of network protection devices as many fault locations could present similar fault current. To overcome this problem, protection devices are often time-graded, thus operating at a slower protection speed, leaving the electrical network exposed to fault conditions for a larger time period [170, 172-174]. In turn, this would further disrupt power supply and power quality to flight-critical loads throughout the network.

Overall in the current literature, the protection challenges and requirements of an interconnected network at a systems-level have received little attention. Whilst a small part of the literature/research has taken under consideration the power quality requirements under normal operating conditions, the implications of paralleled generation schemes under abnormal operating conditions are not well documented. This is an important area as MEA/E are demanding ever-increasing amounts of electrical energy to power an ever-increasing multitude of loads, several of which are flight-critical and safety-essential. To meet this demand, MEA/E electrical generation systems are getting larger and more complex, however this in turn increases the stress on the aircraft electric system in terms of power handling, fault tolerance and reliability [66]. Consequently, interconnected MEA/E power networks require novel protection schemes and innovative distribution architectures capable of meeting the stringent power quality requirements under normal and fault conditions.

3.5 Chapter summary

This chapter reviewed the state of interconnected generation in the past and present aviation industry and presented the challenges associated with paralleled architectures. These challenges include adherence to airworthiness standards and regulatory power-quality requirements, as well as limitations within the current field of protection devices. It identified that the key challenge prohibiting AC interconnection options is the variable-frequency output of novel MEA/E generators, which does not feasibly permit the direct paralleling of generation sources.

It also identified key technological drivers that may provide a more feasible route for the implementation of paralleled DC architectures, including efficiency gains that could be afforded by utilisation of multi-shaft power offtakes and the growing use of DC distribution in airborne platforms. Lastly, it summarized the benefits and drawbacks of proposed interconnected approaches in the relevant literature, and also illustrated that the system-level impact paralleled generation may have under abnormal operation conditions is not well documented. Moreover, it illustrated that the certification implications of airworthiness standards and requirements are not addressed by proposed designs.

Chapter 4

DC Network and Simulation Analyses

This chapter will present the paralleled two-, three- and four-bus DC power networks considered in this thesis and investigate the behaviour of each interconnected system under fault conditions. This study will show that solid short-circuit faults can breach certification requirements and potential solutions to this issue will be presented. Each of the three solution options considered is a representative example of different mitigation approaches, and include solid state switching, current limiting and smoothing filtering. To examine the viability of each potential solution approach, software models of a solid state power controller (SSPC), a current limiting diode (CLD) and a smoothing filter are developed. Simulations will show that the SSPC and the CLD do not appear to achieve voltage compliance when used as a bus-interconnecting mechanism, whilst a suitably designed smoothing filter has the potential to stabilize the voltage within the defined limits.

4.1 Selection of interconnection level

As discussed in Chapter 3, the main focus of this thesis is a 270 V DC interconnected power network. As MEA/E are equipped with variable-frequency AC generators, the only logical approach to feasibly achieve any interconnection options would appear to be at a DC level. This section will briefly justify why a 270 V DC interconnection option was chosen as the main research platform over a 28 V DC interconnection option.

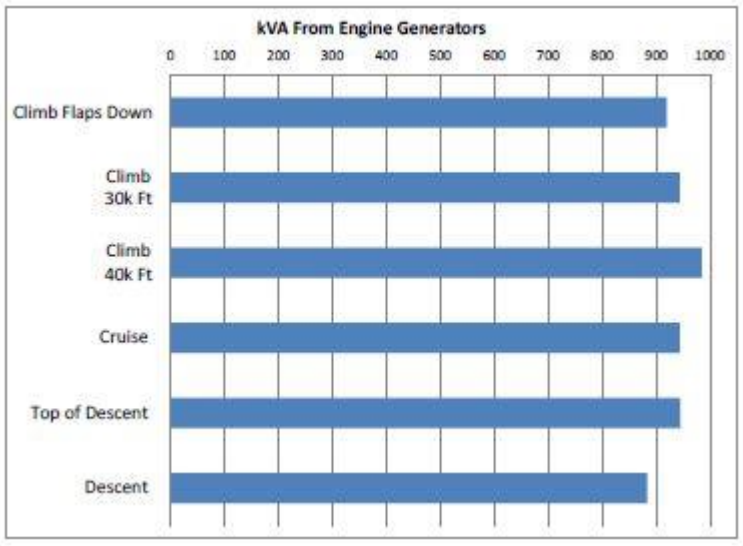

Figure 14. Electrical loading on B787 generators during different flight phases [175].

Table I. Bus loadings of B787 during cruise conditions [175].

Bus:	**230 V AC**	**±270 V DC**	**115 V AC**	**28 V DC**
Loads (kW):	Ice protection 60	ECS/Pressurisation 320	ICS 40	Flight Controls 14
	Galleys 120	Hydraulics 40	Various 140	Various 20
	Fuel pumps 32	Cooling equip. 40		
	Forward cargo AC 60	ECS fans 32		
Total Bus Loading (kW):	272	432	180	34
Total demanded power: 918 kW				

Fig. 14 shows the electrical power requirements of the B787 during major segments of its flight profile. It can be seen that the electrical demand on the generators is relatively constant throughout the various segments. In general, an aircraft spends the larger portion of its flight profile under cruise conditions, and specifically for the B787, at cruise conditions, the ±270 V DC bus is the most loaded bus-level, as can be seen in Table I. From the 918 kW of the total electrical demand, 432 kW are needed at the 270 V DC level and 34 kW of power are needed at the 28 V DC level.

In terms of percentage, it can be seen that approximately 47% is converted to ±270 V DC, and only 3.7% of power is rectified to 28 V DC. Therefore, any benefits afforded by the interconnection of buses could be better taken advantage of at the 270 V DC level.

On the other hand, the 28 V DC bus powers directly a greater magnitude of loads, approximately 150 compared to the 10 loads powered through the ±270 V DC bus (see Fig. 5) [32]. These loads however include avionics and flight displays, which require relatively low amounts of power, in the region of a few tens of kilowatts, and feature built-in redundancy such as power bus switch-over. Also, by ATRU oversizing (as on the McDonnel Douglas F-18, the Boeing 727 and 737) adequate power can be made available to 28 V DC loads in case of an ATRU failure by existing units. In the B 787's network, an ATRU malfunction requires that the essential loads of the respective DC bus be powered by secondary circuits built-in for redundancy, while non-essential loads would be shed.

Lastly, in case of a 115 V AC bus failure or emergency, critical AC and DC loads are powered by the 28V DC bus via DC/AC and DC/DC power converters respectively [176]. Therefore, it can be argued that by strengthening the 28V DC bus, with regards to security of supply achieved via interconnection, the network may potentially perform better in case of an emergency. These types of emergencies however occur relatively rarely in comparison with the amount of flight-time an airplane spends in cruise conditions. Consequently, for the reasons mentioned above and also for those in Chapter 3, the primary interconnection focus in this study will be at the 270 V DC level.

4.2 DC Network models

For a quantitative evaluation of the effectiveness of potential solutions for the attainment of voltage-regulations compliant DC interconnections, two-, three- and four-bus DC power networks have been realized using the Matlab/Simulink software

package. The two-bus DC network is representative of a partially-interconnected system, i.e. an on-engine DC-distribution interconnection of a more-electric engine, whilst thee- and four-bus networks are more indicative of multi-channel engine systems and fully-interconnected aircraft systems. This section will present the modelled power networks and address the rationale under which the software models and simulations were designed and carried out.

4.2.1 Methodology and design approach

As stated in Chapter 3 (Section 3.2.2), the power quality requirements for aircraft electrical systems set out in MIL-STD-704F do not distinguish between interconnected and isolated generation systems. In contrast to isolated power networks, a transient event developing within an interconnected system may propagate across the entire aircraft power network, disrupting flight-critical and flight-safety loads. The reduction in the level of isolation within the electrical system presents an even bigger issue especially for MEA/E, as an ever increasing number of loads and aircraft/system functions are electrically powered. Therefore, it would seem logical that during a large transient event, i.e. electrical fault, the non-faulted segments of the power network should adhere to the stricter non-faulted condition requirements, which are defined in the standards as the 'normal transient limits' (Fig. 10), whilst the faulted segments of the power network should adhere to the 'abnormal transient limits' (Fig. 11).

However, as power networks become more interconnected, defining which segments can be classified as faulted and non-faulted may be challenging. To overcome this issue, the analogy of the radial network paradigm was adopted. In an isolated radial network, a transient event or fault midstream can affect units and devices upstream and/or downstream, in a vertical manner, but it will not affect any adjacent radial systems in a horizontal manner. This approach will form the basis of the interconnected network segmentation into faulted and non-faulted sectors. Therefore, a faulted segment constitutes all the affected buses that are connected vertically, whilst non-faulted segments are defined as the remaining sectors of the power

network that are connected horizontally. This is illustrated in Fig. 15 for a four-channel interconnected system, where a fault on DC Bus 2 renders the respective vertical sector ‘faulted’, whilst the horizontal segments of DC Buses 1, 3 and 4 are considered to be ‘non-faulted’.

In effect, this approach dictates that during an electrical transient or fault, the faulted bus or portion of the power network adheres to the abnormal operation limits, whilst adjacent interconnected (in a horizontal manner) buses or portions of the power network remain compliant with the normal operation limits for the duration of the fault and until system recovery. This interpretation of the power quality requirements with respect to the peculiarity of MEA/E will be the foundation stone of the simulation studies carried out in this chapter.

An initial prerequisite for the design and modelling of a main DC architecture is the definition of the rated power of the 270 V DC system. Typically, such detailed sub-system information is proprietary, especially with new civil aircraft. However, it was stated earlier that the ±270 V DC loads of the B787 at cruise conditions demand 432 kW, and it is known that a variant of the Lockheed Martin F-22 has a ±270 V DC generation capability of 165 kW (Section 2.3). It was therefore decided to use the approximated mean of these two values as an arbitrarily-set rated power value. Consequently, all three modelled power network architectures were designed with a total rated power of 300 kW.

As the basic principle of this research is to assess voltage compliance of an interconnected power network during fault conditions, line-to-line short-circuits were chosen as the primary fault option. From a power quality perspective, this type of electrical fault is considered the most severe type of fault as it is characterized by low impedance, high fault current and extreme voltage profile deterioration (voltage collapse) [177, 178]. Other types of faults, i.e. high impedance or intermittent faults, are typically less severe, may cause transients that do not exceed predefined thresholds, and time requirements for fault clearing may be less strict [179]. Consequently, the impact of these faults on voltage compliance is expected to be less significant than for short-circuit faults.

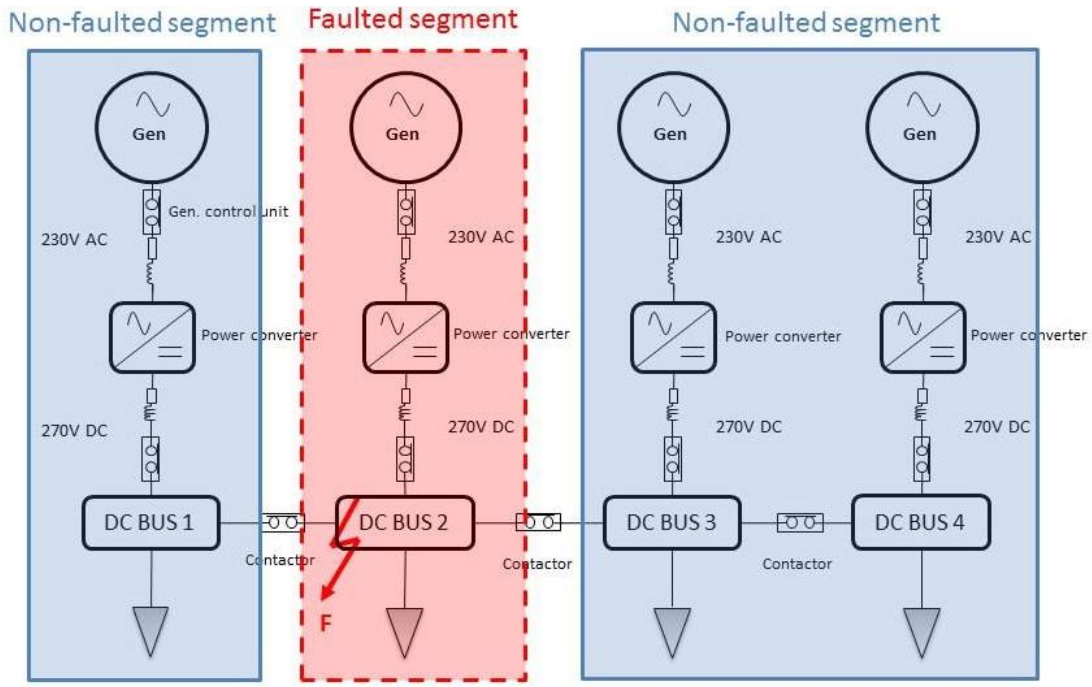

Figure 15. Definition of faulted segment (dashed, red line) and non-faulted segments (solid, blue line) in a multi-channel interconnected network for a DC Bus 2 fault.

To further increase the impact of the electrical fault introduced onto the power network, the short-circuit is introduced with the generation systems operating at full-load conditions. Additionally, a relatively large amount of capacitance has been installed in the power networks, which further worsens the current transient response of the electrical system during the fault. This is attributed to capacitive discharge, where due to the presence of the short-circuit, the energy stored in these larger capacitors is released into the system as fault-current. Consequently, this larger overall capacitance creates larger magnitudes of fault-currents than if less capacitance was installed in the power systems, therefore it adversely affects the performance of the network (i.e. voltage collapse).For example, in similarly rated converters as with those simulated herein, the filter capacitor is rated at 10 µF [180] or 100 µF [181], however filter capacitors in this study are rated at 10 mF. In the four-bus DC architecture therefore, a total of 40 mF of capacitance is made available only from the converters, without taking into consideration additional capacitive loads.

If less filter capacitance was installed in the simulated power networks, for example 10 µF instead of 10 mF, the current transients during the fault would be lower in magnitude for all architectures. As will be explained in more detail at a later section, the current transient directly affects the rating and size of the interconnecting solution options, subsequently smaller-rated interconnecting solutions would be required in this case. For the twin-bus DC network, it was estimated that the smaller filter capacitance would result in an 8% smaller interconnecting solution option for a fault-clearance time of 5 ms. Additionally, in comparison to the 10 mF capacitors, the smaller-rated 10 µF capacitors would expedite recovery of the bus-voltage to nominal levels after clearance of the fault, thus resulting in a network less stiff to voltage changes.

4.2.2 Modelling of components

The interconnected DC-architecture models created for this study were developed at a functional level of fidelity and accurately capture the initial transient response of the generation system [182]. These functional models neglect switching-level transients in order to minimise the computational burden and facilitate time-efficient extensive simulations, but still capture the power system and controller dynamics with sufficient fidelity. An overview of the different hierarchical levels of modelling fidelity is illustrated in Fig. 16.

The generation systems are comprised of permanent magnet machines representing 230 V AC HP and LP/IP generators, and are rated according to the number of generation sources and desired power rating for each architecture. By design, the HP and LP/IP turbine systems have different operational constraints, i.e. speed ranges, and different shaft rotational speeds [183]. Depending on the engine, an HP shaft may rotate between 9,000-14,000 rpm [184-186], whilst an LP shaft may spin at a lower range of 2,600-4,000 rpm [184-187] (with the IP shaft rotating at 5,000-9,000 rpm [185, 186, 188]). The amount of power produced by each compressor/turbine blade is proportional, but not limited to, the rate of gas mass flow and the speed of the blade [189]. Therefore the shaft power, and in turn the electrical power, produced

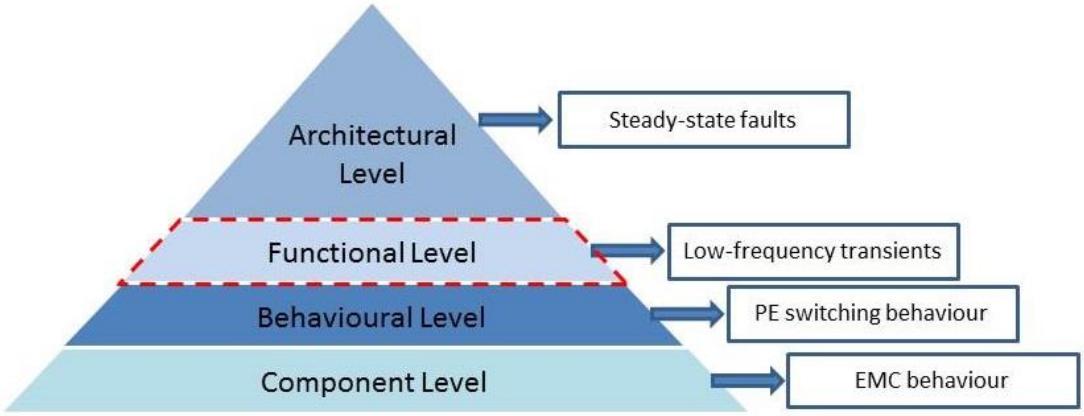

Figure 16. Hierarchical levels of modelling fidelity (adapted from [190]).

by the same electrical machine from the HP turbine is greater than that of the LP or IP turbine [191]. Consequently, for the simulations in this study, the LP generator will be rated to half the nominal power of the HP generator, unless stated otherwise.

The specification parameters of the HP and LP generator are summarized in Tables II and III respectively. The HP-generator variants are designed to produce 150 kW, 100 kW and 75 kW at 12,000 rpm for the two-, three- and four-bus DC architectures respectively. Similarly, the LP-generator variants are designed to produce 100 kW, 75 kW and 50 kW at 3,000 rpm for the two-, three- and four-bus DC architectures respectively. HP generators are designed with two pole pairs, whilst the less powerful LP generators are designed with 5 pole pairs.

The generation systems operate in parallel with drooped voltage control, explained in more detail in the next section, and are interfaced with controlled rectifiers. The purpose of the rectifiers is to provide 270 V DC from variable-speed AC generators, with variable terminal voltage. An additional requirement for the paralleled-generation computer models is that each converter must be capable of regulating its own voltage output to 270 V DC. To achieve this, two-level voltage source converters are used, consisting of six IGBT devices, and the output of these devices is regulated through voltage control. In the simulation results that will be presented however, the generators are loaded at 100% of their nominal power output with no further loads being switched on or off, thus the speed of the generators will be held

Table II. Specification parameters of HP generator model

Parameter	Value
Rated power	Variable 75 kW - 200 kW
Rated speed	12,000 rpm
Mechanical input	Speed
Stator phase resistance	19 mΩ
Stator inductance	102 µH
Pole pairs	2

Table III. Specification parameters of LP generator model

Parameter	Value
Rated power	Variable 50 kW - 100 kW
Rated speed	3,000 rpm
Mechanical input	Speed
Stator phase resistance	13 mΩ
Stator inductance	12 µH
Pole pairs	5

constant throughout the simulation, therefore it is not necessary for the rectifiers to vary their switching pattern to maintain the 270 V DC output.

The specification parameters of the rectifiers are presented in Table IV. The switching frequency of the six-switch voltage source converter is 5,000 Hz, with a DC link capacitance and inductance of 10 mF and 250 µH respectively. Lastly, the parasitic series inductance of the DC cable is 6 µH and the resistance is 4 mΩ.

A single power channel of the simulated architecture comprising of three-phase 230 V AC generation and 270 V DC rectification, along with corresponding control systems, is depicted in Fig. 17. The generator receives as input the engine shaft speed and closed-loop voltage control is employed to regulate the power output. Rectification is achieved via a two-level VSC, designed in a three leg, six switch configuration. To provide voltage control in average-value models, the PWM generator can be directly controlled by the reference voltage in order to achieve the desired 270 V DC output.

After rectification, the generated power is fed via DC buses to lumped loads, consisting of resistive and capacitive loads, forming a ‘DC bus’. For each DC architecture, the load resistance is varied according to the nominal generator output

and is 0.49 Ω, 0.73 Ω and 0.97 Ω for the two-, three- and four-bus architectures respectively. However, the capacitance of the bus loads is kept constant at 10 µF, due to the large amount of added capacitance at the terminals of the converters. The length of the main feeders was arbitrarily set to a quarter of the B787 length, i.e. 14.2 m, and the per-meter feeder resistance and capacitance was adapted from [182] accordingly. The implementation of multiple single power-channels enables the formation of multichannel architectures, which can be paralleled or isolated at the 270 DC bus level via ideal contactors.

Table IV. Specification parameters of rectifier models

Parameter	**Value**
Filter capacitance	10mF
Filter inductance	250 µH
R_{load}	4.1 Ω (300kW at 270V)
L_{line}	6 µH
R_{line}	4 mΩ
Switching frequency	5,000 Hz
Sapling frequency	20,000 Hz

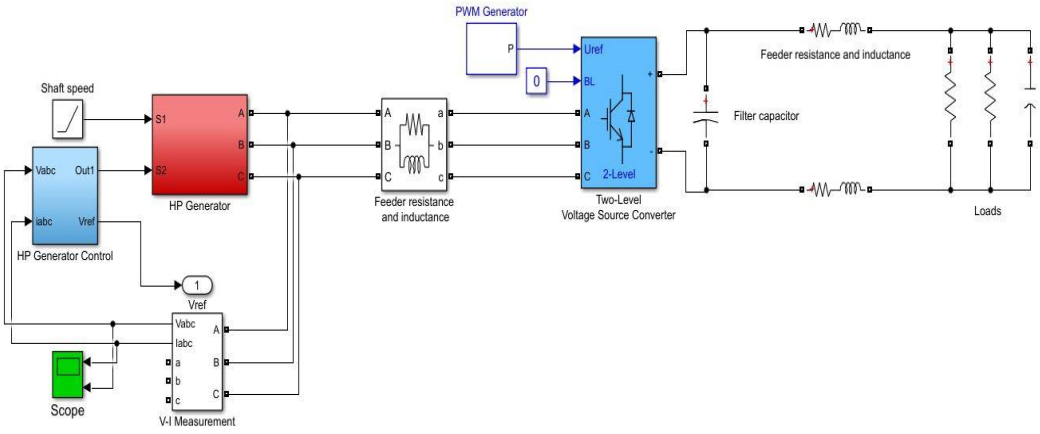

Figure 17. Single channel block diagram of simulation model featuring 230 V AC generation, 270 V DC rectification and DC bus loads.

4.2.3 Parallel generation regulation

For the required power network simulations, dual/plural generation sources are paralleled, therefore there is the need to efficiently control each generator power output. This is particularly important in the case of HP-LP paralleling where, as stated previously, the simulated LP generator is rated to half the nominal power output of the HP generator. Due to the mismatch in generator power output, independent control of the generation sources, whereas each generator individually regulates 270 V DC, may lead to excessive generation demands on the less powerful LP generator. Instead, a more fair distribution of electrical loading depending on generator capability can provide better use of generation capacity. Other means of power sharing control, such as current control, master-slave control and concentrated/distributed control require communication between generation units [192], and in turn this can lead to a reduction in system redundancy [193].

Voltage droop control however can function locally, without any communication between generation sources, and allows for a better exploitation of generator capacity whilst maintaining the level of system redundancy provided by voltage control [180, 194-197]. Therefore, voltage droop control was implemented to regulate the HP/HP and HP/LP generator power output under parallel generation conditions. Suitable droop control profiles are incorporated into their respective control systems, as described next.

To achieve parallel 270 V DC voltage regulation, each control system requires a voltage reference which the generation systems aim to achieve. This voltage reference can be derived from references [198-200] to be:

$$V_{Ref} = V_{Nom}(1 + a) - mP_{Gen} \qquad (1)$$

where V_{Nom} is the nominal voltage level, α is a constant governing the desired level of voltage control, the constant m represents the voltage/power gradient (slope of droop control) and P_{Gen} is the rated generator power. Numerical values for α vary in the literature between 0.012 and 0.06 [193, 201, 202], but given that tight voltage control is necessary for the 270 V DC loads, a value of 0.02 was selected. The

constant m can be calculated for both types of generators by setting in (1) V_{Ref} equal to V_{Nom}, when the generator is operating at half of its nominal power output, which gives

$$m_{HP} = \frac{aV_{Nom}}{\frac{P_{Gen_{HP}}}{2}} = \frac{10.8}{P_{Gen_{HP}}} \qquad (2)$$

$$m_{LP} = \frac{aV_{Nom}}{\frac{P_{Gen_{LP}}}{2}} = \frac{10.8}{P_{Gen_{LP}}} \qquad (3)$$

Lastly, for the specific generator power requirements of each architecture, the droop control profiles are finalized by inputting the appropriate generator power output in equations (2) and (3). In this implementation, the control systems aim to achieve a changing voltage reference instead of a constant 270 V value, in a manner dependant on generator capability. This way, parallel operation coordination is achieved, whilst at the same time allowing for better exploitation of generator capacity.

4.2.4 Twin-bus DC architecture

To investigate the behaviour of a partially-interconnected power network under fault conditions and the effectiveness of potential solutions to achieve voltage-requirements compliance, a paralleled twin-DC bus software model was created, shown in Fig. 18. Two variants of this model were designed, featuring HP/HP and HP/LP generation systems. For a total model power rating of 300 kW, in the HP/HP configuration both generators are rated at 150 kW, whilst for the HP/LP configuration, the HP generator is rated at 200 kW and the LP generator is rated at 100 kW. Interconnection of DC buses is achieved via an ideal switch acting as a contactor. The network model parameters are summarized in Table V.

For a behavioural analysis of an interconnected system during a fault, solid short-circuit faults of 1 mΩ fault impedance are introduced on DC bus 2.These external faults are ‘artificially’ introduced by shorting the terminals of the busbar using an ideal switch, producing in this manner the most severe type of fault response, but at

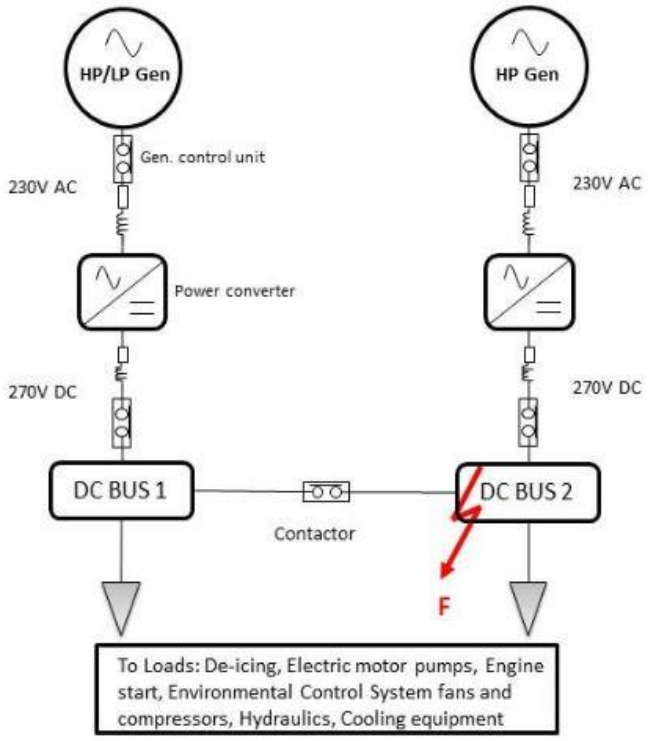

Figure 18. Representative single-line diagram of twin-bus DC architecture.

Table V. Network model parameters of twin-bus DC system

Parameter	**Value**
Rated power	300 kW
HP/HP generators	150 kW each
LP/HP generators	100 kW / 200 kW each
Operating voltage	270 V DC
Nominal current	555 A
Feeder resistance	0.801 mΩ/m [9]
Feeder inductance	0.65 μ/m [9]

the same time without isolating the faulted DC bus from the rest of the network. These faults are then cleared in a pre-set time margin by un-shorting the busbar terminals. The pre-set time margin, representing the fault-clearing time the protection system is capable of operating within, will vary for different simulation scenarios. In this manner, the effect of different fault clearing times on the network voltage can be investigated, as will be illustrated at a later section.

Fig. 19 depicts the baseline voltage profile of the non-faulty, or healthy, DC bus 1 during a short-circuit on DC bus 2. The fault is applied at t=0 s and cleared at t=50

ms, realising a protection operation speed of 50 ms, indicative of an average CB as typically, CBs have a tripping time of 10 ms – 100ms [117, 203]. During this transient event, the simulated voltage (blue line) collapses to near-zero and then overshoots the compliant voltage breadth (red lines) once the fault has been cleared. Evidently, the simulated voltage profile of the healthy bus exceeds the bounds of the normal voltage envelope defined in MIL-STD-704F.

Additionally, with a fault clearing time of 50 ms, it is clear that the protection system is not fast enough as to eliminate the fault within the initial, wider voltage area provided by the standards. This would suggest that any protection system designed for use on an interconnected network should have an operating speed of a maximum of 40 ms, the time after which the allowed voltage zone is reduced to the steady-state voltage limits, making voltage compliance even more difficult to achieve. In an attempt to derive a more useful baseline voltage profile, and thus provide the protection system with the possibility to clear the fault within the wider voltage zone, a simulation with a fault clearing time of 10 ms was carried out, indicative of a very fast CB. The baseline voltage profile of the healthy bus during the short-circuit is illustrated in Fig. 20. It is therefore apparent that even with a much faster CB, voltage compliance cannot be achieved.

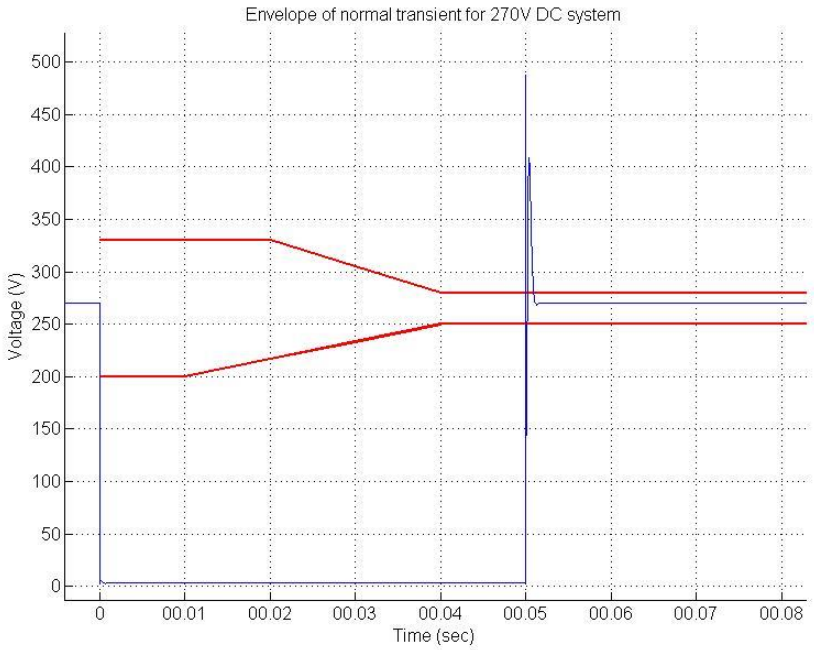

Figure 19. Voltage profile of the non-faulted bus during a fault with a fault clearing time of 50 ms.

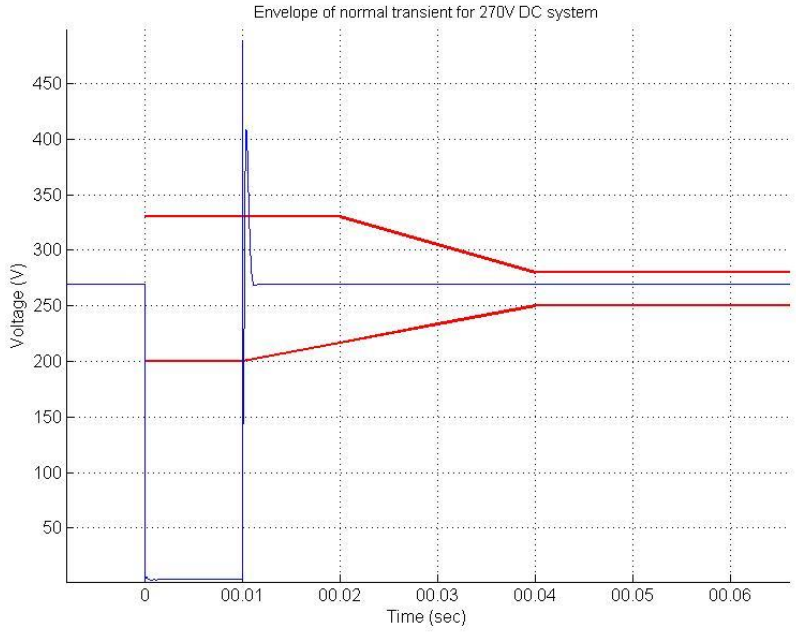

Figure 20. Voltage profile of the non-faulted bus during a fault with a fault clearing time of 10 ms.

4.2.5 Three-bus DC architecture

To study the behaviour of a more interconnected power network under fault conditions, a three-bus DC network was created, shown in Fig. 21. Two variants of this simulation model were built, the first one features three 100 kW HP generators, and the second one is comprised of two 120 kW HP generators and one 60 kW LP generator. The three DC buses are interconnected via ideal switches representing inter-bus contactors. The network model parameters are summarized in Table VI.

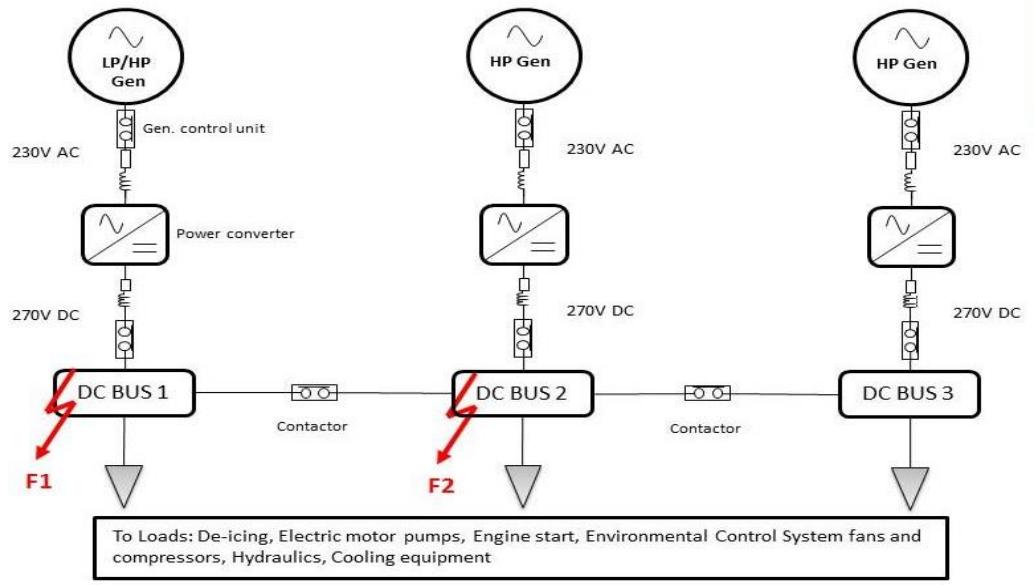

Figure 21. Representative single-line diagram of three-bus DC architecture.

Due to the symmetry of the network, only two fault locations are examined, DC bus 1 and 2. For each individual fault location, a short-circuit is introduced onto the network by shorting the terminals of the respective bus. The fault duration, representing the protection system's operation speed, will vary for different simulation scenarios, highlighting the effect of different protection operation speeds on the system/bus voltage.

During a fault on DC bus 1, the voltage profile of the non-faulted DC bus 2 is illustrated in Fig. 22. The fault is applied at t=0 s and cleared at t=10 ms, realising a protection operation speed of 10 ms. During this transient event, the voltage profiles

of the healthy interconnected buses have breached the power quality limits of MIL-STD-704F.

Table VI. Network model parameters of three-bus DC system

Parameter	Value
Rated power	300 kW
HP generators	100 kW each
LP/HP generators	60 kW / 120 kW each
Operating voltage	270 V DC
Nominal current	370 A
Feeder resistance	0.801 mΩ/m [9]
Feeder inductance	0.65 μ/m [9]

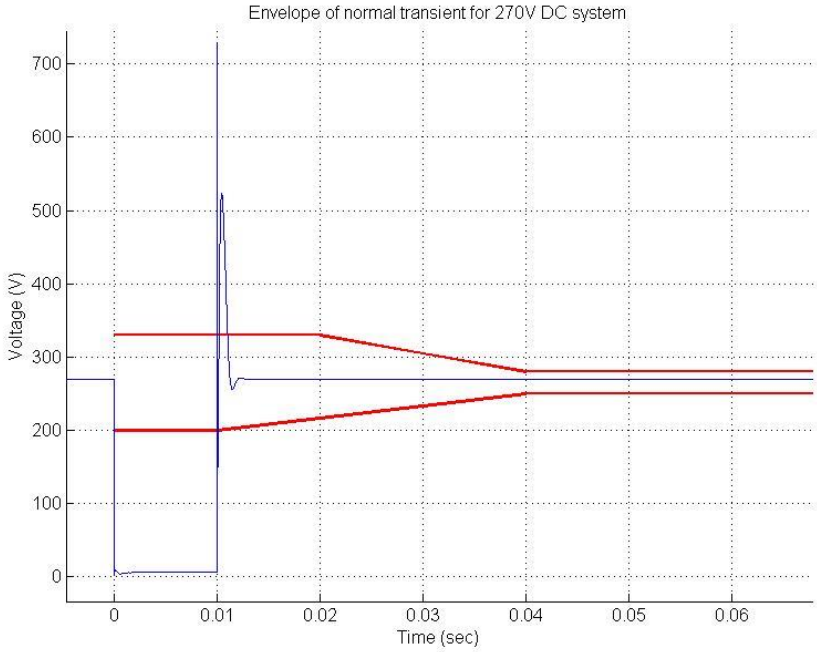

Figure 22. Voltage profile of the non-faulted bus during a fault with a fault clearing time of 10 ms.

4.2.6 Four-bus DC architecture

To assess voltage-envelope compliance of a fully interconnected power network under fault conditions, a four-bus DC network was designed, shown in Fig. 23.

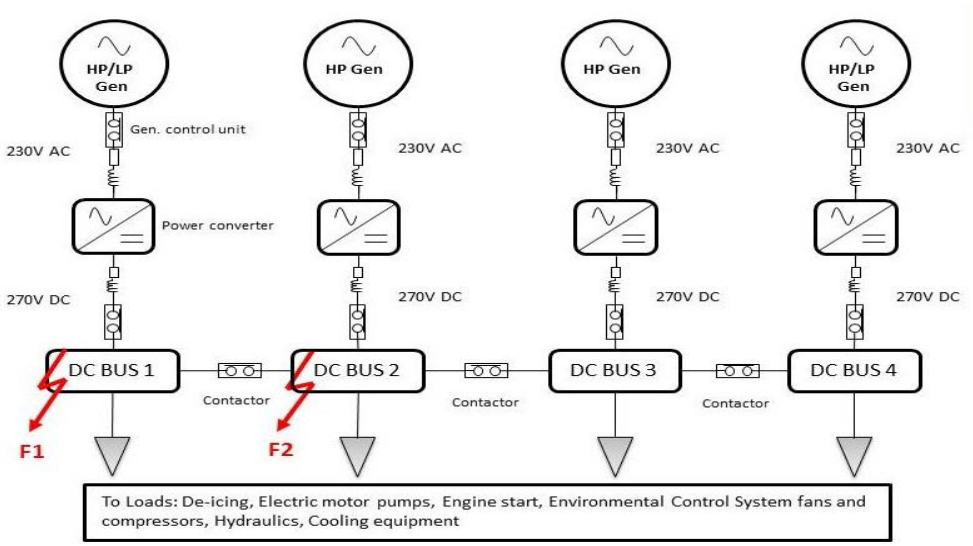

Figure 23. Representative single-line diagram of four-bus DC architecture.

Table VII. Network model parameters of four-bus DC system

Parameter	**Value**
Rated power	300 kW
HP generators	75 kW each
LP/HP generators	50 kW / 100 kW each
Operating voltage	270 V DC
Nominal current	278 A
Feeder resistance	0.801 mΩ/m [9]
Feeder inductance	0.65 µ/m [9]

Again, two variants of the simulation model were created, the first featuring four 75 kW HP generators, and the second featuring two 50 kW LP generator and two 100 kW HP generators. The four interconnected DC buses are interconnected using ideal switches acting as contactors. The network model parameters are summarized in Table VII.

Due to the symmetry of the network, only two fault locations are considered, DC bus 1 and 2. Similarly, for each individual fault location, a short-circuit is introduced onto the network by shorting the terminals of the respective bus. The fault duration, representing the protection system's operation speed, will vary for different simulation scenarios, highlighting the effect of different protection operation speeds on the system/bus voltage.

During a fault on DC bus 1, the voltage profile of the non-faulted DC bus 2 is illustrated in Fig. 24. The fault is applied at t=0 s and cleared at t=10 ms, realising a protection operation speed of 10 ms. During this transient event, the voltage profiles of the healthy interconnected buses have breached the power quality limits of MIL-STD-704F.

For all simulated architectures, it has been demonstrated that the voltage profile of the healthy interconnected buses collapses to near zero during the low-impedance short-circuit. In general, the severity of an electrical fault depends on the magnitude of fault impedance, as the lower the fault impedance is, the higher the voltage drop is. Additionally, with negligible bus-tie inductance offered by the interconnecting contactors, the total impedance of the network is not capable of sufficiently limiting/suppressing the contribution of fault current from the paralleled generators. An additional issue with DC-system faults is the contribution of fault current from individual components such as converters, capacitors and feeders, which further worsens the fault-current transients [204]. In effect, low-impedance faults with negligible inter-bus inductance result in significant current transients and the unavoidable voltage collapse of the interconnected DC buses. Consequently, the impact/influence of the fault is transferred almost instantaneously to the non-faulted parts of the network.

The instantaneous transfer of the influence of the fault across the entire network suggests that traditional fault-clearance speeds of EMCBs may not be sufficient in protecting the healthy segments of the network from voltage collapse. Any increase in the speed of the protection operation system will result in a reduction of the duration of the transient, thus reducing the amount of time the voltage is at near zero, however it will not prevent the voltage level from collapsing in the first place. Voltage compliance to the normal power-quality requirements during a fault cannot be maintained if the voltage level cannot be stabilized at or above 200 V during the initial 10 ms from the onset of the fault.

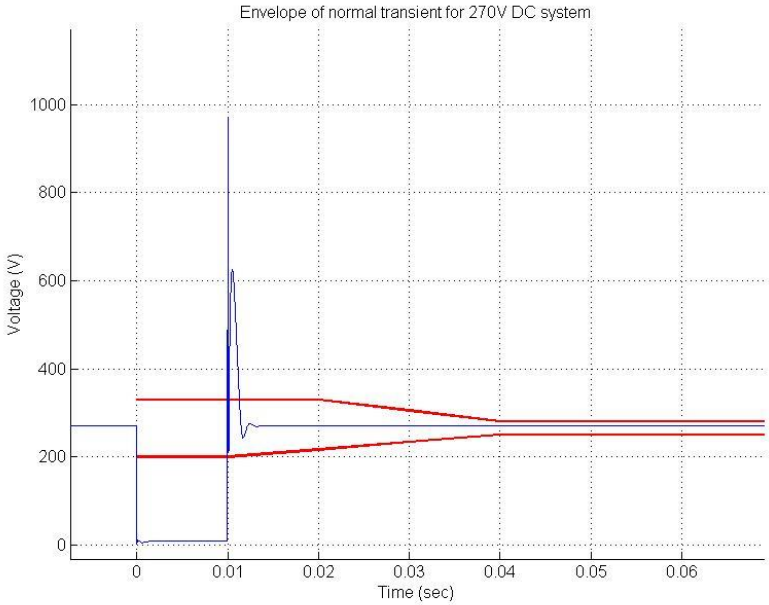

Figure 24. Voltage profile of the non-faulted bus during a fault with a fault clearing time of 10 ms.

To mitigate the voltage collapse of the non-faulted interconnected buses, means other than that of traditional protection appear to be needed, which can suppress the voltage drop in such a way that the voltage profile of the non-faulted interconnected buses does not exceed a lower-limit value of 200 V during the fault. In essence therefore, the voltage-transient fault responses of the non-faulted segments of the network must be decoupled to some extent from the fault response of the faulted segment of the power system. In this manner, the faulted segment of the system can adhere to the abnormal transient voltage limits, which permit a voltage collapse for up to seven seconds, and at the same time, the non-faulted parts of the system can retain compliance with the normal transient voltage limit.

4.2.7 Model validation

This section will briefly demonstrate that the simulation models presented within this thesis accurately capture the steady-state and transient behaviour of the 270 V DC system. For each DC architecture, a mathematical analysis was undertaken to

identify key system parameters to be simulated. First, nominal currents for all networks were calculated using the following equation:

$$I = \frac{P}{V} \qquad (4)$$

which then allowed the calculation of the overall resistance values for all networks using:

$$R = \frac{P}{I^2} \qquad (5)$$

where *P* is the rated power (W), *V* is the nominal voltage (V), *I* is the nominal current (A) and *R* is the required resistance (Ω).

For the two-bus DC architecture for example, it was calculated that in order for the HP generator to provide 150 kW of power at a voltage of 270 V, the nominal current output would be 555.5 A, a value almost identical to the 555 A of Table V with 0.49 Ω of total resistance. Similarly, the calculated nominal current for the three-bus architecture was 370.4 A, in comparison to the simulated 370 A, and for the four-bus network, the calculated nominal current was 277.7 A, in comparison to the simulated current of 278 A. Overall, although the key simulated parameters for the 270 V DC system were almost identical to the calculated values, the simulated AC voltage was 10 V higher than the nominal 230 V. This was attributed to the overall losses of the power network operating at full-load conditions.

Additionally, the electrical behaviour of the 270 V DC system from start-up to steady-state operation was considered to be acceptable. Fig. 25 depicts the current profile of the DC bus of the three-bus architecture during start up. Initially, the current is zero, but as the HP generator reaches 12,000 rpm, the current spikes to 400 A and then stabilizes at its nominal value of 370 A. Similar behaviour is exhibited by the voltage profile, shown in Fig. 26, where the voltage briefly peaks at 290 V before stabilizing at its nominal value of 270 V.

After the simulation model has reached stead-state operation, a low-impedance short-circuit is introduced at the terminals of one of the DC buses. Typical low-impedance faults are characterized by large fault-currents and extreme voltage deterioration

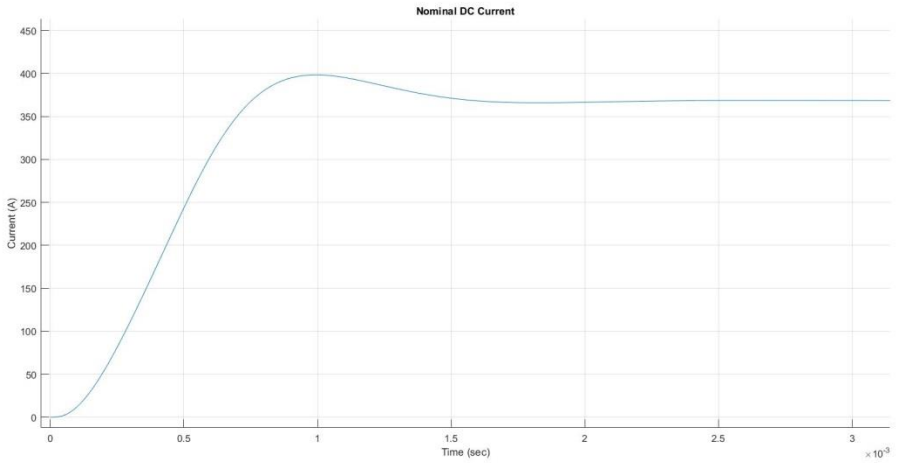

Figure 25. Current profile of healthy DC bus of the three-bus architecture during start-up.

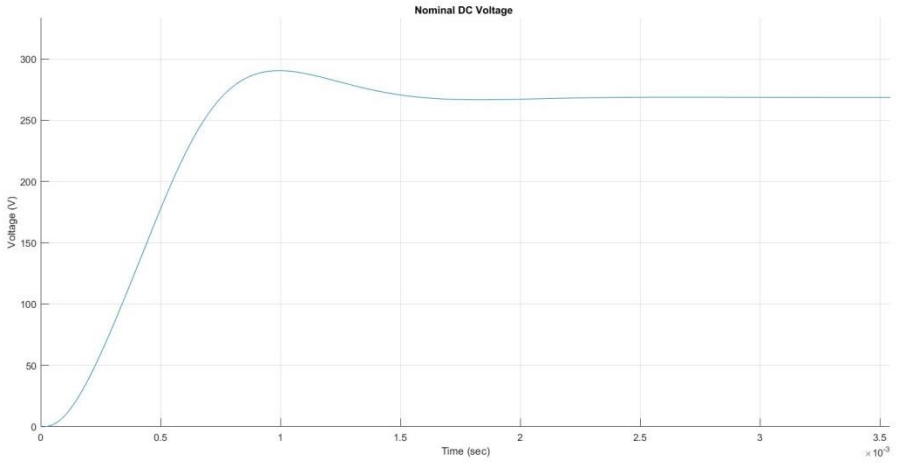

Figure 26. Voltage profile oh healthy DC bus of the three-bus architecture during start-up.

(voltage collapse) [177]. After the clearing of the fault, the voltage overshoots its nominal value and oscillates around it, before eventually stabilizing. Such behaviour is observed in Fig. 20, therefore the transient response of the 270 V DC system during and after the fault is believed to follow the expected trend.

4.3 Potential solutions for voltage compliance

In the previous section, it was shown that for all three simulated paralleled-generation architectures, an electrical fault on one of the DC buses forces the voltage profile to collapse across all interconnected buses. It is apparent that a fault on any DC bus propagates throughout the entire 270 V DC system, rendering all interconnected buses across the power network 'faulted'. Consequently, to achieve voltage-requirements compliance, there is the need to decouple to some extent the transient responses of the interconnected DC buses.

To this end, three interconnecting-solution approaches are considered. First, novel very fast-acting protection operation and fault clearing, as extremely fast protection speeds could potentially tackle the almost instantaneous propagation of current and voltage transients throughout the power network. Second, a current-limiting approach, as limiting the magnitude of fault-current transients, and therefore the voltage sag, could potentially maintain the bus voltage within permissible limits. Third, a smoothing filtering approach, in an effort to mitigate transient conditions by limiting the high current pulses and control the non-faulted bus voltages during the fault. To examine the effectiveness and feasibility of each potential solution function, a representative example of each approach was implemented, consisting respectively of:

- A solid-state power controller (SSPC)
- A current-limiting diode (CLD)
- A smoothing reactor

A solution consisting of a dual active bridge (DAB) DC/DC converter as a bus-interconnecting mechanism was also considered, mainly for its galvanic isolation capability, but was subsequently discarded for two main reasons. Firstly, due to high switching losses at light load conditions and high conduction losses (due to circulating currents) under heavy load conditions [205], and secondly, due to the complexity of control strategies across the whole power range and possible operating

conditions (power flow direction, emergency operation conditions) [206]. However, the behaviour observed for the three candidate solutions listed above can be extrapolated to determine the impact of a DAB based solution. The next section will assess potential compliance of candidate solutions with the power-quality requirements.

4.3.1 Solid state power controller

SSPCs are broadly considered to be the next generation in protection and load-management devices. In addition to providing power (voltage and/or current) control to supply a load, these semiconductor devices are capable of accurately monitoring power quality and load conditions, allowing the system controller to instantaneously react to power fluctuations and fault conditions [207]. Similarly to electronic circuit breakers, these devices can protect against short-circuits and overload conditions, however are faster at switching power off and are more reliable [208]. Smart, programmable SSPCs also permit power-management systems to adapt to arising fault conditions by isolating the faulted section and reconfiguring the power network. This feature may be very beneficial for interconnected systems, by feasibly realizing a dynamically-reconfigurable network depending on given operational power-system conditions.

An SSPC's main function is to switch a device or load on or out of a power network. In general, SSPCs offer i^2t protection, where power is cut off when the device senses that there is too much energy transfer, unlike circuit breakers that trip when the current reaches the tripping threshold. This allows an SSPC to achieve very fast power cut-off times, in the range of 3 µs – 10 µs [117, 209], depending on the power rating of the device. Current commercially available SSPC devices for 270 V DC appear to be limited to 80 A [210], with research and development going in to prototype ratings of 100 A [211] and 120 A [164], and with future industry targets of 300 A [212].

The nominal current levels in the two-, three- and four-bus DC architectures presented earlier, were 555 A, 370 A and 287 A respectively, far higher than any available SSPC's current rating. Although the power ratings of existing SSPC devices may be still lower than required for many applications, their fast operating speed and compact size may potentially make them ideal candidates for the protection requirements of future higher-voltage DC aerospace applications. In an effort to explore potential benefits arising from the use of an SSPC as a bus-interconnecting mechanism in order to feasibly achieve voltage compliance, a functional software model of such device was created and adapted to the power ratings of each DC architecture, shown in Fig. 27.

For all simulated architectures, Mosfet SSPC devices were installed in place of the pre-existing contactors, serving as bus-interconnecting mechanisms. The control system of each device was configured to operate within the normal voltage transient limits, with emphasis being placed on the 'turn off' specifications rather than the 'switch on', as the main focus of these simulations was to assess the appropriateness of the candidate solution to maintain voltage-profile compliance of the healthy buses during a short-circuit. To this end, the input voltage range was set to 200 V- 330 V and the drop-out voltage ranges were set for voltages below 199.99 V and above 330.01 V. i^2t parameter specification was carried out for each DC architecture, according to guidance provided within references [117, 120], and the most optimistic switching time of 3 μs was employed. These specification parameters used for all DC architectures are summarised in Table VIII.

The simulated voltage profile of the healthy bus in the twin-bus DC architecture is shown in Fig. 28. When the fault is applied, the low fault impedance causes the voltage of the healthy bus to collapse almost instantaneously, but quickly recovers after the operation of the SSPC. In comparison with Fig. 20, it appears that the voltage profile is qualitatively better, however the implementation of SSPCs does not help in maintaining the voltage within the permissible limits during a short circuit. Consequently, the use of an SSPC used in isolation as bus-interconnecting mechanism does not appear to be a viable option for voltage-requirements compliance.

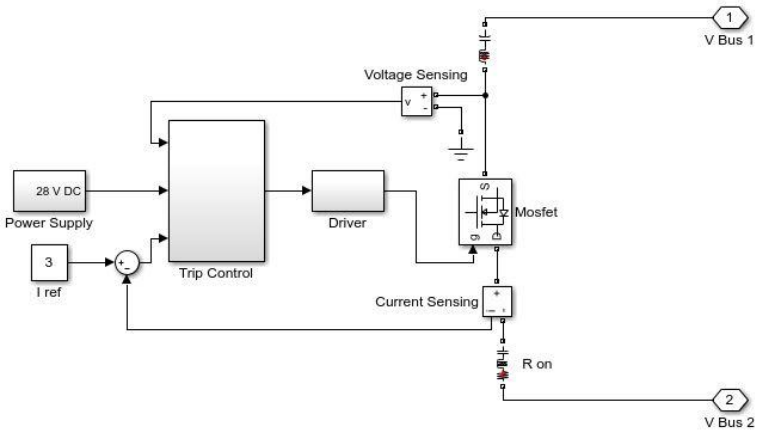

Figure 27. Block diagram and control of simulated inter-bus SSPC (Mosfet).

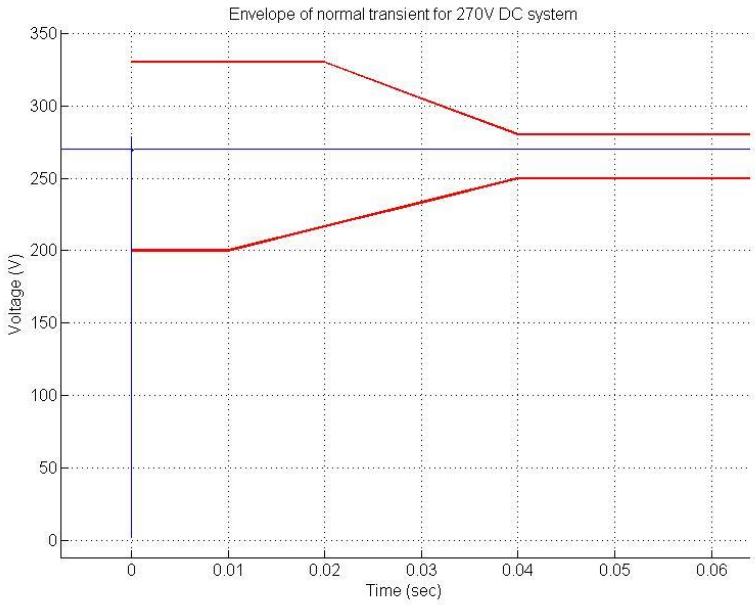

Figure 28. Voltage profile of the non-faulted bus during a fault with a fault clearing time of 3 μs in the twin-bus architecture.

Table VIII . Specification parameters of modelled SSPC devices for all DC architectures

DC Architecture	Twin-bus	Three-bus	Four-bus
Power voltage (V)	270	270	270
Nominal current (A)	555	370	280
Max. current (A)	1,665	1,110	840
Nominal power (kW)	150	100	75
Instant trip	I > 300%		
i^2t trip	110% < I < 300%		
Fall time	t_{fall} < 3 μs		

4.3.2 Current limiting diode

Current-limiting devices provide a means of reducing fault current to a certain level rather than it being regulated by the power network. Several benefits afforded from the implementation of such devices include reductions in circuit-breaker ratings and system-component stress during faults [9]. A current-limiting approach was implemented for the interconnection of the 28 V DC buses on the McDonnel Douglas F-18 (Fig. 6), although exactly what kind of the device was used is unknown. For the purposes of this study, a CLD was simulated as a bus-interconnecting mechanism, to assess whether current-limiting solutions can contribute towards achieving power-quality compliance.

A CLD is a silicon carbide JFET with the gate shorted to the source, functioning as a two-terminal current limiter. If a potential between the gate and the terminals is applied, the JFET will become more resistive to the flow of current, increasing the effective series resistance. Therefore it allows the current passing through it to rise to a certain value and then level off at a specified value. Additionally, a CLD can keep the current flowing through the device unchanged when the voltage changes.

After an extensive search in the literature, it was realized that a 270 V DC CLD with the desired current ratings of each interconnected architecture did not appear to exist. To overcome this issue, a 50 A CLD software model was created with guidance from [213, 214], and multiple CLDs were connected in parallel in-between DC buses to

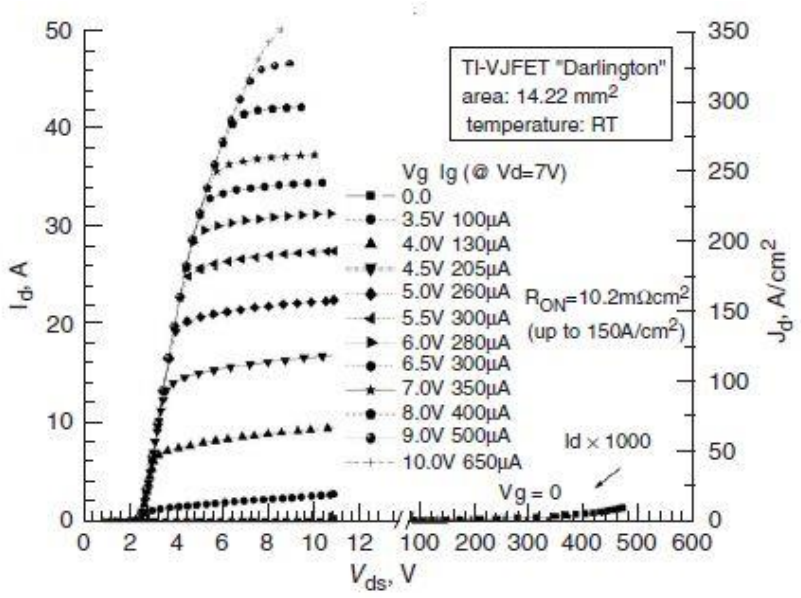

Figure 29. I-V data used as input for the controlled current source of the CLD [213].

achieve the required current limiting capability (for power ratings as stated in Table VIII for each architecture). The modelled CLD consists of a controlled current source which uses as an input I-V data from a lookup table, extracted from Fig. 29, and is shown in Fig. 30. Due to the inability to locate a suitably rated CLD and subsequently, accurate thermal data, temperature characteristics were not taken into consideration. Additionally, given the parallel connection of many smaller-rated CLDs, the heat dissipated by the CLDs would not have been representative, therefore a thermal model for such configuration was considered to be inaccurate.

Fig. 31 depicts the voltage profile of the healthy bus in the twin-bus architecture for a fault-clearing time of 10 ms using an interconnecting CLD. Again, the low fault impedance results in high fault-current which causes the voltage to drop almost instantaneously. In turn, the inter-bus CLD starts blocking the current transient almost instantaneously, which does not permit the voltage to collapse to zero, but instead be maintained at 80 V – 90 V throughout the duration of the fault.

From this simulation, it is evident that the implementation of CLDs does not appear to be an interconnecting solution that achieves voltage compliance, although the CLD did not allow the voltage to collapse to zero as in the case of the SSPC (Fig. 28). Also, an inherent disadvantage of CLDs is that they are unidirectional

components, allowing current to flow only in one direction. Consequently, anti-parallel CLDs would have to be implemented to allow power transfers between buses, either during normal operation of the power network, or in emergency situations potentially requiring network reconfiguration.

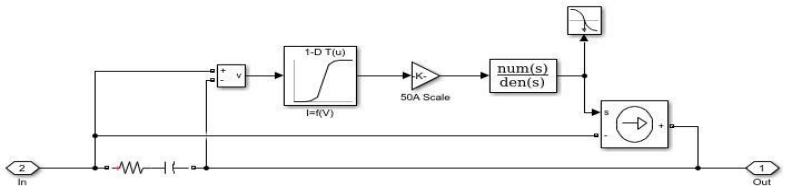

Figure 30. Block diagram of simulated CLD.

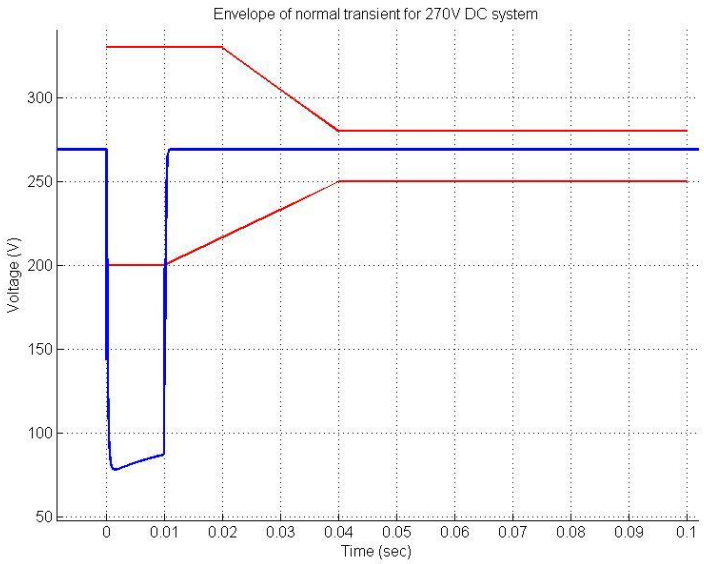

Figure 31. Voltage profile of non-faulted bus during fault with an interconnecting CLD.

4.3.3 Smoothing filter

Smoothing filters consisting of reactors and capacitor banks have successfully been used in high-voltage DC (HVDC) distribution networks to reduce current ripple and overcurrent transients, and prevent steep voltage waves and spikes [215-217]. Shunt capacitance also aids in lowering the harmonic content and distortion in DC lines, as

well as limiting the inrush current following the switch-on of large inductive loads [218, 219]. Although the current and voltage ratings of HVDC networks exceed those of MEA/E, the operating principle of smoothing filters remains the same, therefore it is worth considering them as a candidate solution for aircraft voltage compliance.

This approach can arguably receive further validation from a recent invention by Siemens, which utilizes smoothing reactors in DC distribution systems within ship power networks. A reactor, coupled with a very fast isolation switch, was chosen as a means to interconnect the main distribution switchboards on-board a novel class of more-electric, dynamic position marine vessels, as illustrated in Fig. 32 [220].

Similarly to the MEA concept, electrical-power equivalents are used to replace pneumatic, mechanical and hydraulic power transfer systems in different sea vehicles [221]. In this more-electric ship concept, the ship's propellers/thrusters are turned by inverter-fed electric motors that are powered from diesel-powered generators. Dynamic position vessels are designed on the principle that enough thruster power has to be available at all times to keep the vessel in the desired position, even in the event of a major part of the electrical system failing [222]. In the past, these requirements resulted in diesel-electric ships having two or more independent switchboard systems. In an effort to optimise performance, new designs enable the paralleling of switchboards during normal operation, however the systems are isolated during critical operations.

Interconnection of the main AC switchboards is achieved by a very fast solid state bus-tie breaker, the Intelligent Load Controller (ILS), which is believed to have a breaking time of 10 μs – 20 μs [223]. A suitable ILS for DC-breaking applications was also built, featuring the same breaking time for low-impedance faults, with nominal voltage and current ratings of 1,000 V and 2,000 A respectively [222]. As a design requirement, several ILSs may be paralleled to achieve greater power ratings. The very fast breaking time of the ILS, paired with the reactor's buffering ability, is thought to prevent the fault current from exceeding twice the nominal rating, therefore opening the possibility of parallel switchboard operation even during critical operations, such as dynamic positioning.

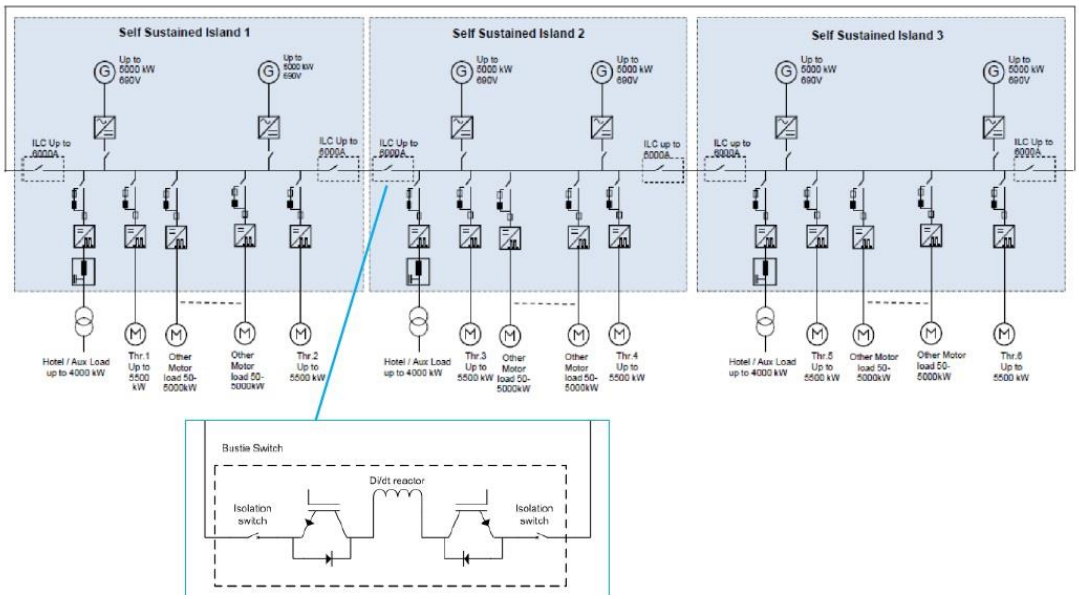

Figure 32. Typical Siemens diesel electrical propulsion featuring main DC distribution [220].

A candidate solution featuring a fast-breaking SSPC was trialled in a previous section, therefore this section will focus purely on the implementation of a smoothing filter acting as an interconnecting mechanism. A reactor is essentially an inductor, which is often fitted with a ferrous core to concentrate the magnetic flux lines, thus making the inductor more effective. In general, an inductor stores energy in the magnetic field induced by its coils and resists any change in current flow. Consequently, an increase in the rate of current flow will induce a voltage of opposite polarity to the applied voltage, ε_{ind}, given from the equation

$$\varepsilon_{ind} = -L\frac{di}{dt} \qquad (6)$$

where L is the inductance and di/dt is the rate of change of current flow through the inductor. Therefore, if an inductor was to be connected in-between two adjacent DC buses and either one experiences a short-circuit, the increasing rate of change of fault-current would induce a voltage that opposes the voltage drop on the healthy bus. Based on this principle, for the case study considered, an inductor is connected in-between two adjacent DC buses and a capacitor is installed parallel to the inductor, to provide shunt capacitance.

Due to the novelty of this approach within the MEA/E literature, arbitrary inductance and capacitance values of 1 mH and 10 mF respectively were used, but the same 10 ms fault-clearing time simulation was carried out as with other candidate solutions. The simulated voltage profile of the healthy bus during a short-circuit is depicted in Fig. 33. Evidently, the bus voltage is not maintained within the requirements-limits, however, the voltage does not drop below 100 V and there is no voltage-envelope overshoot upon fault clearance. This is attributed to the voltage of opposite polarity induced from the increasing rate of fault-current flow through the inductor, opposing the voltage collapse on the non-faulted bus. When the fault is cleared, the rate of current-flow through the inductor changes again, as no more current is passing through due to balanced operation conditions. Again, this decreasing rate of current flow induces a voltage which causes the bus voltage level to rise to 330 V, before stabilizing to the nominal value of 270 V. Overall therefore, this approach appears to show better potential compared to all other candidate solutions considered.

It is apparent that in order to decouple the transient responses of the interconnected DC buses, an effective smoothing filter is required. Deeper analysis may permit the identification of suitable inductance and capacitance ratings, for a smoothing filter capable of achieving voltage-compliant interconnections. In this implementation, although the voltage of the faulted bus will collapse, the non-faulted bus should only experience a voltage transient compliant with the power-quality requirements. The next chapter will focus on the design parameters of such a smoothing filter.

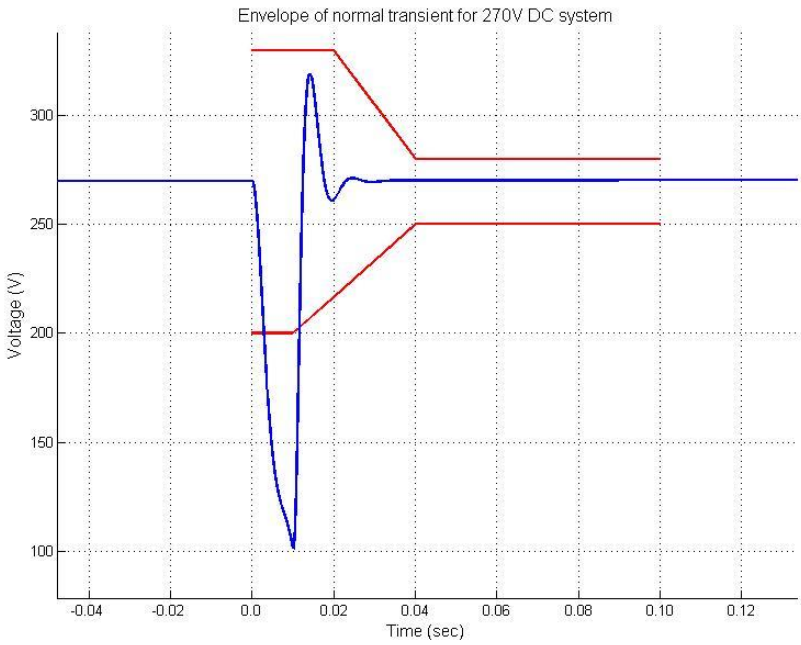

Figure 33. Voltage profile of non-faulted bus during fault with arbitrary smoothing filter.

4.4 Chapter summary

This chapter has presented the simulation models and the design rational of two-, three- and four-channel interconnected DC architectures that were analysed with regards to their fault response for low impedance faults. It was shown that traditional means of protection do not prevent the non-faulted segments of the power network from breaching the power quality requirements (voltage collapse) suggesting that to achieve voltage-requirements compliance, the transient responses of these segments must be decoupled from that of the faulted part of the system.

To this end, three solution options were considered, an SSPC, a CLD and a smoothing reactor, as a DC bus-interconnecting mechanism. From this assessment, it was concluded that despite the fast fault-clearing operation offered by the SSPC, the voltage collapse was not avoided. The implementation of the CLD aided in blocking the current transient, thus suppressing the voltage drop, however this was not sufficient as to allow the DC bus to maintain voltage compliance. Lastly, the smoothing reactor showed better potential compared to all other candidate solutions

considered, although the power-quality requirements were still breached. A deeper analysis that could permit the identification of suitable inductance and capacitance ratings for a smoothing filter capable of achieving voltage-compliant interconnections will be the focus of the next chapter.

Chapter 5

Implementation and impact of smoothing filter solutions

This chapter will focus on the design and implementation of effective smoothing filters, capable of achieving normal and steady-state voltage compliance for candidate DC architectures under full-load conditions. Simulations will show that shunt capacitance has an adverse effect of the bus voltage during an electrical fault, subsequently purely inductive interconnecting solutions will be pursued. It will be demonstrated that there two main variables which impact the size of inductance required to achieve bus-voltage compliance: the type of compliance required and the operation speed of the protection system. A mass estimation analysis will quantify the added weight penalty, and thus the feasibility, of the proposed inductive solutions. The apparent trade-off between the size of inductance and these variables will be highlighted, and adverse factors acting on these inductance ratings will be identified. Additional inductance ratings for partial generator loading will be presented, to exploit benefits afforded by load optimization schemes in interconnected power systems. It will also be shown that inductive solutions have the potential to influence architectural design and electrical machine selection. Lastly, the feasibility of the proposed solution approach will be examined on novel, parallel-generation network patents.

5.1 Designing an effective smoothing filter

In the previous chapter, it was shown that a smoothing filter has the potential to decouple the transient response of the interconnected DC buses during an electrical fault. Through simulation, this section will focus on the identification of suitable

design parameters for the desired smoothing filter, in order to develop an interconnecting mechanism capable of maintaining voltage compliance during a short-circuit fault. This analysis will initially concentrate on the twin-bus DC architecture, and potentially meaningful conclusions will be transferred onto the three- and four-bus networks. To permit a normalized comparison across architectures, the equally-rated HP variants of the architectural simulation models will be investigated first. LP-generator software models and their influence on the necessary smoothing filters will be analysed in a later section.

To maintain voltage compliance during a fault, an effective smoothing filter must perform two main functions. First, possess the buffering ability that does not allow the voltage to drop below a minimum value of 200 V during the initial 10 milliseconds from the onset of the fault, and second, ensure that the entire bus voltage profile stays within the defined voltage-area limits (Fig. 10). To investigate the potential feasibility with regards to the first main function of the filter, and thus identify the required inductance and capacitance ratings for the reactor and filter capacitor respectively, extensive combinations of values were simulated. The range of inductance and capacitance values simulated was from 0 mH to 40 mH and 0 mF to 40 mF respectively, in 1 μH/μF increments. Additionally, the fault-clearing speed of the protection system was varied in order to simulate different protection strategies and assess below which fault-clearing time this approach is potentially viable.

Figures 34 to 38 illustrate the minimum sensed voltage of the non-faulted bus during a short-circuit that is cleared within 50, 25, 10, 5 and 1 ms respectively. Each voltage value (z axis) of the surface plot corresponds to a distinct pair of capacitance (x axis) and inductance (y axis) values, and depicts the lowest voltage sensed on the non-faulted bus during the electrical fault, by using these capacitance and inductance values as reactor ratings.

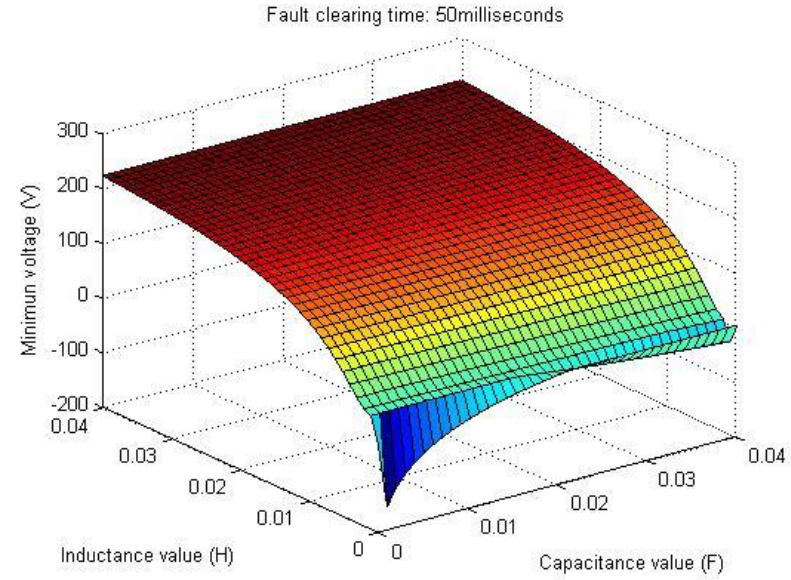

Figure 34. Minimum sensed voltage of interconnected non-faulted bus during a fault for varying filter inductance and capacitance values for a 50 ms protection operation speed.

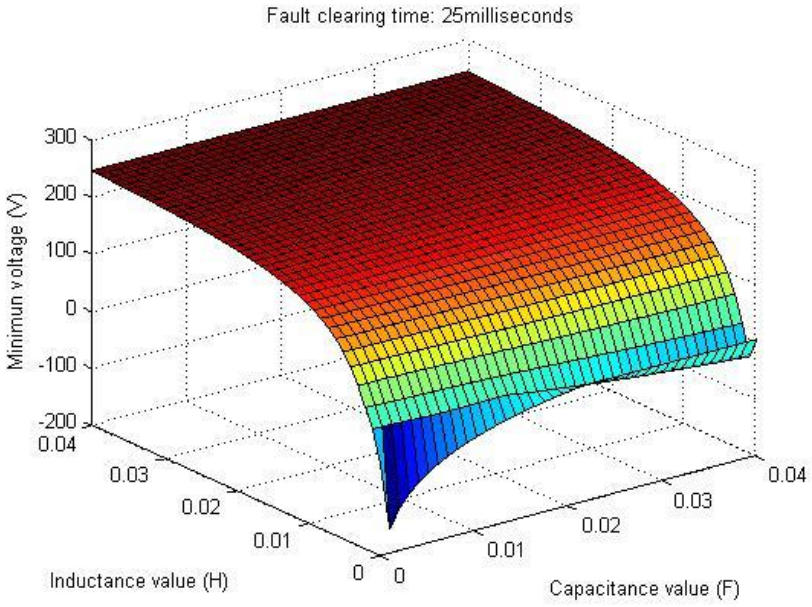

Figure 35. Minimum sensed voltage of interconnected non-faulted bus during a fault for varying filter inductance and capacitance values for a 25 ms protection operation speed.

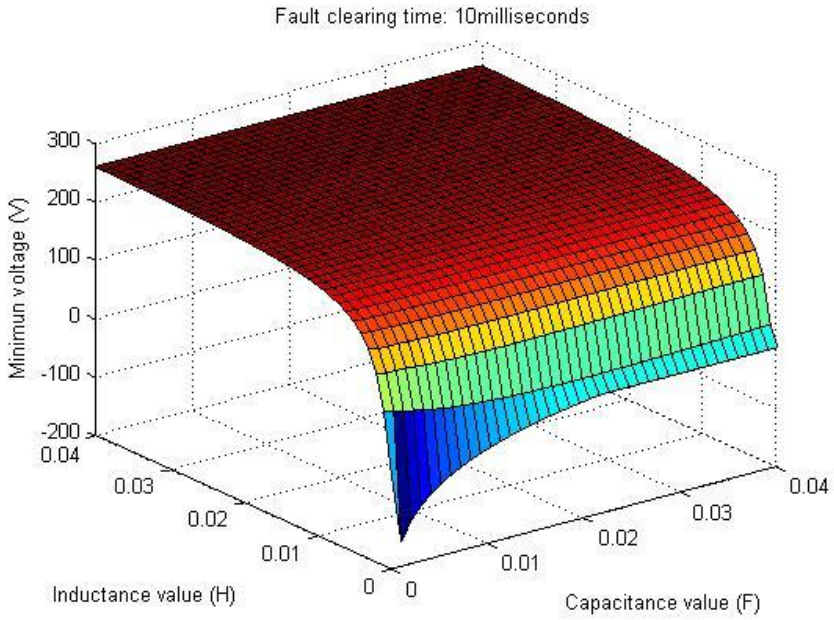

Figure 36. Minimum sensed voltage of interconnected non-faulted bus during a fault for varying filter inductance and capacitance values for a 10 ms protection operation speed.

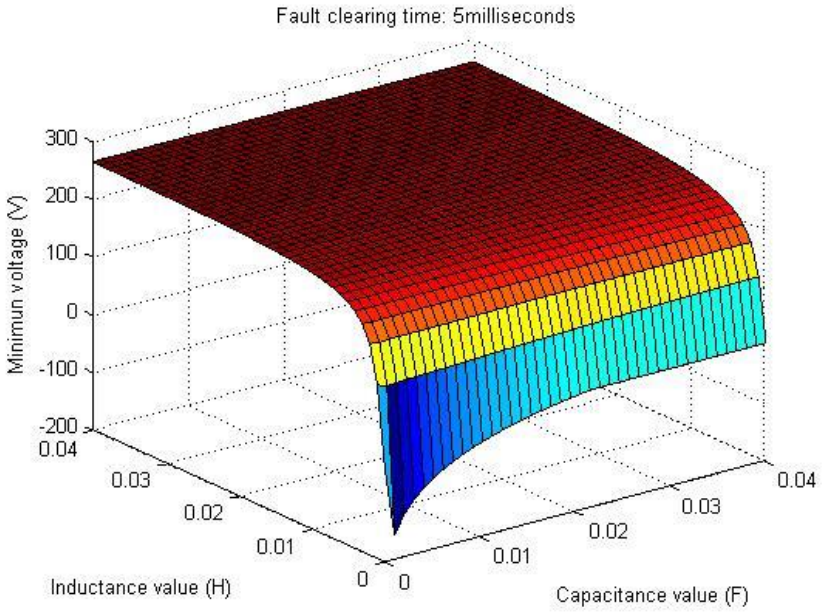

Figure 37. Minimum sensed voltage of interconnected non-faulted bus during a fault for varying filter inductance and capacitance values for a 5 ms protection operation speed.

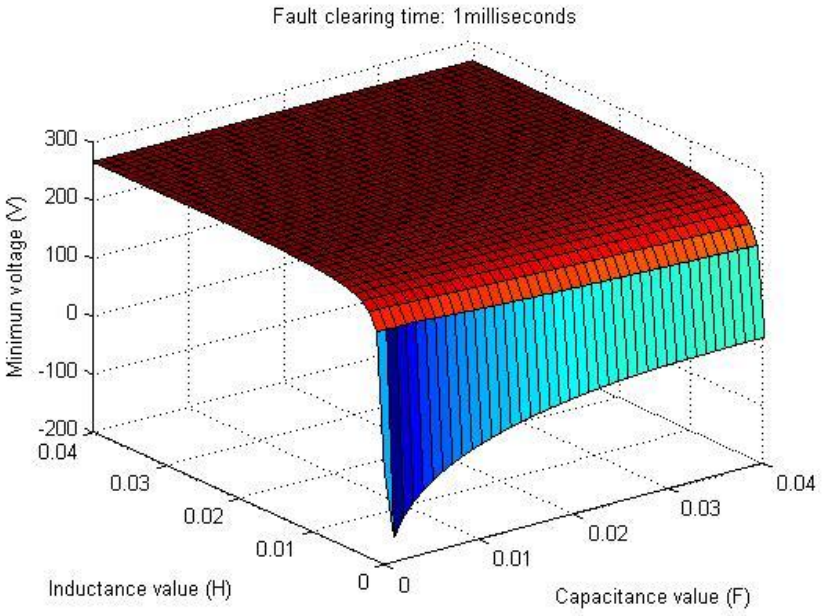

Figure 38. Minimum sensed voltage of interconnected non-faulted bus during a fault for varying filter inductance and capacitance values for a 1 ms protection operation speed.

From an initial, visual comparison of these figures, it would appear that the minimum sensed voltage is more sensitive to changes in inductance and is insensitive to changes in capacitance. This is more evident in Fig. 34, where the minimum sensed voltage increases significantly for increasing values of inductance, yet appears to remain stable for increasing values of capacitance. Additionally, it is evident that faster fault-clearance speeds result in higher voltage values for the same pair of reactor ratings, this is more easily noticeable for 0.04 H of inductance and 0 F of capacitance. Lastly, it is clear that transitioning to faster fault-clearance times results in the surface plots gradually being more flat and less curved, suggesting that smaller amounts of inductance are required for a specific minimum voltage value.

From a deeper analysis of the twin-bus DC architecture, several key observations can be made. First, the voltage drop caused by the short-circuit decreases as the protection operation speed becomes faster. The variation in voltage drop against fault clearing time can be quantified by examining the minimum voltage sensed for fixed inductance and capacitance values, as illustrated in Table IX. In this example, for an interconnecting smoothing filter with 15 mH of inductance and 16 mF of

capacitance, the difference in voltage drop between the fastest and slowest fault clearing time is approximately 92 V. Perhaps intuitively, this suggests that the protection operation speed is a key factor towards mitigating voltage-disturbance propagation, and thus potential voltage compliance of interconnected systems.

Second, for a given filter inductance value larger than 1 mH, an increase in filter capacitance results in a decrease in the minimum bus voltage sensed. For example, for a fault-clearing speed of 50 ms and with a filter inductance of 10 mH, the decrease in bus voltage caused by different shunt capacitance values is illustrated in Table X. This suggests that shunt capacitance does not aid in maintaining the nominal bus voltage level, but on the contrary has an adverse effect, further increasing the fault current through capacitive discharge. For this reason, the parallel capacitor was removed and a purely inductive approach is further pursued.

Third, this analysis enabled the visualization of the greatest minimum voltages sensed on the non-faulted bus for different filter inductance values and protection operation speeds. For fault clearing times faster or equal to 25 ms, the maximum minimum sensed voltages appear to be greater than 200 V, suggesting that suitably rated inductors can maintain the voltage drop during the short-circuit within the initial permitted voltage breadth of the ‘normal transient’ limits.

It is therefore apparent that the first desired function of the smoothing reactor is achievable, however identification of inductor ratings alone is not sufficient for voltage compliance, as the entire bus voltage profile has to be maintained within the defined voltage-limits area. Subsequently, it must be verified that after the removal of the fault, the bus voltage returns to nominal fast enough as to stay above the ‘slope’ provided by the power-quality standards and that it does not overshoot the voltage envelope. The necessary filter inductance capable of achieving overall voltage compliance will be investigated in the next section.

Additionally, for this particular modelled network and the range of filter inductance and capacitance considered, it is not possible to meet the steady-state power quality requirements for a protection operation speed of 50 ms and 25 ms (Fig. 34 and 35 respectively). This can be concluded from the fact that for these fault-clearance

Table IX. Protection operation speed against minimum sensed DC bus voltage with a smoothing filter with 15 mH of inductance and 16 mF of capacitance

Protection operation speed	Minimum sensed voltage
50 ms	167.3 V
25 ms	210.1 V
10 ms	240.6 V
5 ms	251.5 V
1 ms	259.4 V

Table X. Effect of shunt capacitance on minimum sensed DC bus voltage for a 50 ms fault-clearance time and a smoothing filter with 10 mH of inductance

Shunt capacitance	Minimum sensed voltage
1 mF	127.7 V
10 mF	127 V
20 mF	125.7 V
30 mF	124.8 V
40 mF	124 V

times, the greatest minimum sensed voltages are 221.7 V and 243.6 V respectively, whilst the lower steady-state voltage limit imposed by these requirements is 250 V.

Lastly, minimum voltage plots for the three and four-bus DC architectures for fault-clearing times of 50, 10, 5 and 1 ms are presented in Appendix. From these plots, similar conclusions as for the twin-bus DC architecture can be reached. Likewise, steady-state voltage compliance does not appear to be achievable for fault-clearance times of 50 ms and 25 ms for either architecture, as the bus voltage level cannot be maintained above 250 V.

5.2 Implementation of purely inductive solutions

As was previously stated, shunt capacitance appeared to have an adverse effect on the sensed voltage, subsequently the shunt capacitors were removed, and solely an inductor acts as a candidate interconnecting mechanism, as illustrated in Fig. 39 for

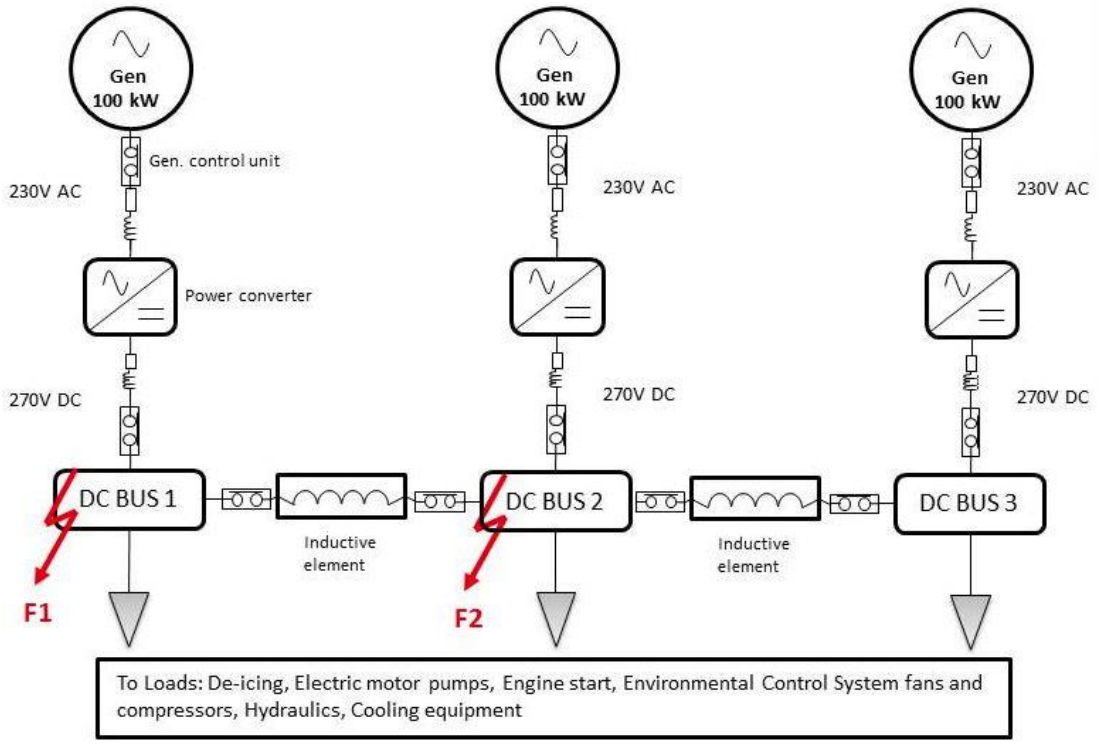

Figure 39. Representative single-line diagram of the three-bus DC architecture with candidate interconnecting inductors.

the three-bus DC architecture. The minimum voltage graphs presented in the previous section enable the identification of suitable inductor ratings that aid in stabilizing the voltage drop caused by the fault above the necessary 200 V level. Through additional simulations, this section will investigate the impact of purely inductive connections on the transient response of the healthy bus/buses and the potential of the identified inductor ratings in achieving normal-transient and steady-state voltage compliance.

5.2.1 Normal transient compliance

For each DC architecture and protection operation speed considered, simulation studies where undertaken in which candidate inductor ratings capable of maintaining the voltage above 200 V during the fault were simulated, and the smallest-rated components that restricted the voltage profile of the non-faulted bus within the

‘normal transient’ limits were determined for each case. Fig.40 depicts the voltage profile of the non-faulted DC bus 2 of the three-DC bus architecture, for a fault in location F1, interconnecting inductors rated at 2.8 mH and a protection operation speed of 5 ms.

Evidently, the voltage profile of the non-faulted bus appears to be maintained within the ‘normal transient’ limits, subsequently the healthy part of the power network retains normal-voltage compliance throughout the duration of the fault. Aggregated data regarding inductor ratings identified for normal voltage compliance for different simulated protection operation speeds for all DC architectures are summarized in Table XI. Also, the fault current that passes through the nearest interconnecting inductor relative to the fault is presented for each scenario, as this will contribute to the weight penalty estimation presented at a later section.

For fault-clearance speeds of 50 ms, 25 ms and 10 ms, it was not possible to identify inductance ratings that could retain normal voltage compliance, as the bus voltage profile could not be maintained within the required voltage envelope. However, inductance ratings were derived for fault-clearance speeds of 5 ms or less. In most of the simulation cases where inductance ratings could be derived, faster fault-clearance speeds result in less fault-current flowing through the interconnecting inductor, and less inductance is needed to maintain normal voltage compliance. In comparison, the twin-bus architecture appears to require larger interconnecting inductance than the three- and four-bus architectures, which in turn results in lesser currents through the inductor. It can also be seen that although there does not appear to be any relation between fault-clearance speed and required inductance, in some cases for clearance speeds of 5 ms and lesser, the relationship appears to be linear or almost linear.

Overall, from these results, it can be seen that the achievable speed of operation of the protection system within an architecture directly impacts the size of the inductor required to retain voltage-envelope compliance during the specified fault conditions. In this manner, faster fault-clearance times reduce the propagation of the voltage transients following the fault, and hence reduce the inductance required to achieve compliant interconnection.

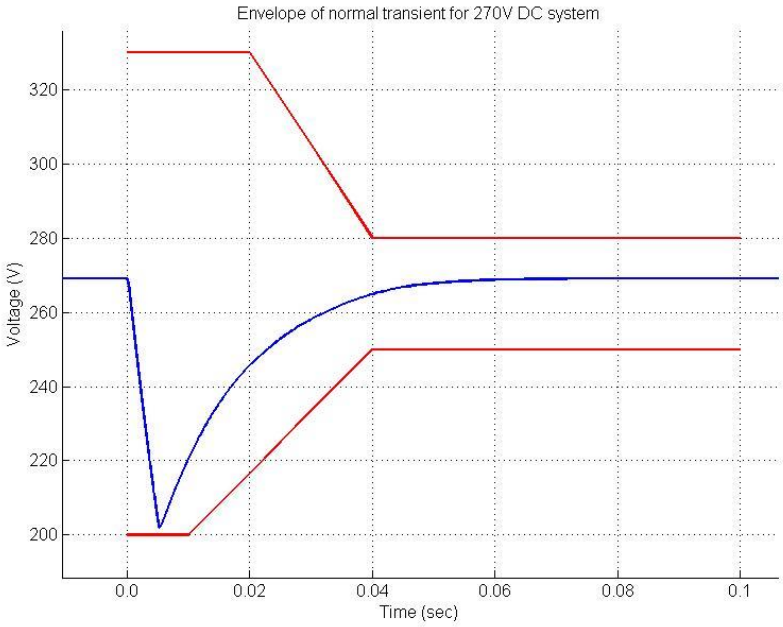

Figure 40. Voltage profile of non-faulted bus with 2.8 mH of interconnecting inductance for a fault-clearance time of 5 ms.

However, inductive interconnections do not appear to be able to provide normal voltage compliance for fault-clearance times of 10 ms and slower. This can be attributed to the fact that for slow fault-clearance times, relatively large amounts of inductance are required to stabilize the bus-voltage level above 200 V, which subsequently delay voltage recovery, thus pushing the voltage profile outside the gradient of the lower-limit envelope. As this behaviour is exhibited for all simulated candidate DC architectures, fault-clearance times of 10 ms and slower are discarded from further analyses.

For this inductive solution approach, the requirement for fault-clearance speeds to be less than 10 ms creates significant implications with regards to traditional protection equipment, in particular mechanical circuit breakers. In Chapter 3, it was stated that at the ±270 V DC level, it is typical for EMCBs with similar tripping times to be employed. This suggests that for the attainment of voltage compliance in an interconnecting network, inductive interconnections cannot be utilised along with traditional EMCBs with tripping times of 10 ms or greater.

Table XI. Inductance ratings for normal transient compliance under full-load HP generator operation

DC Architecture	Fault-clearance time	Fault current through inductor	Inductance rating
2 Bus	50 ms	-	-
	25 ms	-	-
	10 ms	-	-
	5 ms	139.5 A	4.5 mH
	1 ms	128.5 A	2 mH
	0.5 ms	136 A	1 mH
	0.1 ms	151.5 A	0.2mH
	0.02 ms	175 A	0.03 mH
3 Bus	50 ms	-	-
	25 ms	-	-
	10 ms	-	-
	5 ms	406 A	2.8 mH
	1 ms	281 A	0.8 mH
	0.5 ms	198 A	0.6 mH
	0.1 ms	321 A	0.07 mH
	0.02 ms	153 A	0.03 mH
4 Bus	50 ms	-	-
	25 ms	-	-
	10 ms	-	-
	5 ms	404.5 A	2.8 mH
	1 ms	229 A	1 mH
	0.5 ms	171.5 A	0.7 mH
	0.1 ms	162.5 A	0.15 mH
	0.02 ms	131 A	0.035 mH

On the other hand, the apparent applicability of this approach in retaining voltage compliance for relatively fast protection operations speeds opens up the possibility to investigate even faster fault-clearance times, further reducing the inductor ratings and thus the added weight penalty on the architecture. Subsequently, three additional fault-clearance times were considered in this analysis, 0.5 ms, 0.1 ms and 2 μs, indicative of potential very fast protection systems (i.e. SSPCs).

5.2.2 Steady-state compliance

A similar analysis was carried out to identify potential inductor ratings capable of providing the much stricter steady-state voltage limit compliance. To achieve steady-state voltage compliance, the bus voltage level must be maintained between 250 V and 280 V. From this analysis, it was verified that particularly for these modelled networks and the range of inductance values considered, it is not possible to meet the steady-state power quality requirements for a protection operation speed of 50 ms, 25 ms and 10 ms for any DC architecture. It was however possible to determine the required inductor ratings for protection operation speeds faster or equal to 5 ms for all simulated DC architectures.

For comparison reasons, the same parameters as for the voltage profile of Fig 40 were simulated, but in this case the inductors were rated for steady-state compliance. Fig. 41 depicts the voltage profile of the non-faulted DC bus 2 of the three-bus DC architecture, for a fault in location F1 and a protection operation speed of 5 ms. In this case, the interconnecting inductors are rated at 13 mH, compared to the 2.8 mH inductors necessary for normal voltage compliance.

Aggregated data regarding inductor ratings for steady-state voltage compliance for different simulated protection operation speeds for all DC architectures are summarized in Table XII. In the simulation cases where inductance ratings could be derived, faster fault-clearance speeds result in less fault-current flowing through the interconnecting inductor, and less inductance is required to maintain steady-state voltage compliance. The twin-bus architecture appears to require larger interconnecting inductance in comparison to the three- and four-bus architectures. Lastly, it can also be seen that in most cases for clearance speeds of 1 ms and less, the relation between fault-clearance speed and required inductance appears to be linear or approximately linear.

As in the case of normal transient compliance, faster fault-clearance times have a direct impact on the necessary inductor ratings, however, it is evident that steady-state compliance requires larger inductor ratings compared to normal transient compliance for identical fault-clearance times. It can therefore be concluded that the

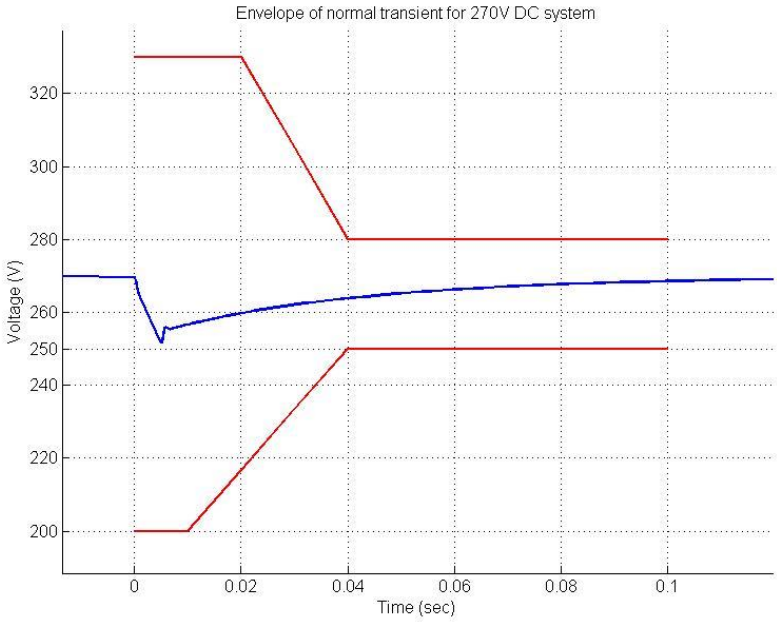

Figure 41. Voltage profile of non-faulted bus with 13 mH of interconnecting inductance for a fault-clearance time of 5 ms.

tighter the voltage envelope, the larger the size of the required inductance, and thus the greater the impact of these solutions on the power-system mass. Additionally, the employment of larger rated inductors for steady-state compliance results in significantly smaller fault-current flows compared to those sensed in normal transient compliance.

So far, it has been shown that via the implementation of bus-interconnecting inductive components, both normal transient and steady-state voltage compliance is potentially achievable for an interconnected system during a short-circuit under specific fault-clearance times. However, the feasibility of these solutions with regards to their impact on the total weight of the electric system has yet to be examined. The following section will attempt to address this issue.

Table XII. Inductance ratings for steady-state transient compliance under full-load HP generator operation

DC Architecture	Fault-clearance time	Fault current through inductor	Inductance rating
2 Bus	50 ms	-	-
	25 ms	-	-
	10 ms	-	-
	5 ms	118 A	17 mH
	1 ms	86 A	7.5 mH
	0.5 ms	69 A	4 mH
	0.1 ms	63 A	1.5 mH
	0.02 ms	52 A	0.2 mH
3 Bus	50 ms	-	-
	25 ms	-	-
	10 ms	-	-
	5 ms	99.5 A	13 mH
	1 ms	66 A	4 mH
	0.5 ms	54 A	2.7 mH
	0.1 ms	52 A	0.75 mH
	0.02 ms	35 A	0.15 mH
4 Bus	50 ms	-	-
	25 ms	-	-
	10 ms	-	-
	5 ms	99.5 A	13 mH
	1 ms	58.5 A	4.5 mH
	0.5 ms	48 A	3 mH
	0.1 ms	34.6 A	1.2 mH
	0.02 ms	34.4 A	0.15 mH

5.3 Mass estimation of inductive solutions

To better depict and quantify the apparent trade-off between inductor sizing and protection operation speed, and assess the feasibility of the proposed inductive solutions, system mass, or added weight penalty, would be an effective illustrator. However, given the multitude of required inductor ratings and desired nominal current levels, it was not possible to identify suitable commercially-available components for all simulated scenarios in order to carry out a system mass analysis.

To overcome this issue, and at the same time perform a uniform and normalized comparison, a mass index from a lightweight, aviation-grade inductor in [224] was derived. From the device's weight and power ratings, a kg mass per unit mH-A was calculated to be 0.025 kg/mH-A. Although this number may be highly approximated, nevertheless it can aid in the quantitative estimation of the added weight inductive solution incur on the power network.

As has been previously stated, the simulation studies have been carried out under full-load operation conditions, subsequently, for each scenario, the current that flows through the interconnecting inductor during the fault would be the greatest fault-current contribution of the healthy part of the network to the fault. Subsequently, by using the largest instantaneous value of sensed current passing through the inductor, along with the known required inductor ratings, it is possible to estimate the inductor weights, W_{Ind}, for all simulated scenarios from the following equation:

$$W_{Ind} = k \cdot L \cdot I_{max} \qquad (7)$$

where k is the inductor weight index of 0.025 kg/mH-A, L represents the required inductance rating in millihenries and I_{max} is the largest value of amperes passing through the immediate interconnecting inductor during the fault.

By definition, the weight estimation of the required inductor in each simulated case is derived in part from the exact maximum value of fault current passing through the interconnecting inductor under full load and balanced operating conditions. Typically however, it is not uncommon for aircraft generation systems to be designed with overrated capabilities (overload), i.e. for equipment failure or emergency operating conditions. A fault under overload conditions will result in larger fault currents flowing through the interconnecting inductor, subsequently overrated inductance ratings are required to maintain voltage compliance. Overload inductance ratings are identified in a later section, however a weight estimation study is not carried out.

Aggregated inductor weight results for protection operation speeds of 5 ms, 1 ms, 0.5 ms and 0.02 ms both for normal and steady-state voltage compliance are summarized in Fig. 42 to 44 for the twin-, three- and four-bus DC architectures respectively. It should be noted that these weights are an estimate of the necessary inductance

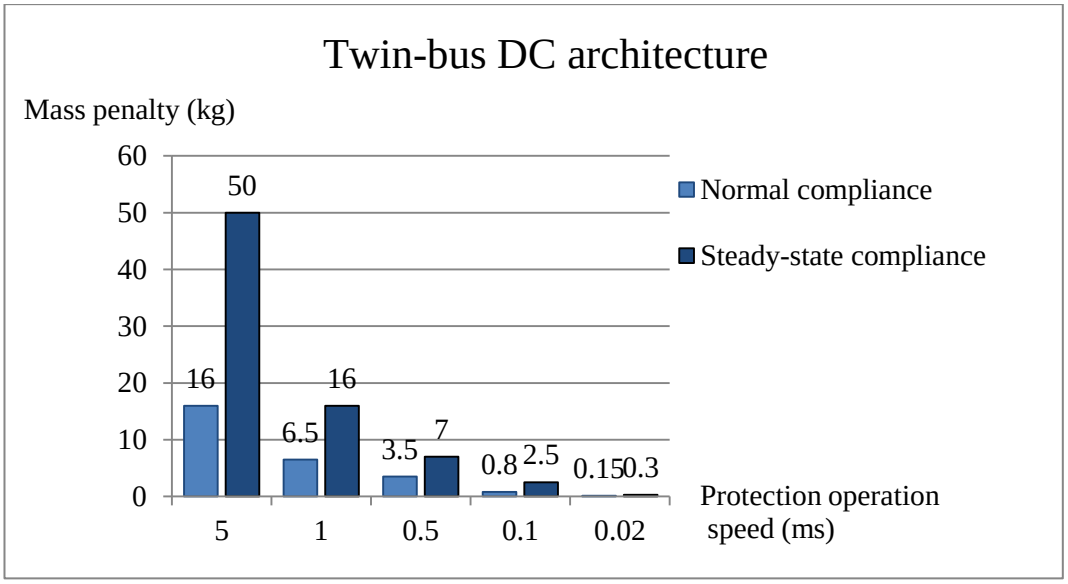

Figure 42. Mass penalty estimation for the twin-bus HP DC architecture.

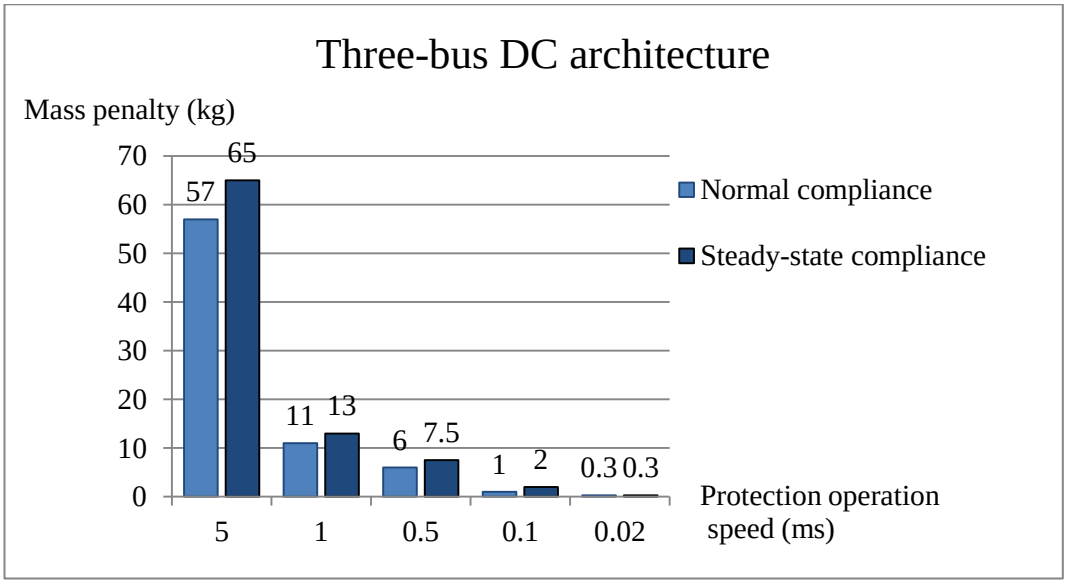

Figure 43. Mass penalty estimation for the three-bus HP DC architecture.

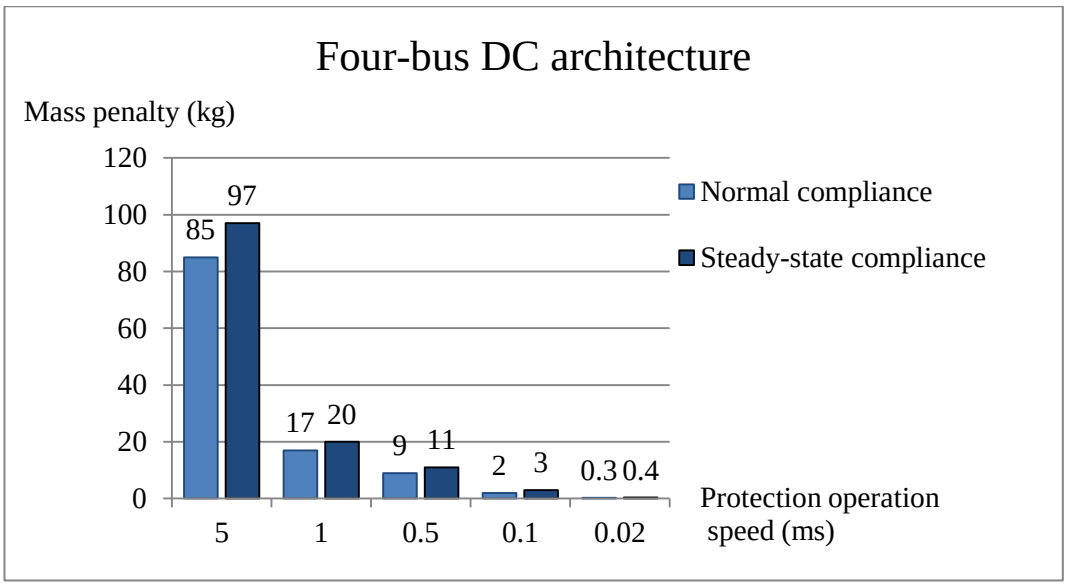

Figure 44. Mass penalty estimation for the four-bus HP DC architecture.

connection and do not include the new, overrated bus-tie breakers and/or contactors that would be required following the interconnection of the power system.

Fig. 42 estimates the quantified weight penalty on the twin-bus architecture. It is evident that steady-state compliance incurs a larger weight penalty in comparison to normal compliance across all protection operation speeds, ranging from twofold to threefold depending on protection speed. For normal voltage compliance and fault-clearance speeds of 1 ms and less, the relationship between mass and protection speed appears to be approximately linear.

In the three- and four-bus architectures (Fig. 43 and 44 respectively), the mass difference between normal and steady-state compliance is not as acute as seen in the twin-bus. Additionally, the relation between mass and protection speed appears to be approximately linear across all protections operations speeds and types of compliance. For a protection operation speed of 0.02 ms, similar inductance ratings are required for either type of compliance. Lastly, the largest weight penalty is incurred at 5 ms and the least is incurred at 0.02 ms across all architectures, for both types of compliance.

Overall, it is clear from these figures that for any given architecture and type of compliance, voltage limits can be adhered to with lighter inductors if faults are cleared within a shorter time frame. This demonstrates that fast protection operation speed is crucial to the potential feasibility of interconnected systems. Also, for any given architecture and fault-clearance time, these results highlight that the tighter the required voltage envelope, the larger the weight of required inductance. Therefore, there is an apparent trade-off between the type of compliance required and the added weight penalty incurred on the electrical architecture.

Additionally, the multitude of DC buses within an architecture also impacts the total added weight penalty on the power system. Although three- and four-bus DC networks require smaller-rated, thus lighter inductors compared to the twin-bus architecture to achieve the same type of compliance, they incur a greater mass penalty due to the need for multiple inductors for the implementation of this interconnection approach. The implications of this on the electrical design of an architecture will be illustrated in the next section.

Lastly, to highlight the importance of inductor design and its impact on the system mass, if the same weight estimation analysis was carried out using a larger, heavier inductor with a weight index of 0.12 kg/mH-A [225], the mass results presented in Fig. 42 to 44 would been approximately five times larger, significantly worsening the feasibility of this approach.

5.4 Influence of inductive solutions on generation source and architectural design selection

Previous simulation studies were undertaken with equally-rated HP generators across the power network for all DC architectures. To explore the implementation of inductive solutions in multi-shaft power off-takes schemes, this section will focus on the HP/LP model variants presented in the previous chapter. The substitution of the left HP generator with an LP in the twin- and three-bus architectures, and the two

outer generators in the case of the four-bus architecture, requires the reconfiguration of existing generation sources so that the LP generator is rated at half the power output of the HP, whilst maintaining the power output of the DC power system limited to 300 kW.

Although the initial twin-bus architecture for example was equipped with two identical 150 kW HP generators, the multi-shaft twin-bus architecture variant is equipped with one 100 kW LP and one 200 kW HP generator. The new HP generator output constitutes a 50 kW increase compared to the initial HP generator suitable inductance ratings were derived for. Similarly, a 20 kW increase per HP generator is observed for the three-bus architecture, and a 25 kW increase per HP generator is observed for the four-bus architecture. Consequently, new inductance ratings for the multi-shaft off-take variants are necessary to mitigate the induced increase in HP generator power output. Following the same simulation analysis as for the case of the identical HP generators studies, the new inductance ratings for normal transient and steady-state compliance are summarized in Tables XIII and XIV respectively for all DC architectures.

Table XIII. Inductance ratings for normal transient compliance under full-load LP/HP generator operation

DC Architecture	Fault-clearance time	Fault current through inductor	Inductance rating
2 bus	5 ms	142 A	8.5 mH
	1 ms	106 A	2.5 mH
	0.5 ms	127 A	2 mH
	0.1 ms	135 A	1 mH
	0.02 ms	151 A	0.04 mH
3 Bus	5 ms	385 A	3 mH
	1 ms	238 A	1 mH
	0.5 ms	181 A	0.7 mH
	0.1 ms	328 A	0.07 mH
	0.02 ms	170 A	0.03 mH
4 Bus	5 ms	334 A	3.5 mH
	1 ms	197 A	1.2 mH
	0.5 ms	173 A	0.7 mH
	0.1 ms	166 A	0.15 mH
	0.02 ms	133 A	0.035 mH

Table XIV. Inductance ratings for steady-state compliance under full-load LP/HP generator operation

DC Architecture	Fault-clearance time	Fault current through inductor	Inductance rating
2 bus	5 ms	42 A	35 mH
	1 ms	41 A	7.5 mH
	0.5 ms	43 A	4 mH
	0.1 ms	33 A	1.5 mH
	0.02 ms	32 A	0.2 mH
3 Bus	5 ms	98 A	14 mH
	1 ms	65 A	4.5 mH
	0.5 ms	54 A	3 mH
	0.1 ms	58 A	0.75 mH
	0.02 ms	41 A	0.15 mH
4 Bus	5 ms	90 A	13.5 mH
	1 ms	51 A	5 mH
	0.5 ms	46 A	3 mH
	0.1 ms	33 A	1.2 mH
	0.02 ms	33 A	0.15 mH

In Table XIII, it can be seen that the transition to faster fault-clearance times results in smaller inductance ratings. For the two- and three-bus architectures, it would appear that there is no correlation between inductance rating and protection speed, whilst in the four-bus architecture, the relation between protection speed and required inductance is almost linear for speeds of 1 ms and less. Lastly, in the four-bus architecture, the fault-current through the inductor appears to be decreasing as the fault-clearing speed increases, however this is not the case in the two- and three-bus architectures.

Table XIV depicts the required inductance ratings for steady-state voltage compliance. In comparison with normal compliance, it is clear that significantly larger inductors are required, with the largest inductance of 35 mH being needed for the twin-bus architecture for a fault-clearance speed of 5 ms. A direct consequence of the need for relatively large inductor are the considerably smaller levels of fault current flowing through the interconnecting inductor, with the two-bus architecture exhibiting the least amount of fault current and the three-bus architecture exhibiting the most. Lastly, for steady-state voltage compliance, the linear relationship between

inductance ratings and protection speed does not appear to hold for the vast majority of measurements.

Overall from these results, it is evident that the necessary increase in the power output of the HP generators has increased the required inductance ratings for normal compliance, for fault-clearance speeds of 5 ms and 1 ms in all architectures. On the other hand, the increase in HP generator output does not appear to have an impact on the inductance ratings for protection operation speeds of 0.5 ms, 0.1 ms and 2 μs for the three- and four-bus DC architectures. Particularly for steady-state compliance, it would appear that in most cases the previously identified inductance ratings for purely HP-generation network variants are sufficient to provide compliance besides the increase in HP generator output. It should be noted however that for the twin-bus architecture given a 5 ms fault-clearing time, the 35 mH inductance rating appears to be unfeasibly large for any airborne platform.

Aggregated inductor weight results for protection operation speeds of 5 ms, 1 ms, 0.5 ms and 0.02 ms for both types of voltage compliance are summarized in Fig. 45 to 47 for the twin-, three- and four-bus DC architectures respectively. Again, these weights are an estimate of the necessary inductance connection and do not include the new, overrated bus-tie breakers and/or contactors that would be required following the interconnection of the power system.

In Fig. 45, it can be seen that the mass penalty for both types of compliance can be significantly reduced by transitioning from a fault-clearance time of 5 ms to a fault-clearance time of 1 ms, whilst for normal compliance, there appears to be only a marginal benefit from transitioning from a fault-clearance speed of 1 ms to a fault-clearance speed of 0.5 ms. In the three-bus architecture of Fig. 46, again the relation between protection operation speed and added weight penalty appear to be approximately linear for normal voltage compliance, as is the case with the four-bus architecture. Particularly for the four-bus architecture, it would appear that across all fault-clearance speeds, the weight penalty difference between the two types of compliance is negligible, suggesting that the stricter steady-state compliance can be adhered to with marginally larger added weight.

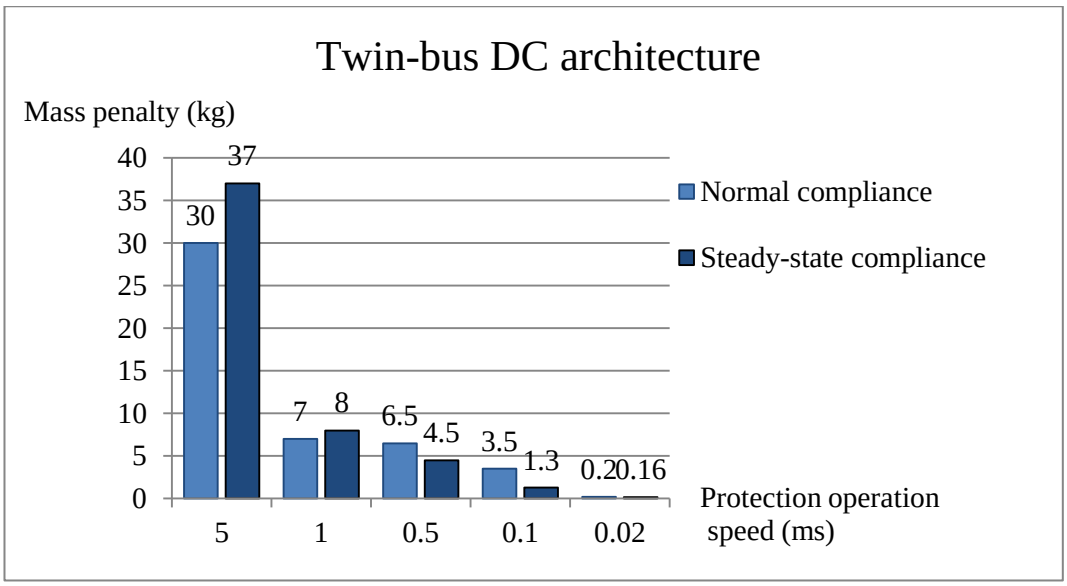

Figure 45. Mass penalty estimation for the twin-bus LP DC architecture.

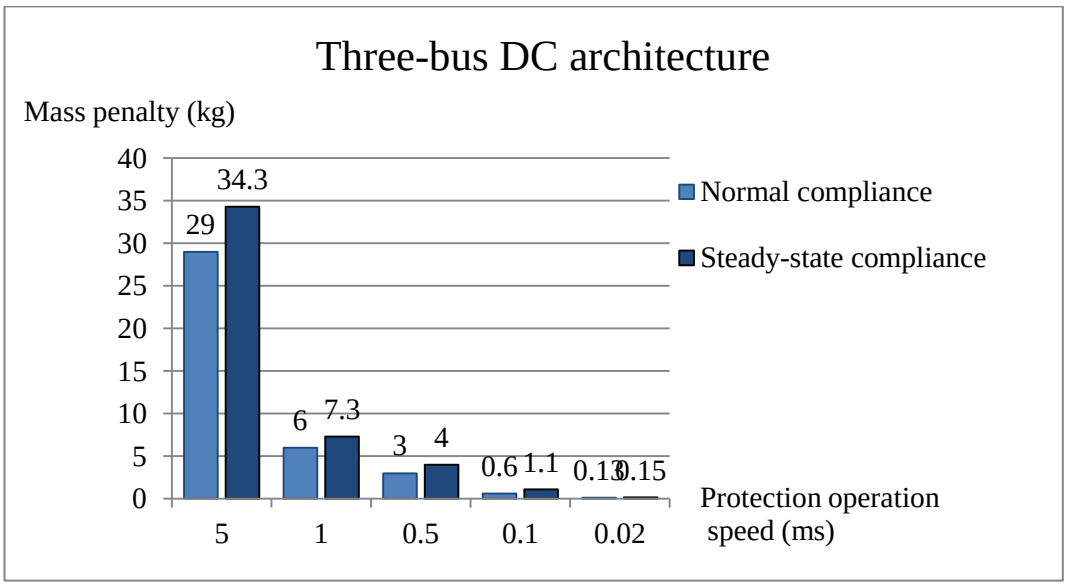

Figure 46. Mass penalty estimation for the three-bus LP DC architecture.

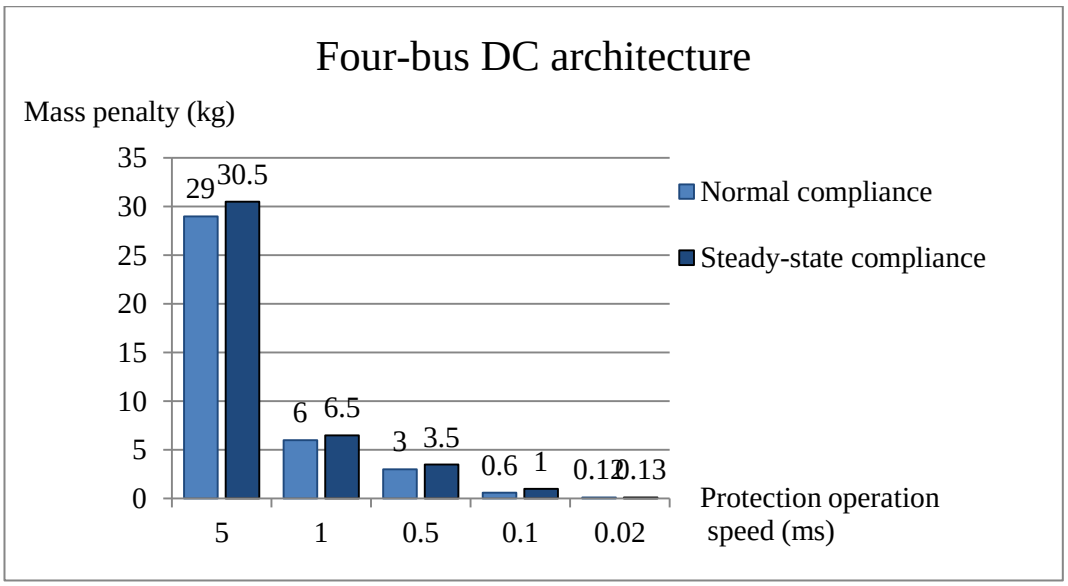

Figure 47. Mass penalty estimation for the four-bus LP DC architecture.

Perhaps intuitively, in all architectures it was seen that the dominant heterodyne short-circuits originated from the respective buses of the HP generators. In comparison, faults on the respective buses powered by LP generators created less fault-current, and smaller-rated inductors were needed to achieve either voltage compliance type. However, the implementation of smaller-rated inductors would mean that voltage compliance could only be retained for a fault on the respective LP bus, and not for a fault on any respective HP bus, consequently these ratings were discarded.

Also, it can be concluded that the main contributor to the need for bigger-rated inductors is not the variance in power mismatch between generation source types across all architectures, and thus the kind of shaft from which power is off-taken, but the greatest nominal power value of the available generators. For example, this would mean that for any two power systems that have the same multitude of generators with the same generator power output, the inductor rating that would be needed would be the same, irrelevantly if the fault was on the LP or HP generator. Accordingly, if an LP is the heterodyne between two given generators with regards to power output, then suitable inductor ratings would be dictated by the LP generator.

Overall, it will be shown that the rating and mass of the required inductance interconnection has the potential to influence the choice of architectural design as well as generation source type. Within this research, it is assumed that the LP generator is rated to half the power of the HP generator, thus this induces a necessary increase in the HP generators outputs. In turn, larger-rated inductors are required to maintain voltage compliance. Table XV presents the aggregated inductance ratings required for normal and steady-state voltage compliance for all simulated architectures, employing both HP and LP generator variants, across all fault-clearance speeds considered. By comparing the inductor ratings in Table VX, it would appear that as the multitude of generation sources within an architecture increases, thus decreasing the nominal HP generator power outputs, smaller-rated inductors are required to achieve compliant interconnections. In this manner, it would be more beneficial for an architecture to be equipped with more, less-powerful generation sources than fewer, more-powerful sources.

On the other hand, an increase in the multitude of generation sources, and thus the multitude of DC buses, corresponds to an increase in the number of inductors that are required to interconnect the DC buses. In turn, this increases the added weight penalty on the architecture. Therefore, there is an apparent trade-off between the multitude of generation sources, and thus their nominal power output, and the degree of interconnection that can be applied within the architecture via the number of interconnecting inductors.

Additionally, the mass of the required inductance connection has the potential to influence the architectural design and degree of interconnection, as will be briefly illustrated in the following architecture-comparison case study. This case study will compare the fully-interconnected four-bus DC architecture presented earlier with a partially-interconnected ‘two twin-DC bus’ architecture, shown in Fig. 48. The latter employs the same multitude of generation sources and DC buses as the former, however, features a smaller degree of interconnection, as the medial inductor has been removed. For ease of comparison, both architectures will be assumed to feature four 75 kW generators, disregarding HP or LP machine selection.

Table XV. Aggregated inductance ratings for all simulated architectures employing both HP and LP generator variants for normal and steady-state voltage compliance across all fault-clearance speeds considered

DC Architecture	Fault-clearance time	Required inductance ratings for:			
		Normal compliance with HP	**Normal compliance with LP**	**Steady-state compliance with HP**	**Steady-state compliance with LP**
2 Bus	50 ms	-	-	-	-
	25 ms	-	-	-	-
	10 ms	-	-	-	-
	5 ms	4.5 mH	8.5 mH	17 mH	35 mH
	1 ms	2 mH	2.5 mH	7.5 mH	7.5 mH
	0.5 ms	1 mH	2 mH	4 mH	4 mH
	0.1 ms	0.2mH	1 mH	1.5 mH	1.5 mH
	0.02 ms	0.03 mH	0.04 mH	0.2 mH	0.2 mH
3 Bus	50 ms	-	-	-	-
	25 ms	-	-	-	-
	10 ms	-	-	-	-
	5 ms	2.8 mH	3 mH	13 mH	14 mH
	1 ms	0.8 mH	1 mH	4 mH	4.5 mH
	0.5 ms	0.6 mH	0.7 mH	2.7 mH	3 mH
	0.1 ms	0.07 mH	0.07 mH	0.75 mH	0.75 mH
	0.02 ms	0.03 mH	0.03 mH	0.15 mH	0.15 mH
4 Bus	50 ms	-	-	-	-
	25 ms	-	-	-	-
	10 ms	-	-	-	-
	5 ms	2.8 mH	3.5 mH	13 mH	13.5 mH
	1 ms	1 mH	1.2 mH	4.5 mH	5 mH
	0.5 ms	0.7 mH	0.7 mH	3 mH	3 mH
	0.1 ms	0.15 mH	0.15 mH	1.2 mH	1.2 mH
	0.02 ms	0.035 mH	0.035 mH	0.15 mH	0.15 mH

The key parameter values of the comparison are summarised in Table XVI, for selected fault-clearance times. From this comparison, it is evident that although the ‘two twin-DC bus’ architecture requires larger inductance ratings to retain normal voltage compliance, it employs one less inductor than the four-DC bus architecture, and the smaller degree of interconnection produces smaller fault currents. Therefore, the overall weight penalty incurred by the interconnecting inductors in the ‘two twin-DC bus’ architecture appears to be less than in the four-DC bus architecture.

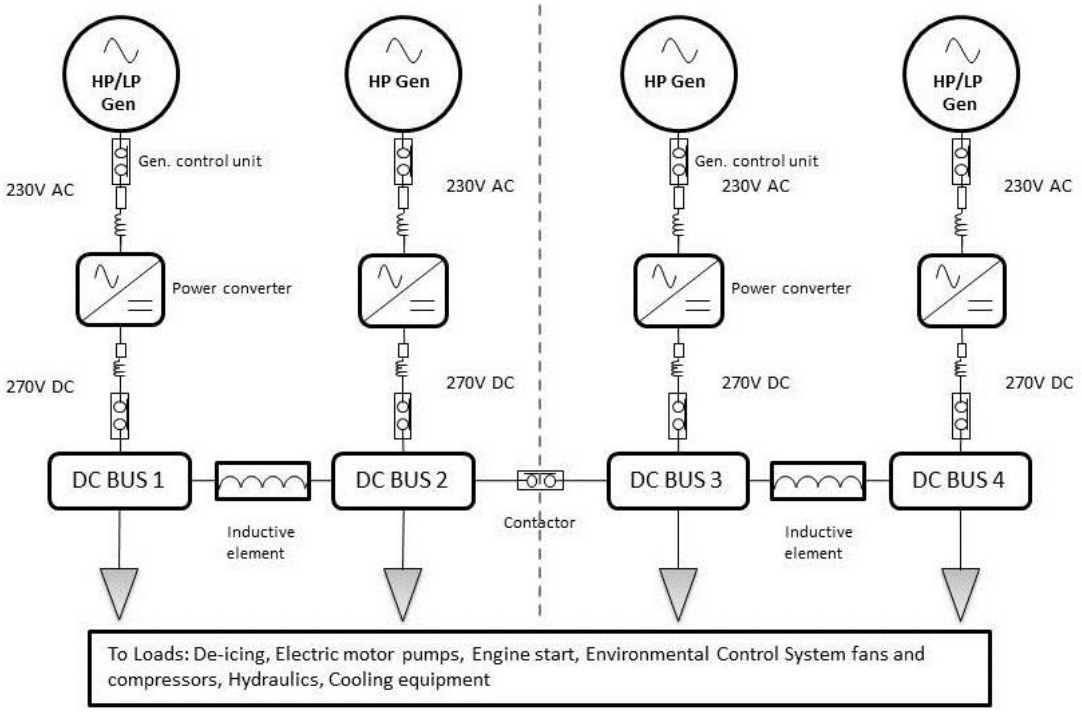

Figure 48. Partially-interconnected 'two twin-DC bus' architecture.

Table XVI. Key parameters of comparison study between four-bus and 'two twin-bus' DC architectures for normal transient compliance

DC Architecture	Fault-clearance time	Fault current through inductor	Inductor rating	Total weight penalty
4 Bus	5 ms	404.5 A	2.8 mH	85 kg
	1 ms	229 A	1 mH	17 kg
	0.5 ms	171.5 A	0.7 mH	9 kg
	0.1 ms	162.5 A	0.15 mH	2 kg
	0.02 ms	131 A	0.035 mH	0.3 kg
2+2 Bus	5 ms	336 A	3.4 mH	57 kg
	1 ms	208 A	1.1 mH	11.5 kg
	0.5 ms	152 A	0.8 mH	6 kg
	0.1 ms	132 A	0.2 mH	1.3 kg
	0.02 ms	103 A	0.045 mH	0.23 kg

Subsequently, strictly in terms of system mass, it would be more beneficial to combine groups of smaller generators, and thus DC buses, into separate channels than opting for fully interconnected DC systems. Moreover, the weight penalty is further aggravated for fully interconnected systems once the need for overrated contactors and bus-ties is factored into the weight comparison. With regards to the

total weight of the electrical system, the examples described in this section illustrated how electrical architectures and protection operation strategies can influence design at a systems and architectural level.

5.5 Beneficial and adverse aspects of inductive interconnections

During an electrical fault, the implementation of interconnecting inductance between DC buses appears to allow the non-faulted part of the power system to adhere to the voltage limits defined in MIL-STD-704F, for both types of voltage compliance under specific fault-clearance times. For the simulation studies presented in previous sections, the electrical fault was introduced at the terminals of the DC busbar, in an attempt to analyse a worst-case scenario in terms of transient response and fault-current within the DC system. To further aggravate this scenario, the DC bus was not isolated from its respective ATRU or upstream AC generation source, perhaps in contrast to how an actual protection system would operate in order to clear the fault.

Nevertheless, the interconnecting inductive components appear to be able to stabilize the voltage profiles of the non-faulted buses within the specified limits without the need of isolating the DC buses. For example, a fault upstream or downstream of a DC busbar would necessitate the removal by the protection system of that particular channel from the network, and the voltage profile of the respective busbar may be affected, or even collapse, but the DC buses would still be able to operate in paralleled mode as the interconnecting components would stabilise the voltage profiles of the non-faulted DC buses within the required limits. Therefore, unlike the approach proposed for AC and/or DC distribution systems on-board diesel electrical propulsion vessels in [220, 222], DC bus isolation or reconfiguration of the distribution network does not appear to be required in this interconnecting method.

Another benefit afforded by this inductive approach is the implementation of an interconnecting mechanism that has no moving parts, which makes it less susceptible

to wear and tear issues, and thus reduces the need of frequent maintenance. Once installed, these components do not need to be programmed or have their operation be continuously monitored, and unlike traditional fuses, are not single-use items.

Moreover, inductors are thought to exhibit high reliability, although high temperature operation or exposure to high current stresses can lead to component failure [226]. The two most common fail modes of an inductor are open circuit (i.e. due to a crack in the coil wire) and short-circuit (i.e. inductance drop due to insulation damage/deterioration) [227]. If an inductor becomes an open circuit, this suggests that at least one power channel is operating in isolated-generation mode, with apparently no further impact to flight operations. Therefore, this failure mode is considered to have a minimal effect on flight safety or continuity, as the electrical system can subsequently be operated in isolated-generation mode.

On the other hand, and perhaps only in the event of an electrical fault, the deterioration of the inductor's insulation could potentially result in the adjacent power channel(s) exceeding the permissible voltage limits and relevant equipment being exposed to larger fault currents. However, it is believed that this can be mitigated by the operation of the protection system and by component inspection during maintenance. In essence, it would appear that an additional advantage of utilising inductors as bus-interconnecting mechanisms is their 'safe fail' characteristic, where following a failure of the component, it can be argued that the only drawback is the reduction in operability and efficiency gains due to the electrical system operating in isolated-generation mode.

However, there are also several disadvantages to this approach. The following sections will briefly discuss the effects of unbalanced operation conditions and power quality on the required inductor ratings necessary to achieve compliant interconnections. The adverse effects of adding inductance in-between buses will also be considered with respect to transient load sharing and protection relay coordination.

5.5.1 Generator Imbalance

In the simulation scenarios of Section 5.2.1, the identified inductor ratings were derived under balanced operation of the power system, however, generator operation may not always be balanced. The electrical generation systems on most civil aircraft are designed with overload provisions (time-limited excess overload capacity) or have over-rated generation capabilities, particularly for the case of abnormal or emergency flight conditions. The A380 is thought to be able to sustain the loss of two of its four generators before an overload situation is established [56], whilst in the twin-engine B777, both main AC buses and all essential electrical services can be provided for under single-generator operation [106]. Additionally, TRUs are designed with incorporated overload features, where the current output can be significantly increased for a limited time period [228].

At the same time, it not uncommon for flight crew to reduce the throttle on a particular engine, and thus the output of the respective generator, in the event of excessive engine vibrations or oil temperature [229, 230]. This section will investigate the impact of overloaded and underperforming generators within a network on the required inductance ratings necessary for normal voltage compliance.

To investigate the effect of unbalanced generator operation on the necessary inductance ratings, a similar analysis as in Section 5.2 was carried out for all DC architectures, however in this case, one generator was set to operate at 50% of rated power and the adjacent generator set to 150% of rated power. From this analysis, it is apparent that if the fault is applied on the respective DC bus of the under-performing generator, there is no breach of the voltage-limits envelope, however a fault applied on the respective bus of the over-performing generator leads to a breach of the normal voltage-limits envelope. As the previously identified inductance ratings are not able to maintain the non-faulted bus voltage within the defined limits, new over-rated inductors are needed in this case, summarized in Table XVII, further increasing the added weight penalty on the DC architectures.

Table XVII. Inductance ratings for normal transient compliance under unbalanced generator operation

DC Architecture	Fault-clearance time	Inductance rating
2 Bus	5 ms	10 mH
	1 ms	3 mH
	0.5 ms	2.5 mH
	0.1 ms	1.2 mH
3 Bus	5 ms	4.5 mH
	1 ms	2 mH
	0.5 ms	1 mH
	0.1 ms	0.2 mH
4 Bus	5 ms	4 mH
	1 ms	1.5 mH
	0.5 ms	0.8 mH
	0.1 ms	0.04 mH

5.5.2 Bus power quality

In the simulation scenarios of Section 5.2.1, the identified inductor ratings were derived under optimum power quality conditions, with a nominal busbar voltage of 270 V DC and no fluctuations. This section will investigate the effect of power quality on the required inductance ratings necessary for normal voltage compliance.

As a means of introducing a degree of instability into the simulated power networks, a 10.05 kVA DC-AC converter-fed constant-power load, representing a three-phase AC motor, was attached to each DC bus across all architectures. A two-level voltage source inverter, featuring six IGBTs in a three leg configuration, outputs three-phase AC power which in turn is fed to the motor, with the block diagram of the simulation model shown in Fig. 49. The control system of the inverter was designed with guidance provided within [231]. The output voltage magnitude of the inverter is regulated using a phase angle controller, and dq0 transformation is used to determine the V_d component magnitude. The V_d component and reference value are then summed with the AC voltage phase angle to provide a frequency for the reference sinusoidal waveform. These waveforms are created for each of the three AC phases and are separated by 120^o. The sinusoids are then compared to the PWM switching

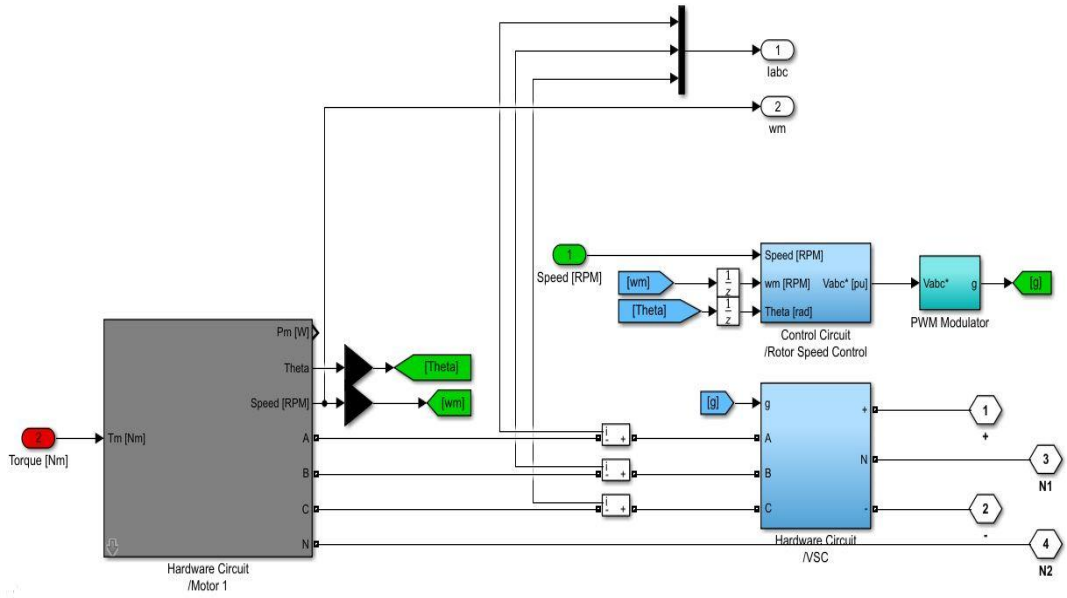

Figure 49. Block diagram of software model used to simulate a constant power load, consisting of a two-level voltage source inverter that drives an AC motor.

pattern, which generates the pulse signals to control the switching of the inverter. Lastly, this specific power rating for the AC motor was chosen so that the generated voltage fluctuations would not exceed the 6 V limit imposed by the power-quality requirements, while producing 12 Nm of torque at a nominal speed of 8,000 rpm.

In all simulated scenarios, the voltage oscillations generated onto the DC buses by the constant-power loads lead to breaches of the normal voltage-limit envelope using the inductance ratings previously identified. This is illustrated in Fig. 50 for a fault-clearance time of 5 ms in the twin-bus DC architecture, using the 4.5 mH inductor previously identified. Consequently, new inductance ratings are required to maintain voltage compliance under voltage fluctuating conditions, which are summarized in Table XVIII.

Although these ratings are slightly larger than the ones identified in Table XI under optimum power quality conditions, the impact of voltage fluctuations on the inductance ratings, and thus on the added weight penalty, is less significant than the impact of unbalanced generator operation on these ratings.

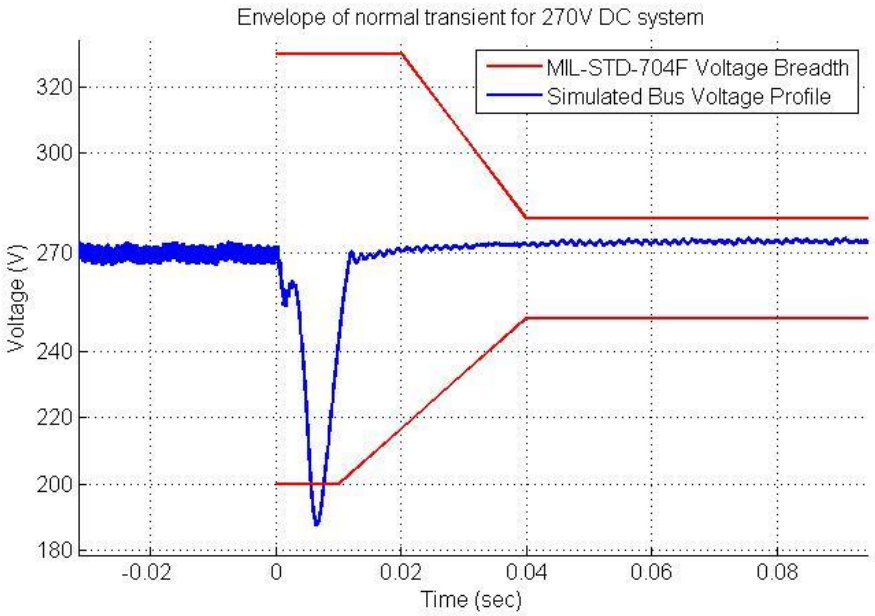

Figure 50. Voltage profile of the non-fault bus of twin-bus DC architecture following the addition of a constant-power load, during a fault with 5 ms fault-clearance time.

Table XVIII. Inductance ratings for normal transient compliance under fluctuating voltage conditions

DC Architecture	Fault-clearance time	Inductance rating
2 Bus	5 ms	5 mH
	1 ms	2.5 mH
	0.5 ms	1.2 mH
	0.1 ms	0.3 mH
3 Bus	5 ms	3 mH
	1 ms	1 mH
	0.5 ms	0.7 mH
	0.1 ms	0.08 mH
4 Bus	5 ms	3 mH
	1 ms	1.5 mH
	0.5 ms	0.8 mH
	0.1 ms	0.2 mH

5.5.3 Undesired effects due to interconnecting inductance

Previous sections identified operational conditions, such as generator imbalance and non-optimal power quality, as issues that have an adverse effect on the proposed

inductance ratings necessary achieve voltage-envelope compliance. This section will briefly discuss the adverse aspects arising from the deployment of interconnecting inductance in-between DC buses within electrical architectures, with respect to transient load sharing and protection relay coordination

First, the addition of inductive components onto the power network can incur a significant weight penalty, particularly for larger DC architectures with slow fault-clearance times. In applications where weight and volume come at a premium, such as in aviation and offshore power installations, there are constraints on the mass and size of components, as the cost of platforms is highly dependent on their weight, and more importantly, volume [14]. Although transitioning to faster fault-clearance times reduces the added weight penalty incurred on the electrical architecture by the interconnecting inductor/s, this may increase the cost and complexity of the protection system.

Additionally, there is a trade-off in inductor design between the rate of rise of fault current and the stiffness of the power system [14]. Higher inductance values can further supress the fault-current rate of rise, but in doing so, create a stiffer network that restricts fast current changes, impacting the response of the power flow control in the grid [232]. This can be illustrated in Fig. 51, which depicts a voltage response comparison following a 50 kW load step-up and down, at time t = 0.3 s and t = 0.33 s respectively, on the three-bus DC architecture with and without the inclusion of inter-bus inductance. It is clear that the response of this particular inductive system is over-damped, reducing the peak of voltage transients but at the same time extending the settling time of the system.

The addition of interconnecting inductance between adjacent DC buses could also potentially compromise the stability of the electrical network with regards to transient load sharing of generators following step changes in load. Although this seems to pose a serious problem in islanded microgrids [233], where poor transient load sharing is exhibited when synchronous generators are paired with inverters, this does not appear to be an issue with more interconnected systems [234], or a wider threat to the stability of the system [235], and there are means of control to mitigate for such issues, such as droop-based or master-slave control.

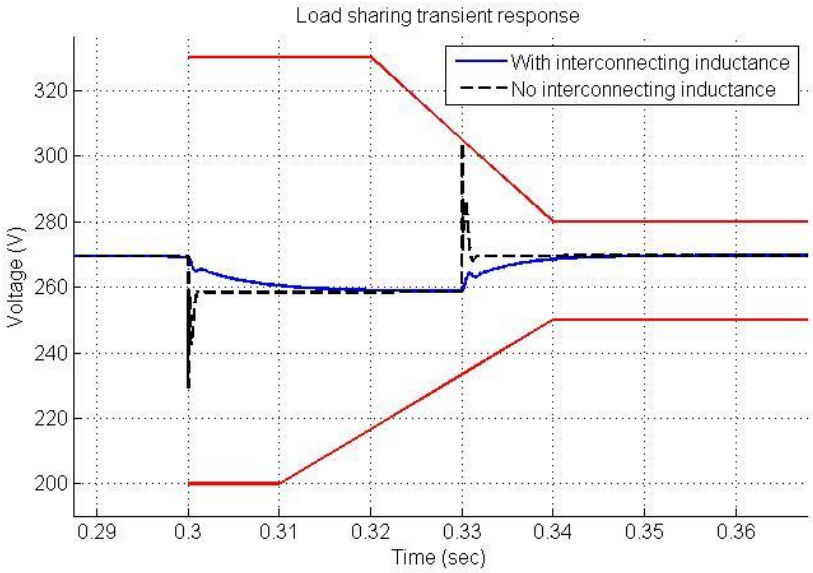

Figure 51. Load sharing transient response during a 50 kW step-up and down with inter-bus inductance (blue line) and without (black line).

Lastly, during an electrical fault, fault-current magnitude and voltage-disturbance propagation are expected to be greater in an interconnected system than in an isolated network. Therefore, protection devices and relays must be configured to operate and coordinate accordingly. Although research has shown that high-impedance faults can result in dampened protection operation [236], or protection blinding [237], in simulations presented in previous sections, the inductance ratings of the proposed interconnecting solutions are driven by low-impedance short-circuit faults. This, along with novel research into high-impedance fault mitigation [238], suggests that relay coordination poses no greater problem compared to other protection issues, however a relay coordination analysis is out of the scope of this research.

5.5.4 Implementation of non-ideal inductor

In all simulation scenarios presented within this thesis, the identified inductor ratings were derived under the assumption that an ideal inductor acts as a bus-interconnecting mechanism. This section will briefly investigate the effect the implementation of a non-ideal inductor has on key system parameters.

Typically, inductors are rated with particular saturations currents, and their effective inductance is temperature-dependent and varies within a specific tolerance [227]. These factors were not considered within this work, as a linear representation on an inductor model was simulated. Also, a non-ideal inductor has a series resistance R and a stray capacitance C, as shown in the equivalent circuit of Fig. 52. The series resistance is dependent on the effective inductance of the inductor, temperature and inductor design/size [227]. Stray capacitance is dependent on the design of the coil and the type of core, however its impact is considered to be less severe than that of the series resistance.

To investigate the effect of a non-ideal inductor acting as a bus-interconnecting mechanism on the network, a simulation model was created from Fig. 52. Relevant R and C values were looked up within the literature, however due to these parameters being design- and temperature-specific, arbitrary values were assumed. Consequently, a stray capacitance of 40 pF and a series resistance of 4 Ohms were chosen, as typically inductor DC resistance does not exceed 4 Ohms [239]. This would therefore create a worst-case scenario with regards to the impact of a non-ideal inductor on the 270 V DC system.

Fig. 53 depicts the voltage profile of the non-faulted DC bus on the three-bus architecture during a 5 ms fault, with two non-ideal inductors with a series resistance of 4 Ω serving as interconnecting mechanisms. For a meaningful comparison with the transient behaviour exhibited by the implementation of ideal inductors (Fig. 40), the inter-bus inductance was maintained at 2.8 mH, as previously identified in Table XI for normal voltage compliance of the three-bus DC architecture. It is evident that the power-quality requirements could not be adhered to using the previously identified inductance rating, due to the 15 V drop incurred onto the system voltage by the series resistance of the non-ideal reactor. A similar voltage drop was observed for smaller values of inductance afforded by faster fault-clearing times, as shown in Fig. 54 for the same architecture, but for a 1 ms fault and 0.8 mH of inter-bus inductance. Again, compliance to power-quality requirements could not be maintained, suggesting that the steady-state voltage profile, and thus voltage-limit compliance, is sensitive to relatively large increases in system resistance.

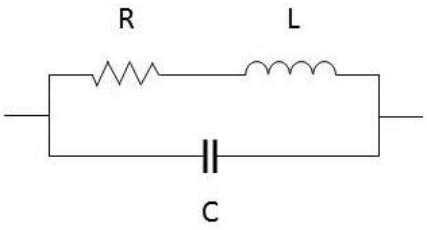

Figure 52. Equivalent circuit of non-ideal inductor.

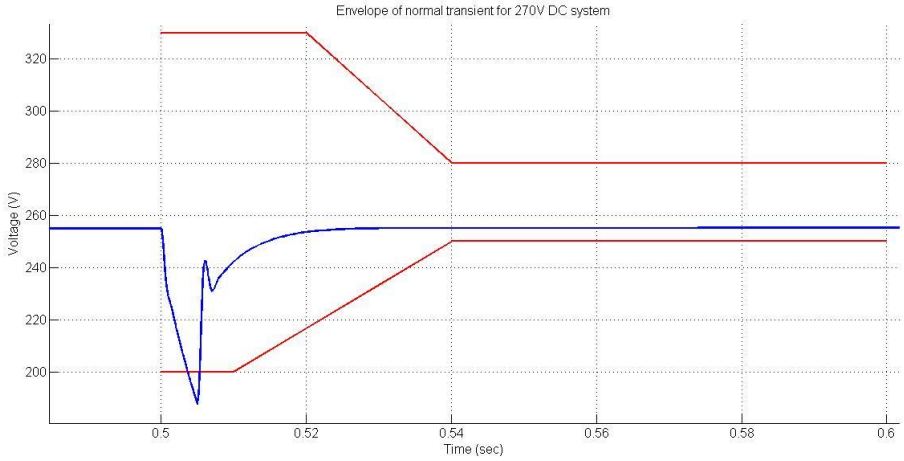

Figure 53. Voltage profile of non-faulted bus on the three-bus architecture during a 5 ms fault with the implementation of 4 Ω, 2.8 mH non-ideal inductors.

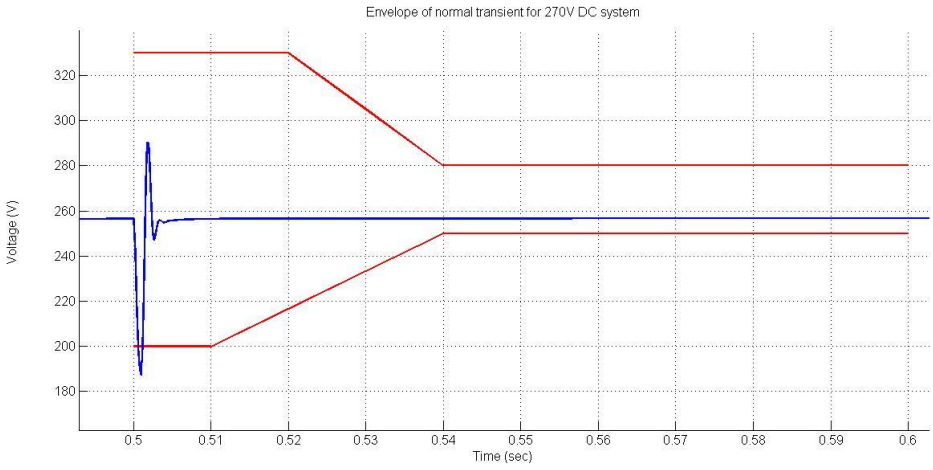

Figure 54. Voltage profile of non-faulted bus on the three-bus architecture during a 1 ms fault with the implementation of 4 Ω, 0.8 mH non-ideal inductors.

At the same time, by comparing Fig. 40 and 53, it is apparent that the transient responses of the network are different, as the implementation of a large inter-bus resistance results in a noticeably less steep voltage collapse and a steeper voltage recovery time. Therefore, the addition of such large resistance appears to qualitatively improve the transient response of the system during the fault, as it reduces the fault-current flowing through the inductor. A steeper voltage recovery gradient is also observed in Fig. 54, which paired with the faster fault-clearance, result in noticeable overshoot of the nominal voltage level, however without exceeding the upper permissible voltage limit.

Arguably, 4 Ohms is a very large value for an inductor's series resistance, however it appears to imply that 15 V is the maximum amount of voltage drop to be expected by the practical implementation of a non-ideal inductor. As expected, further simulations showed that by reducing the series resistance of the inductors, the voltage drop is also reduced. Lastly, it was seen that in order for the non-ideal inductor to have a negligible effect on the system voltage, i.e. less than 1.5 V, the series resistance should not exceed a value of 0.5 Ohms.

5.6 Optimisation under partial generator loading

In the simulation scenarios of Section 5.2.1, the identified inductor ratings were derived under full-load operation of the generation system, simulating in this manner a worst-case type scenario for the network with regards to fault-current and transient response. However, an aircraft's power system does not operate under these conditions throughout the entire flight cycle, as typically, there is less electrical demand from the on-board generators during cruise and descent compared to take-off and climb.

Moreover, with generator operation at or around 100% of nominal power output, it is not possible to perform any kind of generator/load optimisation, thus reducing one of the added benefits that could be afforded by operating the power system under interconnected mode. On the other hand, if for example the generators on-board an

interconnected system were operated at around 70% - 80% of their nominal power output during particular segments of the flight cycle, this could enable the implementation of power optimisation schemes.

Several benefits afforded by such schemes in interconnected networks, like electrical power-transfer between shafts and more efficient generator operation, have been previously mentioned in Section 3.3. Additionally, load optimisation can also allow for a more effective system response to variances in electrical demand and reduce peak loads [240], which in turn reduce power system losses and thermal stress on components [241]. Reducing component stress, thermal and/or fatigue, improves network stability and equipment health [242], leading to reductions in maintenance costs and improved asset utilisation [243].

This section will identify suitable inductance ratings capable of retaining normal voltage compliance for generator operation rated at 70% of the nominal power output. Subsequently, each HP generator in the twin-, three- and four-bus DC architecture is rated at 105 kW, 70 kW and 52.5 kW respectively. Aggregated data regarding inductor ratings for normal voltage compliance under partial generator loading are summarized in Table XIX, and their weight penalty estimation is illustrated in Fig. 55.

From this weight estimation study of the required inductors, it is again clear that significant weight savings can be realized by increasing the speed of the protection system. In absolute value, this is more evident for the four-bus architecture, in particular between fault-clearance times of 5 ms and 1 ms, as it requires the most inter-bus inductors. For the same fault-clearance times, a significant weight reduction can also be achieved for the three-bus architecture. However, lesser weight savings can realized for the two-bus architecture as is requires only one interconnecting inductor.

Overall, it is evident that a 30% reduction in generator output does not result in a similar reduction in inductance ratings. Across all architectures and fault-clearance times, the required inductance ratings either marginally increased for relatively slow fault-clearance times, or remained the same for protection operation speeds of 0.1 ms

Table XIX. Inductance ratings for normal transient compliance under partial-load HP generator operation

DC Architecture	Fault-clearance time	Fault current through inductor	Inductance rating
2 Bus	5 ms	137.5 A	4.5 mH
	1 ms	109 A	2.2 mH
	0.5 ms	176 A	1.1 mH
	0.1 ms	121 A	0.2 mH
	0.02 ms	170 A	0.03 mH
3 Bus	5 ms	404 A	2.8 mH
	1 ms	250 A	0.9 mH
	0.5 ms	170.5 A	0.7 mH
	0.1 ms	315.6 A	0.07 mH
	0.02 ms	147 A	0.03 mH
4 Bus	5 ms	403 A	2.8 mH
	1 ms	180.5 A	1.3 mH
	0.5 ms	137 A	0.9 mH
	0.1 ms	116 A	0.25 mH
	0.02 ms	126 A	0.035 mH

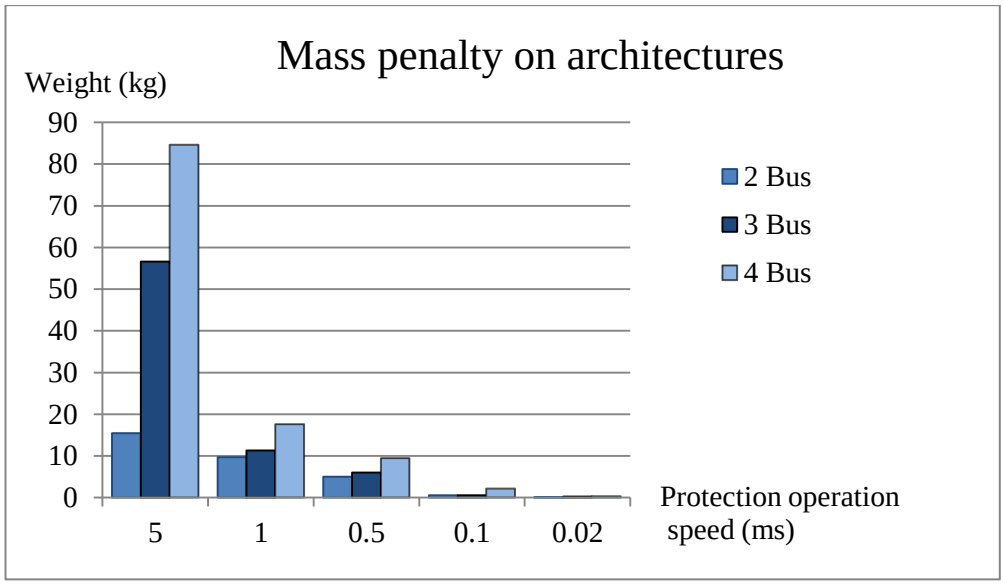

Figure 55. Estimated interconnecting solutions weight under partial loading operating conditions.

and 0.02 ms. In comparison with full-load condition scenarios however, in most cases weight reductions can be realised due to smaller fault currents passing through the interconnecting inductors.

5.7 Implementation of inductive interconnections on novel parallel-generation networks

Previous sections explored the use of interconnecting inductance as a means of achieving voltage compliance on baseline DC architectures. This section will investigate the potential feasibility of this approach on novel interconnected power systems within the relevant literature, presented in Sections 3.3.1 and 3.4, and illustrate the impact of different architecture types on system mass. For a meaningful comparison with the baseline DC architectures, similar fault clearance times are employed at 100 % generator load conditions. The generator power output ratings have been adapted so that the total power rating of the system is 300 kW, and where applicable, the HP generator is rated at twice the power output of the LP generator.

The electrical architecture proposed by Derouineau in [135] is a twin-bus DC architecture comprising of HP and LP generators, identical to the baseline twin-DC architecture studied within, therefore this patent will not be further analysed.

5.7.1 Paralleled HVDC bus

In the paralleled DC architecture proposed by Yue e*t al.* in [160] (Fig. 13), interconnecting inductors were installed in-between adjacent HVDC buses, as shown in Fig. 56. The network model parameters of the paralleled HVDC system are summarized in Table XX. Short-circuits are only introduced onto the terminals of HVDC Bus (Left) and HVDC Bus (Essential) due to the symmetry of the power system. The necessary inductance ratings to achieve normal voltage compliance in this architecture are presented in Table XXI. It is clear from Table XXI that regardless of fault location (Left bus or Essential bus), less interconnecting inductance is required as fault-clearance times become faster. It is also apparent that faults on HVDC Essential require considerable larger inductance ratings in comparison with faults on HVDC Left for the same fault-clearance speed, except for.

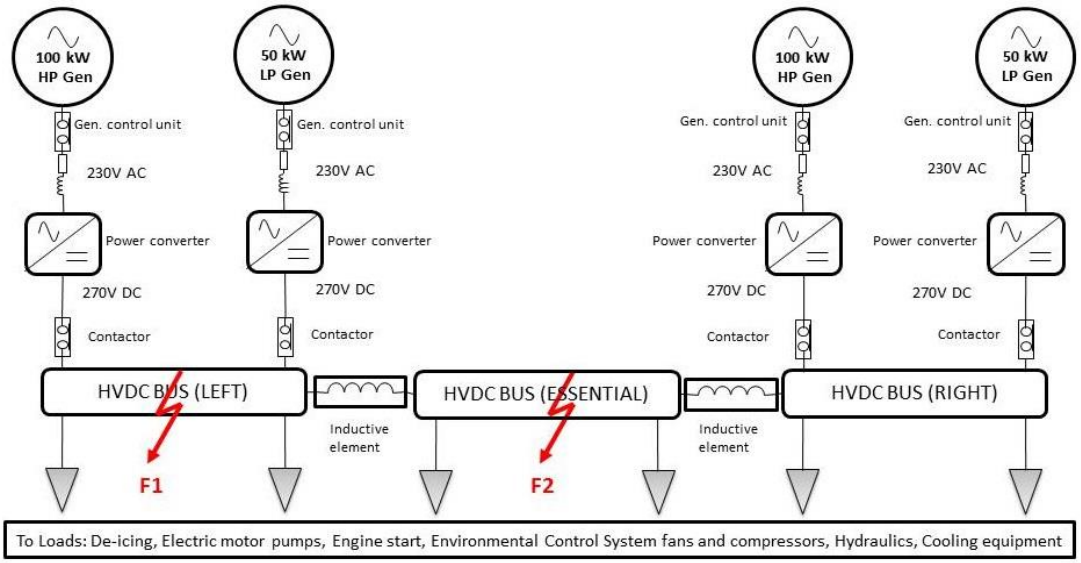

Figure 56. Paralleled HVDC bus electrical power system with interconnecting inductors (adapted from [160]).

Table XX. Network model parameters paralleled HVDC bus electrical power system

Parameter	Value
Rated power	300 kW
HP/LP generator rating	200 kW / 100 kW
Operating voltage	270 V DC
Nominal HP current	370 A
Nominal LP current	185 A
Feeder resistance	0.801 mΩ/m [9]
Feeder inductance	0.65 µ/m [9]

Table XXI. Inductance ratings for normal compliance of HVDC electrical power system

DC Architecture	Fault-clearance time	Inductance rating
Yue *et al.*	5 ms	4.5 mH
HVDC Bus	1 ms	1.2 mH
(Left)	0.5 ms	0.7 mH
	0.1 ms	0.2 mH
	0.02 ms	0.015 mH
Yue *et al.*	5 ms	15 mH
HVDC Bus	1 ms	2.5 mH
(Essential)	0.5 ms	1 mH
	0.1 ms	0.1 mH
	0.02 ms	0.04 mH

a fault-clearance time of 0.1 ms. Lastly, there appears to be no correlation between protection operation speed and inductance rating

Although typically this is a four-generator architecture, each pair of generators is coupled to each of the two outer DC bus, thus essentially resembling a two-bus architecture. For faults on HVDC Left, the required inductance ratings are the same as those of the twin-bus DC architecture for protection speeds of 5 ms and 0.1 ms, and more similar to the candidate four-bus DC architecture for protection speeds of 1 ms and 0.5 ms. For a fault-clearing time of 0.02 ms, this architecture requires lesser inductance than either of the candidate architectures.

An arguably smoother behaviour is exhibited for faults on HVDC Essential, in which the inductance ratings are similar to the two-bus architecture for protection speeds of 1 ms and 0.5 ms, and more similar to the four-bus architecture for protection speeds of 0.1 ms and 0.02 ms. Lastly, the apparent requirement for 15 mH of inductance for a fault-clearance speed of 5 ms is significantly larger than for any of the two candidate architectures.

5.7.2 Paralleled multi-shaft power offtakes

In the AC architecture proposed by Kern e*t al.* in [130], two (or more) constant-frequency HP generators power their respective AC buses independently, with an additional, synchronized LP generator capable of supplying power to each of the two AC buses, as shown in Fig. 57a. In another embodiment of this patent, the LP generator can supply additional AC power to each power electronics module, in parallel with the AC power delivered to each power electronics module by the independent HP generators, as illustrated in Fig. 576b. Lastly, it is envisioned that power electronic modules may “selectively provide either AC or DC power to desired distribution buses”.

In this patent, there appears to be some ambiguity in relation to two main issues. First, it is not specified what type of power electronics module, serving as an

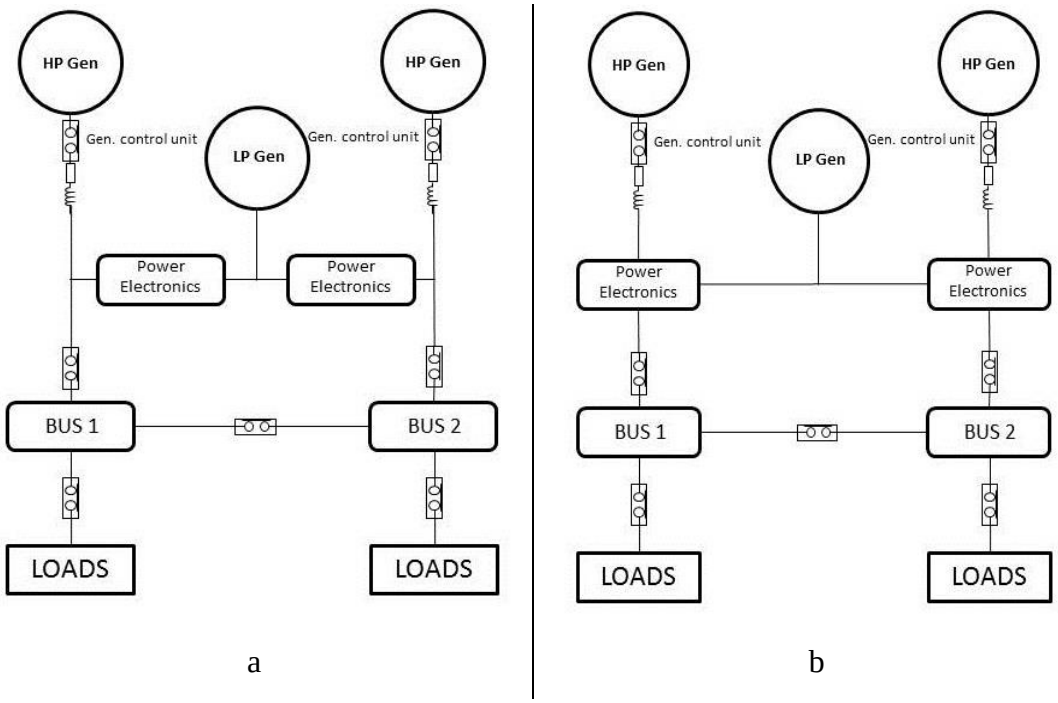

Figure 57. Paralleled multi-shaft power offtakes embodiments proposed by Kern *et al*. in which the LP generator either provides power to either AC bus (a) or provides power to either power electronics module in parallel with the HP generator (b) [130].

interconnector, is used (i.e. SSPC, rectifier). Granted that all generators are defined as constant-frequency AC sources, this would suggest that power electronic modules perform either AC synchronisation functions or DC rectification. In the case of the former, this option is not applicable to modern MEA/E as they are equipped with variable-frequency generators, which do not permit AC interconnection options, thus both topologies of Fig. 57 can be discarded from further analysis.

On the other hand, if the power electronics modules can rectify the generated AC power, then this leads to the second ambiguous issue within the patent, whether the LP generator and/or the power electronics modules provide additional power to both buses simultaneously or only one at a time. If it is the case of the latter, then the topology in Fig. 57b is equivalent to the two-bus HP/LP configuration presented earlier in Section 5.4, therefore no further analysis is justified. However, if the envisioned power electronics modules can power both main HP channels simultaneously, this could enable further analysis into a novel topology, if considered as a variable-frequency AC architecture featuring DC distribution. To this end, the

envisioned power electronics modules are replaced with closed ideal contactors, permitting in this manner the third LP generator to supply both respective HP buses.

An interconnecting inductor was installed in-between the adjacent buses, as shown in Fig. 58. The network model parameters of the paralleled system are summarized in Table XXII. Short-circuits are only introduced onto the terminals of DC Bus 2 due to the symmetry of the power system. The necessary inductance ratings to achieve normal voltage compliance in this architecture are presented in Table XXIII.

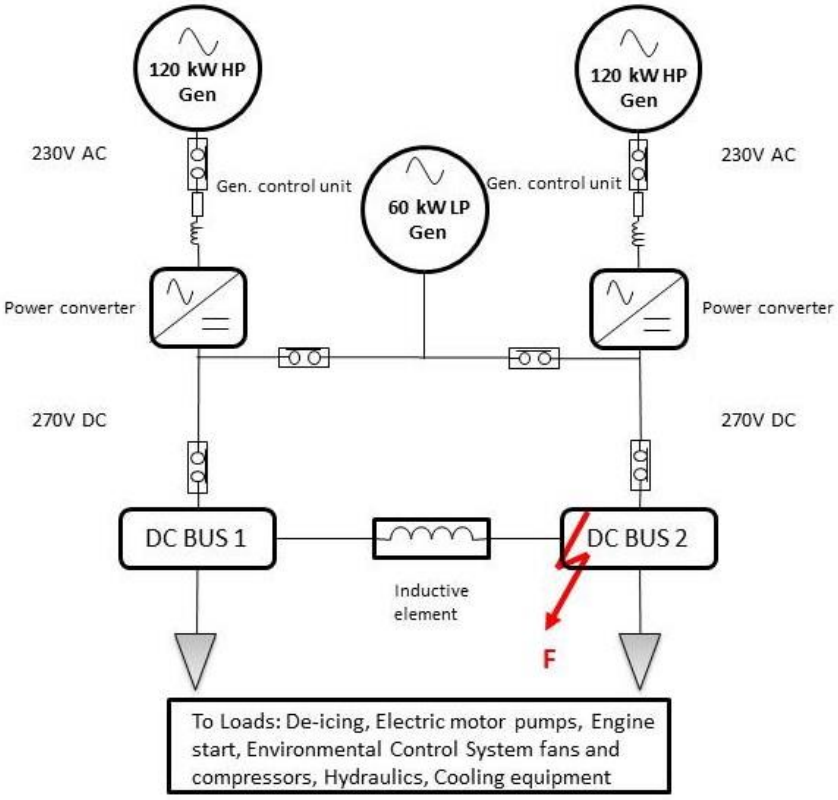

Figure 58. Implementation of interconnecting inductor in multi-shaft power offtakes embodiment proposed by Kern in [130].

For this power network, voltage compliance of the non-faulted bus via the implementation of an inductive interconnecting component appears to be retained only for a fault-clearance time of 2 µs. For slower fault-clearance times and given the topology of this network, the voltage profile of the non-faulted DC Bus 1 cannot be buffered against the fault-response of the generators and subsequent disturbance

Table XXII. Network model parameters paralleled twin-bus electrical power system

Parameter	Value
Rated power	300 kW
HP/LP generator rating	120 kW / 60 kW
Operating voltage	270 V DC
Nominal HP current	444 A
Nominal LP current	222 A
Feeder resistance	0.801 mΩ/m [9]
Feeder inductance	0.65 μ/m [9]

Table XXIII. Inductance ratings for normal compliance of Kern patent power system

DC Architecture	Fault-clearance time	Inductance rating
Kern *et al.*	5 ms	-
Left bus	1 ms	-
	0.5 ms	-
	0.1 ms	-
	0.02 ms	0.025 mH

propagation. This is attributed to the existence of an alternate, lower-impedance fault-current flow route from the left HP generator, via the closed contactors of the LP generator, to DC Bus 2 that bypasses the interconnecting inductor.

To mitigate the additional power-flow route in this network, two alternate implementations of inductive components were tested, as illustrated in Fig. 59. In option A (left), additional interconnecting inductors are placed at the terminals of the LP generators, whilst for option B (right), the interconnecting inductors are installed at the input terminals of the DC buses. For either design option, all three interconnecting inductors installed within are assumed to be equally rated. The necessary inductance ratings to achieve normal voltage compliance for design options A and B are presented in Tables XXIV and XXV respectively.

From these results, it is apparent that the installation of additional inductive elements results in the attainment of normal voltage compliance for all fault-clearance times considered. Moreover, design option B appears to require less interconnecting inductance to retain normal voltage compliance in comparison with option A, for all fault-clearance speeds simulated except for 2 μs. Lastly, both design options feature the same nominal generator outputs and require the same number of interconnecting inductors as with the candidate three-bus HP/LP DC architecture presented in

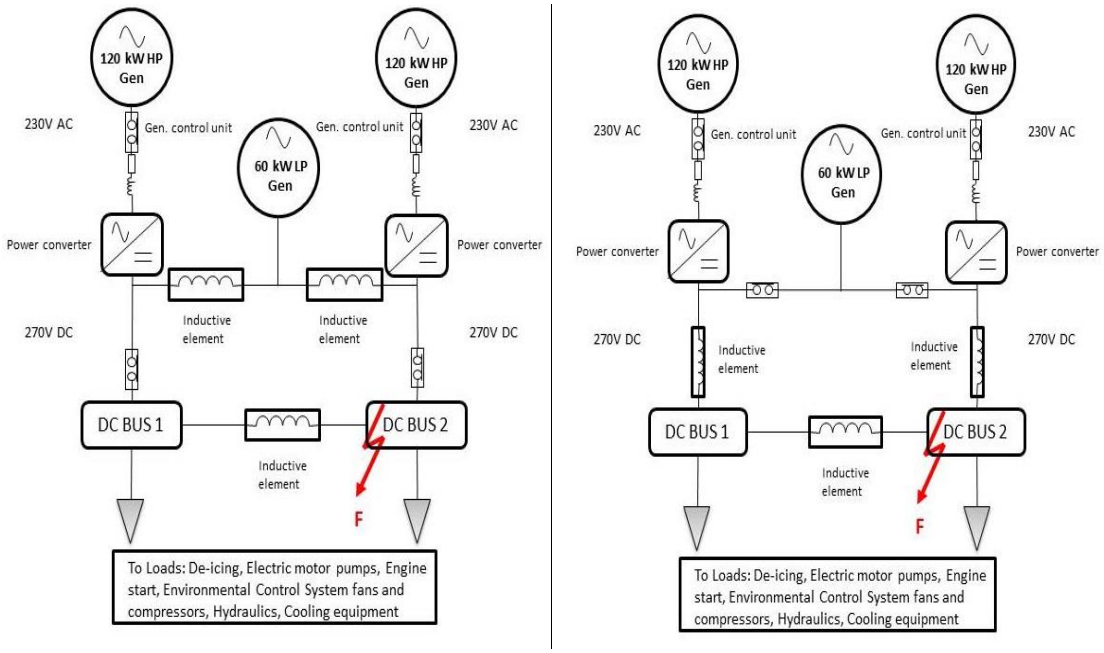

Figure 59. Alternative proposals for the implementation of inductive interconnections on the Kern patent using additional inductors at the terminals of the LP generator (design option A, left), and at the input terminal of the DC buses (design option B, right).

Table XXIV. Inductance ratings for normal compliance of Kern patent option A power system

DC Architecture	Fault-clearance time	Inductance rating
Kern *et al.*	5 ms	14 mH
Option A	1 ms	2.5 mH
	0.5 ms	1.5 mH
	0.1 ms	0.5 mH
	0.02 ms	0.025 mH

Table XXV. Inductance ratings for normal compliance of Kern patent option B power system

DC Architecture	Fault-clearance time	Inductance rating
Kern *et al.*	5 ms	12 mH
Option B	1 ms	2 mH
	0.5 ms	0.8 mH
	0.1 ms	0.2 mH
	0.02 ms	0.03 mH

Section 5.4, however with significantly larger required ratings, with the exception of a 2 µs fault-clearance time. This would suggest that although some weight savings can be achieved by the reduction in the multitude of DC buses, these savings are counteracted by the larger inductance ratings required.

5.8 Chapter summary

This chapter focused on the design and implementation of effective smoothing reactors, capable of achieving normal and steady-state voltage compliance for candidate DC architectures under full-load conditions. Simulations showed that shunt capacitance had an adverse effect on the bus voltage during an electrical fault, subsequently purely inductive interconnecting solutions were further pursued.

This chapter highlighted the two main variables which impact the size of inductance required to achieve bus-voltage compliance: the type of voltage compliance required and the operation speed of the protection system. It was demonstrated that steady-state compliance incurs a twofold to threefold added weight penalty in comparison to normal voltage compliance. Additionally, for all simulated architectures, it was shown that faster fault-clearance times reduce the amount of inter-bus inductance required for any type of compliance, thus significant weight reductions can be realized with fast-acting protection systems. It was also identified that inductive interconnections cannot be used in conjunction with protection equipment with tripping times of 10 ms or greater, creating significant implications for EMCBs with slow tripping times.

To assess the feasibility and applicability of this interconnecting solution approach on airborne platforms, a mass estimation study quantified the weight penalty incurred on the modelled architectures. Additionally, several beneficial and adverse aspects of the implementation of inter-bus inductors were discussed, including bus-voltage quality and imbalanced generator operation. To exploit benefits afforded by load optimization schemes in interconnected power systems, additional inductance ratings for partial generator loading were presented.

It was also shown how inductive solutions have the potential to influence architectural design, as strictly in terms of system mass, it would be more beneficial to combine groups of smaller generators (‘two twin-bus DC architecture), and thus DC buses, into separate channels than opting for fully interconnected DC systems (four-bus DC architecture). At the same time, inductive solutions have the potential to influence electrical machine selection (with regards to HP/LP generators), as it was demonstrated that within an architecture, the main contributor to the need for bigger-rated inductors is not the variance in power mismatch between generation source types, and thus the kind of shaft from which power is off-taken, but the greatest nominal power value of the available generators. Lastly, the feasibility of the proposed solution approach was examined on novel, parallel-generation networks within the relevant literature.

Chapter 6

Discussion on alternate airworthiness power-quality requirements

This chapter will present equivalent airworthiness-standards and power-quality interpretations that may be afforded by the employment of inductors as interconnecting mechanisms. It will illustrate how an electrical fault can be perceived as a normal transient by the non-faulted parts of the power system, and discuss the subsequent implications of this on generation sources and essential loads. A direct consequence of this will be the need to re-evaluate the definition of independent power sources within the framework of interconnected networks. Also, it will briefly address several key factors that distinguish conventional aircraft from MEA/E, and consequently argue the need for dedicated paralleled-generation power-quality requirements for MEA/E.

To this end, four candidate voltage envelopes will be presented and the impact of these envelopes on the feasibility of the inductive interconnecting solutions necessary for compliance will be estimated. It will be shown that extremely fast protection operation speeds have the potential to facilitate compliance of interconnected power systems with these candidate voltage envelopes without the need for bus-interconnecting mechanisms. Lastly, the implications of certification compliance of partially-paralleled systems with regards to critical-load segregation and ‘hybrid’-mode generation will be briefly presented, and it will be shown how such topologies can constitute a compromise between the higher levels or reliability required by a subset of on-board loads and the engine operability and fuel efficiency benefits offered by more-interconnected electrical architectures.

6.1 Alternative interpretation of power-quality requirements with regards to electrical faults

In Section 3.1, it was stated that the on-board electrical system must operate in isolated mode when the aircraft is on approach to land [91], even for systems capable of paralleled generation such as on the B747, so that the multiple autopilot systems are respectively provided with from independent power supplies. In this manner, a fault on any one supply channel would only affect the operation of the respective autopilot system, but not the operation of the remaining channels and autopilot systems, thus allowing for the higher levels of redundancy and reliability that are demanded by the autoland system. The provisions for multiple independent power supplies can also be further extended to all flight critical systems that demand stricter power-quality restrictions for proper operation during relatively more crucial flight phases.

It was also mentioned in Section 5.4, that for short-circuits at particular fault locations in an interconnected electrical network, the power system does not have to perform bus isolation actions or reconfiguration, as the voltage profile of the non-faulted parts of the network remains within the defined normal-compliance voltage limits. Practically therefore, the healthy sectors of the network do not experience an electrical fault and the subsequent voltage-disturbance propagation, but instead, a permissible-by-the-standards normal voltage transient. The way in which an electrical fault can be interpreted as a normal transient by the non-faulted parts of the power system raises the following questions.

- Since an electrical fault is ‘transformed’ into a permissible transient for the non-faulted parts of the power system, does this imply that there are no longer any higher reliability and redundancy issues for the autopilot systems, or any other flight-critical services, if they are powered from non-independent power supplies?

In the case of non-independent power supplies, an electrical fault would affect any one supply channel and the respective autopilot system, as in the isolated-network configuration of the autoland system, whilst the remaining supply channels and autopilot systems would adhere to the normal-compliance voltage limits. At the same time, redundancy is thought to be retained as multiple generation sources continue to power the remaining autopilot systems.

- Are the normal-compliance voltage limits, with an initial voltage range of 200 V- 300 V, sufficiently reliable or tight enough, so that operation of autopilots or other flight-critical services is not compromised or impaired?

If indeed these limits are sufficiently functional and reliable, then this would enable the electrical network to continue to operate under parallel generation mode even during the approach and landing segments of the flight cycle. During these flight segments, relatively low amounts of thrust are demanded from the engines, and engine designs that extract all necessary electrical power from the HP shaft negatively affect engine stability and performance, as described in Section 3.3.1. Paralleled-generation networks however, paired with HP/LP generation systems, may take advantage of the benefits afforded by multi-shaft off-takes, such as improved engine operability and reduced fuel consumption, even during the approach and landing segments of the flight.

Parallel operation of the electrical system could potentially be maintained during other critical flight segments, such as take-off and/or go-around after a missed approach. In both of these critical segments, high amounts of thrust are demanded from the engines, therefore engine stability would not negatively affected even by designs that extract all necessary electrical power from the HP spool. Additionally, for these flight segments, it is assumed that any major failure-event originating from an electrical fault, i.e. a loss of engine, would have taken place regardless if the electrical system was operated in parallel or isolated mode. Nevertheless, the benefits granted by interconnected generation and multi-shaft off-takes during all flight segments will have to be weighed against the larger mass penalty that over-rated protection equipment incur on the power network.

- If the normal voltage envelope does not provide the increased reliability required, can the tighter voltage envelope of steady-state compliance (250 V – 280 V) allow for uncompromised operation of the autoland system or other flight-critical services?

If so, then suitable inductive solutions rated for steady-state compliance may be used as interconnecting mechanisms, therefore permitting the power system to remain interconnected potentially throughout the entire flight cycle. Again, in this manner, an electrical fault would affect any one supply channel and the respective flight critical systems, as in the isolated-network configuration of the autoland system, whilst the remaining supply channels and autopilot systems would adhere to the steady-state compliance voltage limits. From this perspective however, the benefits granted by interconnected generation and multi-shaft off-takes will have to be weighed against the larger mass penalty that adherence to steady-state compliance incurs on the power network, and the necessary larger-rated protection equipment.

If the 30 V variation of the steady-state compliance envelope still does not permit the unobstructed and reliable operation of flight-critical services, then perhaps these systems must be powered from independent circuits/channels at all times. Yet, if the strictest power quality issues lie solely within a limited number of flight-critical systems, then these systems can remain isolated throughout the flight (powered from certain non-paralleled offtakes/spools), whilst allowing the rest of the network to remain under parallel generation mode even until landing. Although such critical systems are of great importance to passenger and flight safety, they are limited in numbers compared to the multitude of electrical circuits on-board MEA/E.

Lastly, if the apparently unmovable constraint of independent power supplies is dominating the operation of the autoland system, then perhaps the definition of ‘independent power supplies’ in the framework of interconnected networks must be re-evaluated, as will be addressed in the next section.

6.2 Alternative interpretation of standards with regards to independent generation sources

The requirements set out by airworthiness standard CS-25 regarding on-board electrical generation sources were presented in Section 3.2.2. At this point, it is useful to briefly revisit several key points in order to provide a foundation for subsequent discussions. The following sections will address and consider, point by point, the current interpretation of independent generation sources and their supply to essential loads, with regards to paralleled power systems. In particular, the general requirements that govern power-source design are briefly presented, and the effect of interconnected generation schemes on the proper operation of essential loads is discussed. The last section debates three possible interpretations of power-source independence that could be offered within the current regulatory standards.

6.2.1 General provisions for power sources

CS 25.1307 requires that aircraft electrical systems have two or more independent sources of electrical energy, excluding batteries and other emergency sources, this way avoiding a single-point-failure in the supply network. According to CS 25.1351, these power sources must function properly when independent and when connected in combination, and that the system voltage and frequency at the terminals of all essential loads is maintained within the limits for which the equipment is designed, during any probable operating conditions. Also, from CS 25.1310, the ability of the remaining power sources to supply essential loads should not be impaired following the failure or malfunction of any power source. CS 25.1355 stipulates that for particular systems or equipment that need two independent power supplies for certification, or by operating rules, an additional, separate power source must be manually or automatically selectable to maintain system or equipment operation. Lastly, CS 25.1431 requires that electronic equipment must be designed and installed

such that they do not cause essential loads to “become inoperative as a result of electrical power-supply transients or transients from other causes”.

Although not directly relevant to the requirements regarding generation sources, additional limitations within CS 25.1165 and 25J1165 demand that main engine and APU ignition systems “are independent of any electrical circuit that is not used to assist, control, or analyse the operation of the system”. For an uneventful flight, engine ignition systems are only required for starting the engine, since once combustion has begun, engine operation is continuous. Nevertheless, it would appear that these types of loads must, by design, remain isolated from the remaining network at all times.

The requirements and provisions necessary for essential loads have shaped modern aircraft architectures into having multiple isolated supplies. It has also been established that an interconnected aircraft electrical system is exposed to larger voltage-disturbance propagations during electrical faults, as the paralleling of generation sources reduces the degree of isolation in the network. However, it has also been demonstrated that inter-bus inductive solutions have the potential to transform these voltage disturbances into normal or steady-state voltage transients. Therefore, it is worth examining the implications of this on the key points set out by the standards regarding generation sources and power supply to essential loads.

For the purposes of this discussion, even if the required inter-bus inductors are perceived as ‘electronic equipment’, as they help stabilize the bus voltage and buffer against inter-bus fault-current flow, it can be argued that their deployment does not cause essential loads powered from the non-faulted buses to become inoperative. Inevitably in an interconnected system, these essential loads would experience a normal or steady-state transient during an electrical fault originating from a different bus, but the effects of these transients on the operation of flight-critical loads can be mitigated, as discussed in the previous section.

6.2.2 Proper function of power sources and essential loads

With regards to the ability of the remaining power sources to supply essential loads following the failure or malfunction of any power source, it can be argued that it is not impaired, both for AC and DC generation systems. In MEA/E, AC generators and buses are kept isolated due to the variable frequency characteristic of novel generation systems, subsequently a fault at the AC level directly affects the respective AC generator and bus, and potentially other devices downstream, but not the remaining isolated AC power sources. At the interconnected DC level, a failure or malfunction of a power source that leads to that power source being dropped offline is believed to be ably sustained, as the existing power sources can maintain power to the DC buses, by potentially increasing their power output and shedding of non-essential loads if needed. For a failure or malfunction of a source that is attributed to an electrical fault, suitable inductance ratings have the potential to retain normal or steady-state compliance of the healthy DC buses during the fault, therefore a permissible voltage transient is not thought to be capable of negatively affecting the ability of the remaining sources to supply essential loads.

It will also be assumed that ‘proper function’ of generation sources when independent and when connected in combination implies operation compliant with the power-quality requirements set out in MIL-STD-704F. The identification of suitable inductive components appears to permit the lawful interconnection of DC generation sources, therefore it can be argued that ‘proper function’ can be warranted in this manner. The necessary provisions that require all essential loads to be provided with voltage within the limits for which the equipment is designed have been addressed in the previous section, and as frequency limits are not applicable to the DC segments of the power network, they will not be further discussed.

For the inductive-interconnections approach proposed within this research for interconnected networks, it can be argued that there do not appear to be any unmovable constraints against the key points dictated by the standards with regards to generation sources, except for the requirement for two or more independent power sources, which is also embedded within the conditions of CS-25.1355. In the pursuit

of standards-compliant paralleled systems that may be entirely operated in interconnected mode throughout the flight cycle, the clause for multiple independent power sources, and subsequently their electrical supply to specific types of loads, may be interpreted as a firm restraining factor. This might not be the case however, as will be explained next.

6.2.3 Definitions of power-source independence

An initial step would be to define what independent power sources are, and within which context, i.e. mechanical, electrical, structural. Within the current airworthiness standards of CS-25 for large turbine-powered aircraft, there does not appear to be a precise definition of power source independency. Some speculation may be offered however in the certification specifications in Book 1 of CS-23 [244], an airworthiness standard relating to, among others, propeller-driven twin-engine commuter aircraft of up to 19 passengers. Although its action area does not apply to large passenger jetliners, it may aid in defining what independent generation sources are at least for smaller passenger airplanes.

CS 23.1331 sets out the requirements governing electrical system design, with similar provisions for instrument and power supply systems as of those for larger, turbine-powered aircraft. CS 23.1331(c) however stipulates that “there must be at least two independent power sources (not driven by the same engine on twin-engine aeroplanes)” and that there must be a means to either manually or automatically select between each power source. These requirements would suggest that regardless of the multitude of engines, airplanes must have at least two independent sources of power, with an additional provision for twin-engine aircraft, as on single-engine airplanes there is no other option other than to have potentially several generators being driven from a single engine off-take. From this, it can be concluded that independent power sources are not defined as those sources of electrical power that are driven from different engines, with regards to some kind of mechanical-power delivery, therefore electrical independence must be implied.

Consequently therefore, it can be argued that aircraft electrical systems must have at least two or more electrically-independent power sources, and load-types requiring two electrically-independent power sources for certification, or by operation, must manually or automatically be able to be provided with an additional, separate power source. The next step would be to define what 'electrical independence' is, and for this, two definitions may be the most plausible. The first, is the conventional interpretation of the definition, in which generation sources and type-essential loads are completely isolated electrically, and with no common feeders, as is the current norm for the autoland systems during approach to land. However, this interpretation would be a direct contradiction to the applicability of paralleled generation on-board current platforms such as the B747.

The second definition may be found within Amendment 5 of CS-23 [245], in which CS 23.2430 regarding power-plant installation, energy storage and distribution systems, states that these systems must "be designed to provide independence between multiple energy storage and supply systems so that a failure in any one component in one system will not result in the loss of energy storage or supply of another system". This 'provision' of independence could imply that even paralleled generation sources can be considered to be independent as long as there are some protection mechanisms or infrastructure in place that can provide the necessary electrical isolation when such a failure occurs. This interpretation of source independence appears to be more suited to past and current interconnected-generation power systems on-board larger, turbine-powered aircraft. Granted that paralleled systems are permitted to function as such on several aircraft, like the B707, B727 and B747, this would appear to be the most dominant interpretation of power source independence.

Moreover, this particular interpretation of the definition of independent power sources does not appear to be contradicted by the power-quality requirements. The first Military Standard to be issued by the U.S. Department of Defence in 1959, MIL-STD-704 [246], which standardized military aircraft power quality requirements for 115/200 V AC and 28 V DC systems, does not make mention of a requirement for independent power sources during normal operation conditions of the electrical

system. In Section 7.3 however, it does stipulate that in the emergency operation case where the primary electric system becomes unable to supply electrical power, “a limited independent alternate source of power is required”. A similar provision for emergency power generation was included in Section 3.10 of MIL-STD-704B [247], released in 1975, however the limited electric source is characterized as “often independent” from the main generation system, implying that even emergency generation options do not have to be isolated form the main network. In the current MIL-STD-704F however, emergency generation sources have to remain isolated from the main generation system.

Indications of an even more relaxed interpretation of power source independency were provided within the Military Specification MIL-E-7016 [248], covering requirements and methods governing the preparation of AC and DC electric load and power source capacity analyses for military aircraft, which was published in 1976 and last validated in 1988 [249]. In Section 6.2.3.1, it is stated that an electrical power source “may consist of multiple unit sources operating in parallel”, suggesting that multiple generators driven from the same engine may be combined into and perceived as a single power source. However, these specifications are believed to have only applied to U.S. military aircraft, as there appear to be no evidence suggesting that these requirements were adopted by civilian aircraft at any time.

Overall however, the interpretation that independent sources consist of those power sources that have the ability to be isolated on demand, provided that there are adequately-rated protection mechanisms in place capable of attending to the greater protection challenges caused by the paralleling of generation sources, appears to comply with the current power-quality requirements and the airworthiness standards. This, paired with mitigating measures relating to the operational safeguarding of essential loads, presented in the previous section, appear to remove the firm constraints that were believed to be unmovable regarding interconnected power systems.

A third, novel definition of source independency can be argued, where generation sources may be coupled in such a way that the operational conditions of one generation source do not impair or affect the operation of the remaining sources out

with pre-defined limits. In effect, this would mean that although several generation sources would be physically coupled via appropriate interconnecting mechanisms, the electrical behaviour and transient response of these sources would be electrically decoupled, consequently therefore be considered as 'electrically independent'. If this would be achievable, then type-essential loads could be powered from a multitude of interconnected but 'electrically independent' generation sources throughout the various flight segments. In essence, perhaps the most appropriate question that could be raised is:

- Does the electrical decoupling of paralleled generation sources, potentially in accordance with some type of power-quality compliance, render them independent?

It is likely that there is no clear and easy answer to this. Even in the case where the electrical power system is able to function properly within an interconnected but 'electrically isolated' manner for certain fault types and locations, the repercussions of this on the operation of other major aircraft systems that will inevitably be affected have to be further investigated. After all, civil aircraft are comprised of such a large multitude of complex heterogeneous components and systems, where possible adverse interactions between different systems regarding performance and safety implications may be difficult to be mapped or anticipated beforehand [90, 250, 251].

Nevertheless, it can be argued that regulatory standards are by nature, first, open to interpretation, and second, have to be broad enough to cover all aspects and provide guidance within a discipline, but at the same time without restricting progress and limiting innovation. Relevant providers are responsible in achieving or complying with specific discipline expectations, but unless explicitly stated, providers should be free to determine how this would be done. It has been stated previously that there is no dedicated airworthiness standard governing the operation of interconnected electrical networks. Additionally, the exploitation and implementation of technological advances in the field of civil aviation and passenger aircraft, such as the MEA and AEA concepts, paired with novel paralleled-generation schemes, could risk having to be based on established standards that may potentially be antiquated or inappropriate. The next section will attempt to address the suitably of existing

airworthiness standards with regards to MEA/E and discuss the need for dedicated interconnected-generation power quality requirements.

6.3 Discussion on the suitability of existing standards for MEA/E

It was seen that within the current airworthiness standards, electrical sources are permitted to operate in parallel arguably under two main conditions, first that power sources ‘function properly’ when doing so and in a manner that does not impair the operation of the remaining power sources, and second, granted the electrical system has the ability to reconfigure itself and operate under isolated generation conditions when necessary (i.e. electrical fault, activation of autoland system). Although airworthiness standards incorporate several provisions regarding the paralleling of generation sources, power-quality requirements specified within MIL-STD-704F do not draw notable distinctions between isolated and interconnected sources or architectures. Therefore, the quantitative restrictions on power quality, such as the normal and abnormal DC voltage-transient envelopes, will have to be satisfied by any architecture, regardless of the topology of the generation system.

Consequently, it can be assumed that the electrical systems of airborne platforms that feature paralleled generation must adhere to the abnormal-operation power requirements under fault conditions, even when interconnected. Some evidence of this can be found in the ARINC Report 413A [252], prepared by the Airlines Electronic Engineering Committee in 1989, whose purpose was to provide guidance for electrical power utilization and transient protection, and also industry interpretations of the MIL-STD-704B, which was current at the time. The report considers AC and DC short-circuits, as well as their subsequent clearance by protection devices, to be abnormal operation of the electrical system, and as such, the less strict abnormal transients limits should be adhered to.

Additionally, Appendix 4 of the report presents the capabilities of the protection system and observed transient behaviours of the B747, without however explicit mention of the model variant. Nevertheless, it is stated that AC faults inside differential current protection zones can be cleared within 40 ms or 115 ms, depending on the exact fault location, and faults outside of these zones can be cleared within 3 s via thermal circuit breakers. During normal operation, the generators function in paralleled mode, where a loss of the excitation system or an open contactor has the potential to reduce the voltage to zero. These "undervoltage conditions on all buses simultaneously are limited to 4 seconds, although a given channel may be subjected to an abnormally low voltage for up to 10 seconds". With regards to the 28 V DC system, low impedance faults that may cause the voltage to collapse to near zero are typically isolated from un-faulted bus sections within 0.3 s and removed in no more than 3 s.

Lastly, a summary of observed AC and DC transient behaviours is presented, accompanied with a recommendation to avionic equipment designers to carefully consider the transient and frequency characteristics of the electrical system in the design of aircraft avionics. It is stated that any transients on the 115 V AC level, owing to load application and removal, as well as AC power source transfers, will result in disturbances at the TRU input terminals, and subsequently, the transients will be injected into the 28 V DC system. With regards to the magnitude and duration of these transients, it was seen that the AC system voltage may approach 175 V for small fractions of a second, spike to 600 V for several microseconds and collapse to almost zero for up to 10 seconds. Similarly, the DC system voltage may go up to 42 V for small fractions of a second, reach 600 V for a few microseconds and be as low as zero for up to 10 seconds.

It is apparent from Report 413A that the entire interconnected power network of the B747 had to adhere to the abnormal voltage limits during an electrical fault and subsequent fault-clearance procedures. This could expose non-faulted paralleled AC parts of the network to undervoltage events with potential durations of up to 4 seconds. The network-wide propagation of fault events sustained for such large durations could have detrimental effects on the operation of all connected loads,

whether flight-essential or not. It could be argued that the operational speed of the protection system on-board the mentioned B747 variant was subject to technological limitations of its time, and that new designs incorporating more recent advances in the field of electrical protection may have significantly reduced the time that is needed to complete fault isolation and clearance actions, however, perhaps the most important issue remains, airplane electrical networks have evolved significantly since then as well.

Technological advances in the field of civil aviation and passenger aircraft, such as the MEA/E concept, have brought with them a broader electrification of on-board systems. Electrical systems are now responsible for functions that previously required mechanical, hydraulic or pneumatic power sources, with a subset of these functions being critical or essential to the continuity and safety of the flight. For example, modern aircraft feature electric actuators and pumps for trim control, which also serve as backup for secondary control-surface actuation, and also electronic systems that work in conjunction with hydro-mechanical controls to operate the turbofan engines. On the B757 for example, there is no mechanical link between the throttle levers in the cockpit and the Pratt and Whitney 2037 engines, as the engine actuators are controlled by a dual-channel digital computer [253], thus a significant part of the electronics have to remain operative for the engine to work [254].

To supply the growing electrical demand of on-board systems, modern jetliners are generating ever-increasing electrical energy, which in turn, has made their power networks larger and more complex. The B747 features two voltage types, for main 115 V AC and secondary 28 V DC systems, while modern MEA may utilise up to four voltage types, for main 230 V AC and secondary 115 V AC systems, as well as DC distribution systems of 270 V and 28 V. The increased complexity of such electrical networks not only requires significant design undertaking to ensure proper and reliable systems operation, but also poses considerable challenges with regards to the thermal management of the heat emitted by the plethora of electrical mechanisms on-board. In restricted environments, such as those typically encountered in aerospace applications, keeping component temperatures within

operational limits, in turn requires complex cooling mechanisms which increase the weight and cost of the system [255].

As well as more electric, modern aircraft have also become more digitalized. The glass cockpit concept facilitated the replacement of analogue gauges and dials with multi-functional display screens, although a few analogue systems are retained as backup [256]. Traditional gyroscopic instruments have been replaced by computer-driven reference systems and satellite-linked GPS receivers aid conventional inertial systems used for navigation [257]. Digital computers have replaced analogue equivalents within flight-management information systems, which simplified aircraft operation and navigation, thus improving the situational awareness of pilots, and also eliminated the need for a flight engineer inside the cockpit. The computational benefits afforded by digital systems enabled the replacement of 17 analogue flight computers on the A310 with 9 digital computers, and the subsequent reduction to 4 and 2 digital computers on the A320 and A330/340 respectively [258].

Modern aircraft also contain large amounts of software and code, which on the A 380 is distributed over 1,000 on-board systems [259]. Within these systems, embedded microprocessors and controllers have provided an unprecedented and affordable opportunity to monitor and manage systems and platform health, thereby enabling diagnostic and prognostic capabilities [260]. These capabilities have reduced maintenance and lifecycle costs for the operator, however the progression to software-intensive digital systems has led to the surfacing of a new issue, the no-fault-found problem [261]. As maintenance crews are faced with a myriad of 'black boxes' full of micro-electronics, one or more of which may not be performing properly, visual inspections previously used to easily identify faults within mechanical of pneumatic systems are now obsolete. Subsequently, maintenance work may be limited to guesswork and unnecessary replacement of boxes, later found to be working properly or not being able to reproduce the fault.

To safeguard the operation and longevity of digital devices and circuits, one mitigating measure would be to protect such equipment from transient events. Although permanent damage to electronic devices can occur from potentially uncontrollable transients caused by lightning strikes [262], such devices can be

shielded from transients caused by the operation of the power system, either through better protection afforded by advancements in PDUs and arc-detection algorithms [260], or by stricter power-quality requirements [263]. Although avionic equipment have experienced significant growth in terms of reliability and performance, they are still bound to large voltage transients and long power interruptions permissible by MIL-STD-704F.

Current platforms such as the B787 have reached nominal power ratings of approximately 1 MW, with future AEA concepts featuring electric propulsion expected to require even more power-dense generators, capable of producing of up to 48 MW of electrical power [264]. Electric propulsion itself will require the development and maturation of new technologies, one example being superconductive machines [265], as conventional means cannot meet the weight and volume requirements with current power-density levels [266]. Moreover, it is expected that the interconnection of generators and motors will be necessary in order to redirect power in case of a failure within a part of the system.

Whether for the MEA or AEA concept, novel paralleled-generation schemes would bring an even greater electrical unification on aircraft platforms, with greater protection and power-quality challenges in comparison with isolated topologies. The exploitation and implementation of such innovative designs however, could risk having to be based on potentially antiquated or inappropriate established standards. In order to meet the ever increasing regulatory and customer demands for safety and reliability, new certification and safety standards will be required for these electrical systems [255].

One example of aircraft operation where increased reliability is demanded is under Extended Operations (ETOPS), which allow airplanes to fly routes that are within a certain amount of flight time between diversion airports under single-engine inoperative conditions. In the past, twin-engine aircraft routes had to be within 60 minutes of flight time under single-engine cruising speed from a diversion airport, while three- and four-engine airplanes had to be within 90 minutes of an alternate airport at single-engine-inoperative cruising speed. This favoured wide-body jets

such as the four-engine B747 and the three-engine MD-10 for trans-Atlantic and trans-Pacific routes.

After 1985, aircraft certified for ETOPS could fly extended routes regardless of number of engines, but within their flight time certification. Over the years, this has made twin-engine aircraft eligible for up to 180 minutes of flight time, and three- and four-engine aircraft for up 240 minutes [267], with new platforms such as the A350 achieving a 370-minute ETOPS [268]. ETOPS certifications however bring additional provisions with regards to fuel reserves, maintenance procedures and pilot training, and also demand the rigorous operational approval of many systems, relating to communication equipment, cargo-fire suppression systems and others [269]. However, they do not bring additional provisions regarding the operation of the electrical system, nor about the quality of electrical power that would be required under the more critical single-engine-inoperative conditions.

Overall, the power quality requirements did not change following the entry into commercial service of several interconnected platforms, such as the B707 and B747. Perhaps it would be unreasonable for regulatory standards to change for every new aircraft platform that is designed and built, however it could be argued that requirements may have to be adapted when considerable step changes in technology and design philosophy are made. Within this section, several key reasons that could justify the need for dedicated paralleled-generation requirements for MEA/E were briefly addressed. The next section will discuss what these potential requirements may be, particularly with regards to candidate voltage envelopes.

6.4 Candidate voltage envelopes for paralleled-generation MEA/E

Since it was first issued in 1959, MIL-STD-704 has undergone many revisions over the years, incorporating inclusions related to increasing AC voltages and the introduction of the 270 V DC bus. However, even in the latest version of 704F which

was released in 2004, there is no dedicated voltage envelope for interconnected systems. Given the greater electrification of on-board systems on MEA/E, and the more perplexed power-quality and protection issues brought on by interconnected networks, this section will present three novel voltage envelopes, as well as the 'normal transient' envelope, as a potential dedicated set of requirements for paralleled generation MEA/E. Additionally, the impact of these voltage envelopes on the feasibility of interconnected generation across different fault-clearing speeds will be evaluated. Simulations will show that for a proposed voltage envelope, fast-acting protection can maintain power-quality requirements compliance without the need for any type of interconnecting mechanism. This would suggest that a potential change in regulatory standards, paired with advances in the field of protection equipment, could facilitate the interconnection of power channels with no added weight penalty, other than that of suitably-rated protection devices.

6.4.1 The normal requirement

In the ARINC Report 413A, AC and DC short-circuits on paralleled-generation networks were considered as abnormal transients, and as such, the entire network had to comply with the abnormal transient voltage limits. In Section 6.3, it was argued that these loose voltage requirements may not be adequate in safeguarding the proper operation of interconnected MEA/E systems. To ensure the unobstructed operation of flight-essential loads, a logical requirement for interconnected MEA/E networks would be that during an electrical fault, the faulted part of the power system complies with the abnormal transient limits, but adjacent, non-faulted segments of the network adhere to the normal voltage transient limits. This candidate requirement was the basis on which the simulation studies in Section 5.2.1 were carried out, subsequently suitable inductance ratings have already been identified and their potential weight has been estimated.

6.4.2 The 5 millisecond ride-through requirement

In Section 6.3, it was seen that AC and DC transient behaviours of the power system may expose electrical components and loads to large transient events of short duration. Consequently, it may be assumed that to some degree, anticipated transient and frequency characteristics are factored into the design of avionics and electrical equipment by respective manufacturers. If large disturbances of short duration can be tolerated by electrical equipment, thus ensuring continuity of service, this could open up the possibility of a power-quality requirement that permits the voltage to considerably overshoot currently-established peak values and collapse to zero for a specified small time-duration, but recover quickly enough so that the operation of the power system in not impaired.

In this approach, the non-faulted part of the interconnected network would experience a significant, but very brief and assumedly sustainable voltage disturbance. However, several key issues that arise from the implementation of this approach include the uncertainty surrounding the order of tolerable magnitude of disturbance caused by the electrical fault, and its subsequent impact on the operation of digital flight control and other avionic systems.

Relevant systems that require very high levels of functional integrity and reliability, such as the Fly-By-Wire assembly, are typically designed in such a way that uninterrupted control may still be provided following a specific number of failures, but it is not clear what type or how severe these failures may be [270]. Also, the duration of the disturbance may be a critical safety factor, particularly for airborne systems that operate outside the stricter safety requirements of commercial passenger transport. For the Space Shuttle for example, an erroneous flight control command persisting for 10 ms to 400 ms, depending on the flight phase, could lead to a loss of vehicle control [271]. Subsequently, it will be assumed that the order of magnitude of the voltage disturbance and its impact on the operation of avionic systems can be militated against by imposing a suitable upper voltage limit or permitting shorter recovery times.

To this end, an upper voltage limit of 810 V DC is imposed, arbitrarily derived as three per unit of the nominal voltage level of 270 V, and a recovery time of 5 ms is selected for this candidate voltage envelope, as shown in Fig. 60. The upper voltage limit of 810 V DC may appear to be a relatively high limit, however in comparison to the 600 V spike seen on the less powerful electrical system of the B 747 (Section 6.3), is assumed to be acceptable for the greater generation capabilities of MEA/E. The selected recovery time seems to be in accordance with the fault ride-through capabilities of DC converters [272] and the time duration VSC valves can withstand the maximum fault current in multi-terminal DC networks [14]. Aggregated inductance ratings for the 5 ms fault ride-through requirement compliance are summarized in Table XXVI for all DC architectures, and their estimated weight is depicted in Fig. 61. Due to the time frame of this voltage envelope, fault-clearance times greater than 5 ms are discarded.

From these results, it is evident that interconnecting inductors cannot maintain the voltage profiles of the adjacent DC buses within the defined limits for a fault-clearance time of 5 ms, as voltage recovery cannot be facilitated quickly enough in the given time frame. Overall, in comparison with normal transient compliance, voltage compliance with a 5 ms fault ride-through envelope requires considerably smaller-rated inductive components, thus significantly reducing the added weight penalty on the electrical architecture. At the same time, due to the need of smaller-rated inductors, the fault currents through the interconnecting inductors are noticeably higher.

Lastly, it is apparent that for all DC architectures considered, fault-clearance times of 0.02 ms may retain voltage compliance without the need of any additional interconnecting mechanism. This would suggest that if large disturbances of small duration could be tolerated by the electrical system and other essential loads, extremely fast protection operation speeds have the potential to facilitate power-quality requirements compliance of interconnected power systems with no added weight penalty, other than that of suitable over-rated protection equipment.

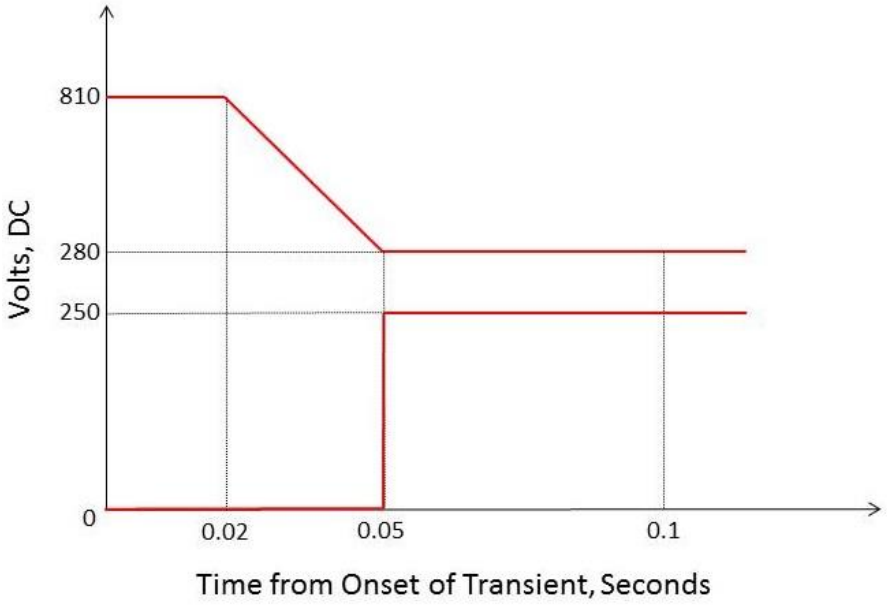

Figure 60. Alternate 5 ms ride-through candidate voltage envelope.

Table XXVI. Inductance ratings for transient compliance with 5 ms fault ride-through voltage envelope

DC Architecture	Fault-clearance time	Fault current through inductor	Inductance rating
2 Bus	5 ms	-	-
	1 ms	556 A	0.2 mH
	0.5 ms	605 A	0.15 mH
	0.1 ms	778 A	0.03 mH
	0.02 ms	830 A	0 mH
3 Bus	5 ms	-	-
	1 ms	771 A	0.25 mH
	0.5 ms	513 A	0.2 mH
	0.1 ms	398 A	0.07 mH
	0.02 ms	1290 A	0 mH
4 Bus	5 ms	-	-
	1 ms	664 A	0.3 mH
	0.5 ms	422 A	0.25 mH
	0.1 ms	200 A	0.15 mH
	0.02 ms	1650 A	0 mH

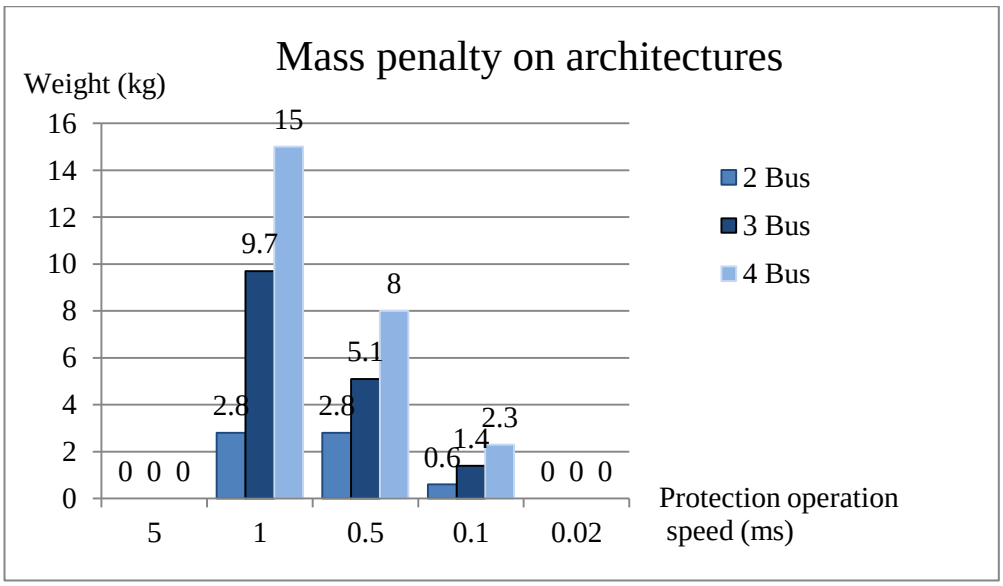

Figure 61. Mass penalty estimation of 5 ms ride-through voltage envelope.

Consequently, the technological maturation of fast-acting, high-power DC protection equipment (i.e. SSPCs), paired with novel power-quality requirements envelopes, could facilitate the most feasible implementation of interconnected-generation schemes on MEA/E in terms of mass penalty.

6.4.3 The 5 millisecond sloped envelope

For the 5 ms fault ride-through requirement presented in the previous section, it was assumed that the electrical system and other loads could tolerate large disturbances of short duration. If however the proper operation of loads and electrical system can be impaired by large transients, an alternate voltage envelope can be proposed, where the maximum permitted voltage is restricted to 350 V DC, as is in the current abnormal transient requirements. Additionally, the permissible voltage collapse for the initial 5 ms is maintained, but the recovery gradient is relaxed, so that the voltage must not be below 200 V after 10 ms and 250 V after 40 ms, as illustrated in Fig. 62. In essence, this sloped recovery time could be regarded as a compromise between the permissible long voltage collapse and abrupt voltage recovery of the current

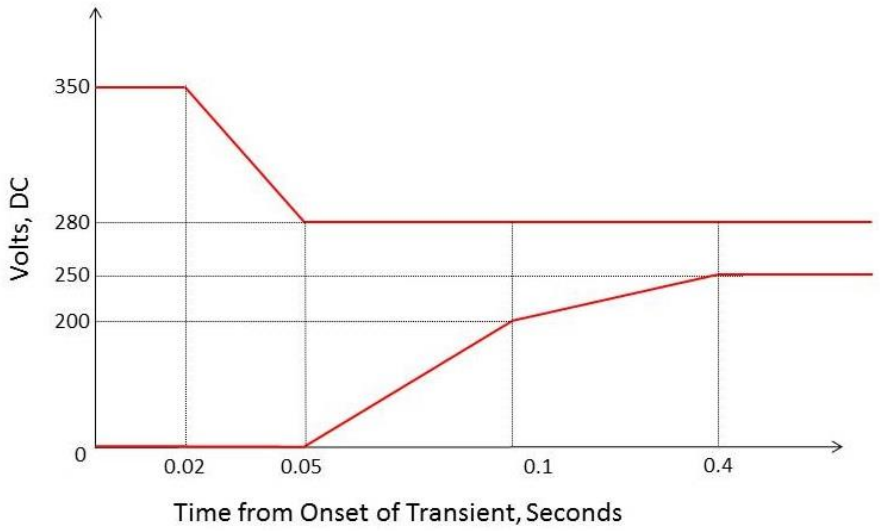

Figure 62. Alternate 5 ms sloped candidate voltage envelope.

abnormal transient limits, and the very short voltage drop and sloped voltage recovery of the current normal transient limits.

The inductance ratings required for compliance are summarized in Table XXVII and their weight estimation is provided in Fig. 63. In contrast to the 5 ms fault ride-through envelope, suitable inductance ratings for protection operation speeds of 5 ms can be identified with these voltage requirements, as the less steep lower voltage limit gradient permits voltage recovery within the given time-frame. Also, in comparison to the normal envelope requirements, it is evident that compliance with this envelope requires considerably smaller-rated inductors, thus significantly reducing the added weight penalty incurred by the interconnecting solutions, which in turn results in noticeably higher fault-current levels. In contrast to the 5 ms ride-through envelope, for extremely fast protection operation speeds, small amounts of interconnecting inductance are required to prevent the bus voltage overshooting the upper voltage limit upon the clearance of the fault.

Table XXVII. Inductance ratings for transient compliance with 5 ms sloped voltage envelope

DC Architecture	Fault-clearance time	Fault current through inductor	Inductance rating
2 Bus	5 ms	551 A	0.3 mH
	1 ms	526 A	0.25 mH
	0.5 ms	604 A	0.15 mH
	0.1 ms	540 A	0.05mH
	0.02 ms	645 A	0.003 mH
3 Bus	5 ms	1925 A	0.3 mH
	1 ms	771 A	0.25 mH
	0.5 ms	513 A	0.2 mH
	0.1 ms	424 A	0.065 mH
	0.02 ms	584 A	0.005 mH
4 Bus	5 ms	1658 A	0.45 mH
	1 ms	664 A	0.3 mH
	0.5 ms	422 A	0.25 mH
	0.1 ms	203 A	0.15 mH
	0.02 ms	331 A	0.012 mH

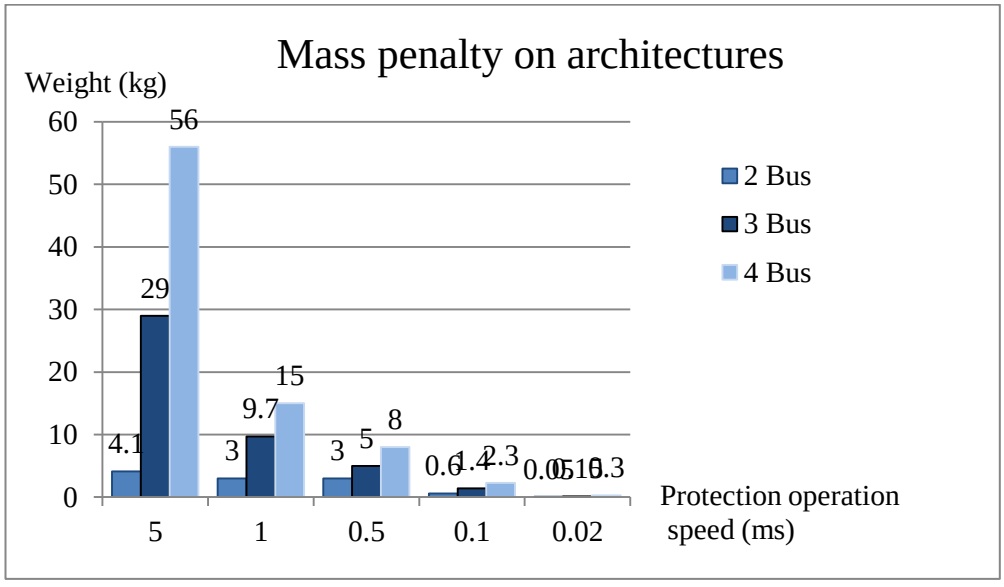

Figure 63. Mass penalty estimation of 5 ms sloped candidate voltage envelope.

6.4.4 25 milliseconds envelope

The last voltage envelope considered in this section is in direct correlation with the operation speed of current protection systems on-board MEA/E. It will be assumed that at the 270 V DC level, bus-interconnecting EMCBs are deployed, capable of breaking and isolating an electrical fault within 20 ms [9]. Subsequently, upon the introduction of the fault, the voltage profile of the paralleled DC buses may collapse for the initial 20 ms until it is cleared by the EMCB adjacent to the fault, and then recover to a lower voltage limit of 250 V within 5 ms, as shown in Fig. 64. In essence, this voltage envelope would create an MEA/E baseline in the case where fast-acting, high-power SSPC equipment are not technologically suitable for the 270 V level.

Suitable inductance ratings for compliance with this voltage envelope are summarized in Table XXVIII, and their weight estimation is depicted in Fig. 65. As with the 5 ms voltage envelopes, 25 ms voltage envelope compliance requires smaller-rated inductors compared to the normal voltage compliance, and presents very high levels of fault current. As in the case of the 5 ms sloped envelope, it would appear that for extremely fast protection operation speeds, small amounts of interconnecting inductance are required to prevent the bus voltage overshooting the upper voltage limit upon the clearance of the fault. Lastly, the similarity in required inductance ratings between the 25 ms envelope and 5 ms sloped envelope is due to the influence of overvoltage conditions on these ratings and not undervoltage.

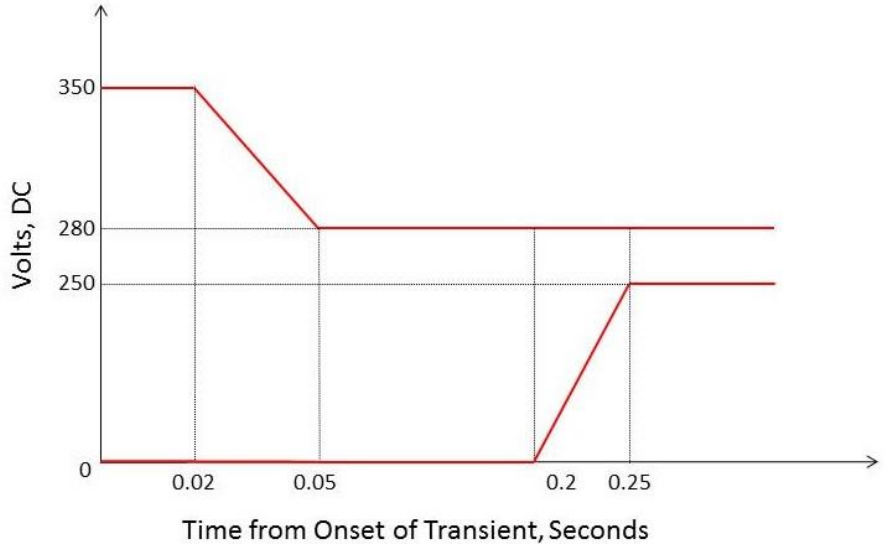

Figure 64. Alternate 25 ms candidate voltage envelope.

Table XXVIII. Inductance ratings for transient compliance with 25 ms voltage envelope

DC Architecture	Fault-clearance time	Fault current through inductor	Inductance rating
2 Bus	5 ms	986 A	0.25 mH
	1 ms	780 A	0.2 mH
	0.5 ms	858 A	0.1 mH
	0.1 ms	814 A	0.02mH
	0.02 ms	550 A	0.005 mH
3 Bus	5 ms	2038 A	0.25 mH
	1 ms	878 A	0.21 mH
	0.5 ms	557 A	0.18 mH
	0.1 ms	424 A	0.065 mH
	0.02 ms	584 A	0.005 mH
4 Bus	5 ms	1780 A	0.4 mH
	1 ms	662 A	0.3 mH
	0.5 ms	421 A	0.25 mH
	0.1 ms	201 A	0.15 mH
	0.02 ms	376 A	0.01 mH

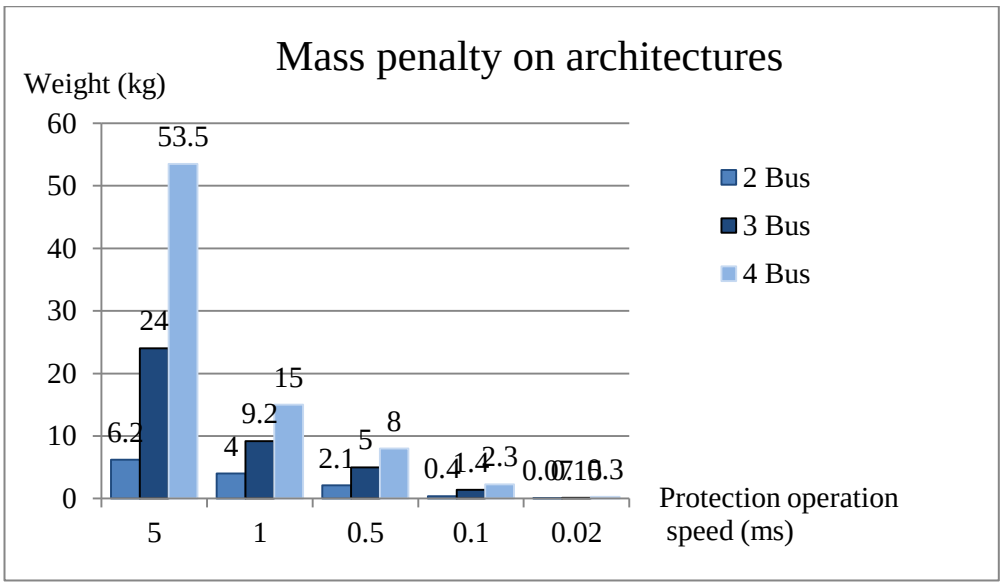

Figure 65. Mass penalty estimation of 25 ms candidate voltage envelope.

6.5 Brief discussion on potential regulatory changes to voltage-limit envelope

Over the last two decades, aircraft design has undergone significant technological step changes which have benefited the efficiency and operability of the platform, reduced emissions and decreased fuel consumption. New electrical systems have further improved aircraft reliability and safety, and at the same time have reduced maintenance costs [273]. These key factors have arguably contributed to making commercial aviation cheaper, thus more accessible to the greater public. The International Air Transport Association (IATA) has forecasted that by 2035, commercial aviation will transport 7.2 billion passengers, approximately double than the 3.8 billion passengers that flew in 2016 [274].

Undoubtedly, this will result in a substantial growth of the aviation industry, and require advancements in technologies and operations, as well as efficiencies in infrastructure [274]. Particularly for aircraft, new design concepts such as the MEA, AEA and MEE are already revolutionising the commercial transport sector. In order to meet the ever increasing electrical demand of on-board systems, as well as future

regulatory and customer demands for safety and reliability, new certification and safety standards will arguably be required for these electrical systems.

As has already been mentioned, the MEA/E concept brings a greater and broader electrification of on-board systems, a subset of which have become critical to the safety and continuation of flight. This, paired with the partial or total electrical unification interconnected systems deliver, could potentially justify the need to re-evaluate the suitability of current airworthiness standards and power quality requirements for these systems.

In an effort to estimate the impact of potential future regulatory changes on the inductive interconnecting solutions described within this research, four candidate voltage envelopes dedicated to paralleled power systems were presented. For each voltage envelope, suitable inductance ratings that could achieve voltage compliance were derived and their mass penalty was estimated. Perhaps the most important conclusion reached from this analysis is that different regulatory power-quality requirements have different impacts on the ratings and mass of the required inductive interconnecting solutions, and thus on the potential feasibility of this approach.

For all simulated DC architectures and fault-clearance times, it would appear that the ‘normal requirement’ voltage envelope incurs the greatest mass penalty on the architecture, whilst the 5 ms voltage envelope incurs the smallest mass penalty where applicable. On the other hand, the larger the required inductance rating, and thus the mass of the interconnecting component, the better the power quality and the less severe the voltage transient is. Subsequently, this highlights the apparent trade-off between the weight penalty incurred on the electrical architecture due to interconnecting solutions and the qualitative improvement in power quality and envelope strictness.

6.6 Brief discussion on regulatory compliance for partially interconnected systems

The discussion and analysis carried out in previous sections of this chapter were focused on fully, and uniformly, interconnected power networks. This section will briefly address the certification compliance of partially-paralleled systems against two key points made earlier in this chapter, in particular critical-load segregation and utilisation of 'hybrid'-generation mode systems.

In Section 6.1, it was argued that flight-critical loads with strict power-quality provisions and/or higher levels of required reliability for type certification could remain isolated throughout the flight, whilst the rest of the power system can remain in interconnected-generation mode. This would require that at least one supply channel (or engine spool) remains isolated from at least two paralleled channels (or one pair of paralleled engine spools). Subsequently, an electrical topology featuring distinct sub-network parts for isolated flight-critical loads and interconnected non flight-critical loads would require at least three power channels, if these channels are powered from three isolated spools respectively.

The existence of three isolated spools satisfies CS 25.1307, which requires all passenger aircraft to have two or more independent sources of electrical energy. In this '2+1 DC bus' topology, and under normal operating conditions, flight-critical loads can be provided with from their dedicated, isolated power supply. Under abnormal operating conditions however, i.e. loss of supply, the automatic crossover to the channel of the interconnected power sources would "maintain system or equipment operation", as stipulated in CS 25.1355. The interconnected supply channel is by design independent from the channel of the critical loads, therefore in this manner, flight-critical loads can be provided with at least two independent sources of electrical power (i.e. main AC sources). An additional, automatically-selectable, back-up power supply can be made available from a different voltage-type bus depending on the location of the load (i.e. via static inverters), thus fulfilling the requirements of CS 25.1355 for type-certification of flight-critical loads.

Although part of the electrical network may operate under isolated mode and other parts under paralleled mode, requirements CS 25.1351 and CS 25.1310, regarding proper operation of power sources, as discussed in Section 6.2 are also fulfilled. Consequently, 'hybrid'generation-mode architectures featuring three supply busses or more do not appear to violate the airworthiness standards. Similarly, this can be extended to the 'two twin-DC bus' architecture presented in Section 5.4 of this thesis. Such 'hybrid' topologies would constitute a compromise between the higher levels or reliability/redundancy required by a subset of loads critical to the safety and continuity of flight, and the engine operability and fuel efficiency benefits offered by more-interconnected electrical architectures.

The potential realization of architectures that feature both modes of generation could open up the possibility of dynamic or multiple voltage-envelope requirements. Segregated flight-critical loads can adhere to strict voltage requirements, i.e. steady-state voltage envelope, whilst at the same time, less-critical interconnected loads can adhere to less strict voltage limits. In this manner, two different sets of requirements must be obeyed by the same power network as a whole, however with different degrees of severity for different sub-parts of the network. Such an approach does not appear to openly reduce the reliability of existing electrical systems and can allow the deployment of more-interconnected schemes at a smaller weight penalty, in comparison to single-envelope voltage requirements or fully-interconnected systems.

Lastly, perhaps a less complicated implementation than the two-envelope approach, and applicable to both partially and fully interconnected systems, would be to have one dynamic voltage-envelope that would account for the different flight phases. In this manner, the electrical architecture would have to adhere to strict power-quality requirements during critical segments of the flight (i.e. take-off, landing) but less strict requirements during less critical phases of flight (i.e. cruise, top of descent). This approach implies that during non-critical flight phases, the impact of an electrical fault on the proper function and reliability of loads and systems is less severe than the impact the same fault would have if it would occur during critical flight segments. Recognition of the different phases of flight for the dynamic voltage

envelope can be carried out through the status of the on-board flight data/management computer.

6.7 Chapter summary

This chapter discussed alternate airworthiness-standards and power-quality interpretations that could be afforded by the employment of inductors as interconnecting mechanisms. It illustrated how an electrical fault can be perceived as a normal transient by the non-faulted parts of the power system, and discussed the subsequent implications of this on generation sources and essential loads. A direct consequence of this was the need to re-evaluate the definition of independent power sources within the framework of interconnected networks. From this, a novel interpretation was debated, wherein interconnected generation sources could be considered as independent power sources if their transient responses can be electrically decoupled in accordance with some type of compliance.

Also, it briefly addressed several key factors that distinguish conventional aircraft from MEA/E, and consequently argued the need for dedicated paralleled-generation power-quality requirements for MEA/E. To this end, four candidate voltage envelopes were presented, and the impact of these envelopes on the feasibility of inductive interconnecting solutions necessary for compliance was estimated. It was shown that very fast protection operation speeds have the potential to facilitate compliance of interconnected power systems with these candidate voltage envelopes without the requirement for a paralleling mechanism.

Lastly, the potential compliance of partially-paralleled systems to certification provisions was briefly presented, with regards to critical-load segregation and ‘hybrid’ mode generation. Such topologies would constitute a compromise between the higher levels or reliability required by a subset of on-board loads and the engine operability and fuel efficiency benefits offered by more-interconnected electrical architectures.

Chapter 7

Conclusions, contributions and future work

The work presented within this thesis covers a number of key issues related to interconnected generation within MEA/E electrical networks. This thesis highlights that the paralleling of generation sources introduces considerable protection demands and presents significant challenges in order for power-quality requirements compliance to be maintained during an electrical fault. Through a detailed analysis of the fault response of two-, three- and four-bus DC architectures, three key interconnecting solution approaches were trialled, and their influence on the attainment of voltage compliance under fault conditions was evaluated. From this analysis, inductive coupling was identified as a suitable interconnecting mechanism capable of maintaining bus-voltage compliance, based on its ability to suppress the propagation of the fault transients throughout the power network. It was demonstrated that there are two main variables which impact the size of inductance required to achieve bus-voltage compliance: the type of voltage compliance required and the operation speed of the protection system.

To assess the feasibility and applicability of bus-interconnecting inductors on aircraft power systems, further analyses were carried out under different operating conditions of the power system and varying protection-speed operation, accompanied with mass-estimation case-studies of the required interconnecting inductor. From these analyses, it was identified that inductive coupling cannot retain normal voltage compliance with traditional protection systems that have operation speeds of 10 ms or greater. It was also demonstrated how the implementation of inductive solutions has the potential to influence architectural design and electrical machine selection (power off-take mix). Finally, the impact of the implementation of bus-interconnecting inductance on the established power-quality requirements is presented and novel interpretations of airworthiness requirements and standards are

discussed. Conclusions and contributions from each of these aspects of this thesis are presented in the following section.

Overall, this thesis demonstrated that a fully interconnected design with fast protection systems can deliver greater efficiency gains but requires more inductors and higher-rated protection equipment, resulting in more added weight on the electrical architecture. This added weight though can be traded against certification requirements that permit the network to operate in parallel mode for a greater duration (potentially throughout all flight phases with the necessary critical-load segregation), therefore realising efficiency and operability benefits over a wider area. On the other hand, partial interconnection is a design solution that incurs a relatively smaller weight penalty (less inductors required, less higher-rated protection equipment) and permits the segregation of critical loads more feasibly, however delivers reduced efficiency gains in comparison to full paralleling. In turn, any gains offered by this approach may be rendered unviable if there is no change in certification requirements.

Purely from a mass-centric scope, fast and lightweight protection equipment can facilitate interconnection solutions with minimal mass penalties, for both fully or partially paralleled networks. The feasible implementation of fully-interconnected configurations will deliver the greatest efficiency gains with the lowest weight penalty. Very fast protection speeds that facilitate adherence to steady-state envelope compliance may even render the need for critical load segregation obsolete. If however, SSPC technology does not reach the necessary maturation for the desired power levels (ratings) and mass requirements, due to the operating characteristics of traditional EMCB equipment, the interconnection of supply channels will incur a significant weight penalty on the electrical architecture.

Moreover, design (architectural) selection and power off-take mix (multitude of HP/LP generators) directly influence the feasibility of inductive solutions. A topology featuring fewer, larger-rated generators will require more inter-bus inductance than an architecture of the same power output featuring more, smaller-rated generators, and will therefore incur a larger weight penalty for a given power output. The larger weight penalty can be mitigated by transitioning to faster

protection-operation speeds and fully-paralleled systems that can deliver higher efficiency gains. At the same time, the degree of interconnection within an architecture depends on the multitude of generators, and thus multitude of channels. Consequently, topologies with relatively few generators/channels have limited paralleling options, in comparison to topologies with a relatively large number of generators/channels. In turn, this affects the segregation of critical loads within any architecture with relatively few and fully paralleled generators/buses.

It is clear that the feasible implementation of inductive coupling on MEA/E electrical networks is not a single-parameter optimisation problem, but a function of architecture topology, protection solutions and regulatory requirements, as illustrated in Fig. 66. Consequently, there can be no single optimum solution or design approach that can suit any potential design/system, for example by aggregating each individual parameter's optimum point into one design. In contrast, the solution space may be optimised if a more holistic approach is taken, where perhaps the contribution of one or more parameters may be sub-optimal, however overall, this delivers the optimum solution for a given set of initial conditions/constraints. In essence, each potential combination of initial conditions (or constraints) can lead to a different optimised balancing point, with this equilibrium being the 'global' trade-off among these three interacting parameters. In this manner, the exploitation and viability of optimised designs or solution approaches can be assessed on a system-specific basis.

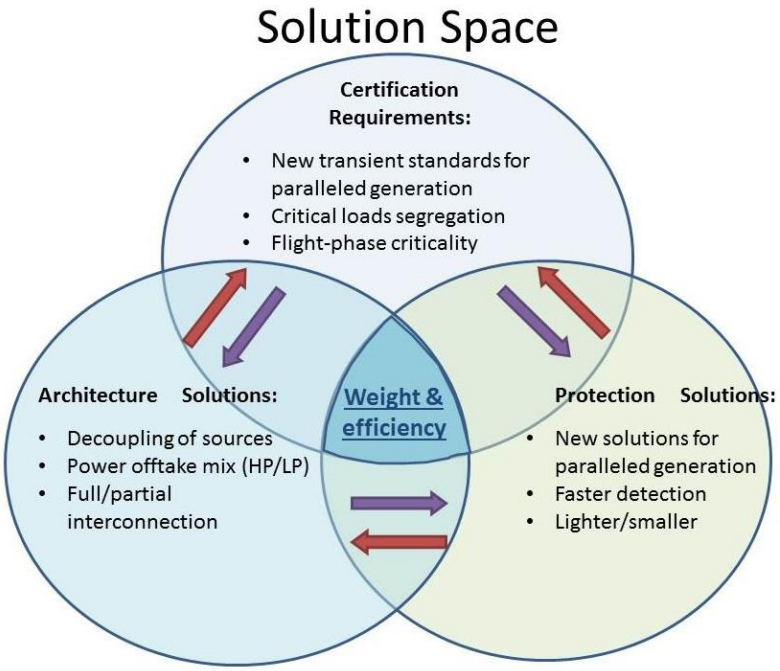

Figure 66. The interaction of certification requirements, architecture solutions and protection solutions within the solution space.

7.1 Summary of chapter conclusions

Chapter 2

Chapter 2 reviewed the MEA and MEE concepts and outlined the key differences between MEA and conventional aircraft. It addressed the technological challenges and breakthroughs of this more-electric shift, and presented novel power generation and distribution systems. Arguably, the latest technological milestone in military and commercial airplane networks today is the advent of ±270 V DC generation and distribution systems. The ever-increasing electrification of MEA/E systems imposes the need for new technologies and novel electrical architectures. To satisfy the need for reduced fuel consumption and improved engine operability, this chapter identified that new power-system design options are needed, with one possible choice being the interconnection of generators to produce a single combined power source.

Chapter 3

This chapter reviewed the state of interconnected generation in the current and past aviation industry and presented the challenges associated with paralleled architectures. These challenges include adherence to airworthiness standards and regulatory power-quality requirements, as well as limitations within the current field of protection devices. It identified that the key challenge prohibiting AC interconnection options is the variable-frequency output of novel MEA/E generators, as frequency-converter technology is not yet sufficiently mature for aviation use with regards to weight and volume.

It also identified efficiency gains (through multi-shaft power offtakes) and the growing use of DC distribution as the key technological drivers that may provide a more feasible route for the implementation of paralleled DC architectures. Lastly, it summarized the benefits and drawbacks of proposed interconnected approaches in the relevant literature, and also illustrated that the system-level impact paralleled generation may have under abnormal operation conditions is not well documented. Moreover, it illustrated that proposed designs do not address the certification implications of airworthiness standards and requirements.

The work presented within this chapter contributed to a conference publication.

Chapter 4

Chapter 4 presented the modelled interconnected 270 V DC architectures that were analysed with regards to fault response for low impedance faults, and described the modelling rational underpinning this analysis. It is shown that traditional means of protection do not prevent the non-faulted segments of the power network from breaching the power quality requirements, suggesting that to achieve voltage-requirements compliance, the transient responses of these segments must be decoupled from that of the faulted part of the system. To this end, three solution options were considered, an SSPC, a CLD and a smoothing reactor, as a DC bus-interconnecting mechanism, to assess voltage compliance of a paralleled power

network during fault conditions. From this assessment, it was concluded that the smoothing reactor showed better potential compared to all other candidate solutions considered.

Chapter 5

This chapter focused on the design and implementation of effective smoothing reactors, capable of achieving normal and steady-state voltage compliance for candidate DC architectures under full-load conditions. Simulations showed that shunt capacitance had an adverse effect on the bus voltage during an electrical fault, subsequently purely inductive interconnecting solutions were further pursued. This chapter highlighted the two main variables which impact the size of inductance required to achieve bus-voltage compliance: the type of voltage compliance required and the operation speed of the protection system. It was also identified that inductive interconnections cannot be used along with protection equipment with tripping times of 10 ms or greater, creating significant implications for EMCBs with slow tripping times.

To assess the feasibility and applicability of this interconnecting solution approach, a mass estimation study quantified the weight penalty incurred on the modelled architectures. Additionally, several beneficial and adverse aspects of the implementation of inter-bus inductors were discussed, including bus-voltage quality and imbalanced generator operation.

To exploit benefits afforded by load optimization schemes in interconnected power systems, additional inductance ratings for partial generator loading were presented. It was also shown how inductive solutions have the potential to influence architectural design, as strictly in terms of system mass, it would be more beneficial to combine groups of smaller generators, and thus DC buses, into separate channels than opting for fully interconnected DC systems. Additionally, the influence of inductive solutions with regards to electrical machine selection was illustrated, as it was shown that within an architecture, the main contributor to the need for bigger-rated inductors is not the variance in power mismatch between generation source types,

and thus the kind of shaft from which power is off-taken, but the greatest nominal power value of the available generators. Lastly, the feasibility of the proposed solution approach was examined on novel, parallel-generation networks within the relevant literature.

The work presented within this chapter has to date contributed to one journal paper and two conference publications.

Chapter 6

Chapter 6 debated alternate airworthiness-standards and power-quality interpretations that could be afforded by the employment of inductive coupling as an interconnecting mechanism. It illustrated how an electrical fault can be perceived as a normal transient by the non-faulted parts of the power system, and discussed the subsequent implications of this on generation sources and essential loads. A direct consequence of this was the need to re-evaluate the definition of independent power sources within the framework of interconnected networks. This re-evaluation led to a novel interpretation of the airworthiness standards with regards to generation source independency, in which the electrical decoupling of paralleled generation sources, and potentially in accordance with some type of power-quality compliance, could render them independent.

Also, it briefly addressed several key factors that distinguish conventional aircraft from MEA/E, and consequently argued the need for dedicated paralleled-generation power-quality requirements for MEA/E. To this end, three novel candidate voltage envelopes were presented and the impact of these envelopes on applicability and feasibility of inductive interconnecting solutions necessary for compliance was estimated. Lastly, it was shown that extremely fast protection operation speeds have the potential to facilitate compliance of interconnected power systems with these candidate voltage envelopes with no added weight penalty.

7.2 Key areas of future work

A number of areas of future work have been identified which have the potential to advance the work presented in this thesis and the wider research area. These are discussed next.

- Evaluation of inductive interconnection approach at an aircraft power system level

The analyses carried out within this thesis mainly focused on the effect and impact the implementation of interconnecting inductance had during an electrical fault at the ±270 V DC level. Whilst suitable inter-bus inductance ratings for normal and abnormal voltage compliance were derived for a fault within the main DC distribution system, it was not examined whether these ratings are still sufficient in maintaining voltage compliance for faults elsewhere in the network.

Additionally, it is not uncommon for electrical systems on-board civil aircraft to have overrated capabilities, potentially time-limited, in the event of an emergency. The presented inductance ratings in this work were derived under full and partial generator loading, and did not take into account the need for capacity overhead which may be required during emergency flight conditions. In this case, larger-rated inductors would be required, however is not known with how much overrated capabilities various aircraft platforms are designed with.

Until this information becomes publicly available, it is up to the aircraft manufacturer to consider the trade-off between the need for larger-rated inductors (thus more added weight penalty) in order to allow the DC distribution system to operate in interconnected mode during abnormal operating conditions, and the frequency by which emergency conditions that require isolated generation occur.

- Model expansion and fidelity

The interconnected simulation models presented within this thesis were designed at a functional level of fidelity. Such models neglect switching-level transients in order to minimise the computational burden and facilitate time-efficient extensive simulations. This permitted the execution of millions of simulations so that suitable combinations of inductance and capacitance could be identified, in order to create an effective smoothing reactor capable of maintaining voltage compliance. Subsequent analyses demonstrated the required order of magnitude for the ratings of the bus-interconnecting inductors for all three DC architectures.

Given that a feasible region of inductance ratings for voltage compliance has been identified, more computationally-intensive and time-consuming software models can improve the fidelity of simulation studies presented in this work. In this manner, more accurate inductance ratings can be analysed and potential transient behaviours not captured by existing models be made visible. At the same time, simulation models of increased fidelity can promote the expansion of these models to a systems-level approach (future work mentioned at the beginning of this section), incorporating in this manner all voltage types of MEA networks.

- Evaluation of the undesired effects incurred due to the implementation of bus-interconnecting inductance

In inductor design, there is a trade-off between the rate of rise of fault current and the stiffness of the power system. Higher inductance values can further supress the fault-current rate of rise, but in doing so, create a stiffer network that restricts fast current changes, impacting the response of the power flow control in the grid. Therefore, a deeper investigation is required into the effect and impact of slower current changes caused by the addition of inter-bus inductance on the operation of flight-essential loads and systems. Moreover, the suppression of the rate of rise of current transients may adversely impact the operation of protection devices. Subsequently, a more thorough protection analysis is required to determine to what degree the employment of inductance impacts the required level of protection performance.

- Adverse effects resulting from the implementation of non-ideal inductors

In all simulation scenarios presented within this thesis, the identified inductor ratings were derived under the assumption that an ideal inductor acts as a bus-interconnecting mechanism. This allowed for a uniform analysis (and comparison) across all simulated DC architectures with regards to fault-clearing time, type of compliance, fault-current magnitude and weight-estimation studies. However, this work did not take into account that non-ideal inductors are rated with particular saturations currents, and that their effective inductance is temperature-dependent and varies within a specific tolerance. Additionally, the series resistance of a non-ideal inductor is dependent on its effective inductance, as well as its design.

This work briefly demonstrated that an inductor's series resistance has the potential to cause the voltage to deviate from acceptable voltage-compliance limits. This is attributed to the significant stead-state voltage drop caused by large values of series resistance. It was also seen that in order for the inductor series resistance to have a negligible effect on the bus voltage, the resistance should not exceed a value of 0.5 Ohms. Overall, this demonstrates that inductor design requires more attention, as the practical implementation of non-ideal inductors as bus-interconnecting mechanisms may have adverse effects on the system voltage of an interconnected power network.

- Quantification of the impact of protection infrastructure on overall system design

From the simulation studies presented in this thesis, it was illustrated that the transition to faster fault-clearance times reduces the added weight penalty incurred on the electrical architecture by the interconnecting inductor/s. However, at the same time this may increase the cost and complexity of the protection system. Additionally, the paralleling of generation sources significantly increases potential fault currents, therefore heavier, overrated protection equipment will be required for interconnected architectures. The influence of cost and mass of overrated protection equipment must be investigated and quantified, since both these factors directly

affect the feasibility and applicability of the inductive interconnection approach in the attainment of voltage compliance for paralleled systems.

SSPCs are considered to be the next generation in protection devices due to their fast operating speed and light weight. Smart, programmable SSPCs also permit power-management systems to adapt to arising fault conditions, by dynamically reconfiguring the power network depending on operational system conditions. To date, the power ratings of existing SSPC devices appear to be lower than required for high-power aviation applications. Future advances however could be the defining step in the feasible realisation and wider adoption of interconnected power networks for commercial aviation.

Appendix

Minimum-voltage plots for the three- and four-bus DC architectures

This section contains the minimum sensed voltage plots of the three- and four-bus DC architectures during an electrical fault, in an attempt to derive suitable inductance and capacitance ratings for the inter-bus smoothing reactor. The range of inductance and capacitance values simulated was from 0 mH to 40 mH and 0 mF to 40 mF respectively, in 1 μH/μF increments. Additionally, the fault-clearing speed of the protection system was varied in order to simulate different protection strategies and assess below which fault-clearing time this approach is potentially viable.

Figures 67 to 70 illustrate the minimum sensed voltage of the non-faulted bus on the three-bus DC architecture during a short-circuit that is cleared within 50, 10, 5 and 1 ms respectively. Similarly, Figures 71 to 74 depict the minimum sensed voltage of the non-faulted bus over the same fault-clearance speeds in the four-bus DC architecture. Each voltage value (z axis) of the surface plot corresponds to a distinct pair of capacitance (x axis) and inductance (y axis) values, and depicts the lowest voltage sensed on the non-faulted bus during the electrical fault, by using these capacitance and inductance values as reactor ratings.

In both architectures, it would appear that the minimum sensed voltage is more sensitive to changes in inductance rather than changes in capacitance. This is more evident for a 50 ms fault-clearing speed in Figures 67 and 71, for the three- and four-bus architecture respectively, where the minimum sensed voltage increases significantly for increasing values of inductance, yet appears to remain stable for increasing values of capacitance. Additionally, by comparing Figures 67 to 70 and Figures 71 to 74, it is evident that faster fault-clearance speeds result in higher voltage values for the same pair of reactor ratings. Lastly, it is clear that transitioning

to faster fault-clearance times results in the surface plots gradually being more flat than curved, suggesting that smaller amounts of inductance are required for a specific minimum voltage value.

In comparison to the twin-bus DC architecture, similar conclusions can be reached for the three- and four-bus DC architectures. Likewise, both normal and steady-state voltage compliance does not appear to be achievable for fault-clearance times of 50 ms for either architecture, as the bus voltage level cannot be maintained above 250 V, but suitable inductance ratings can be derived for both compliance types for fault-clearance speed of 10 ms or faster.

1. Three-bus DC architecture

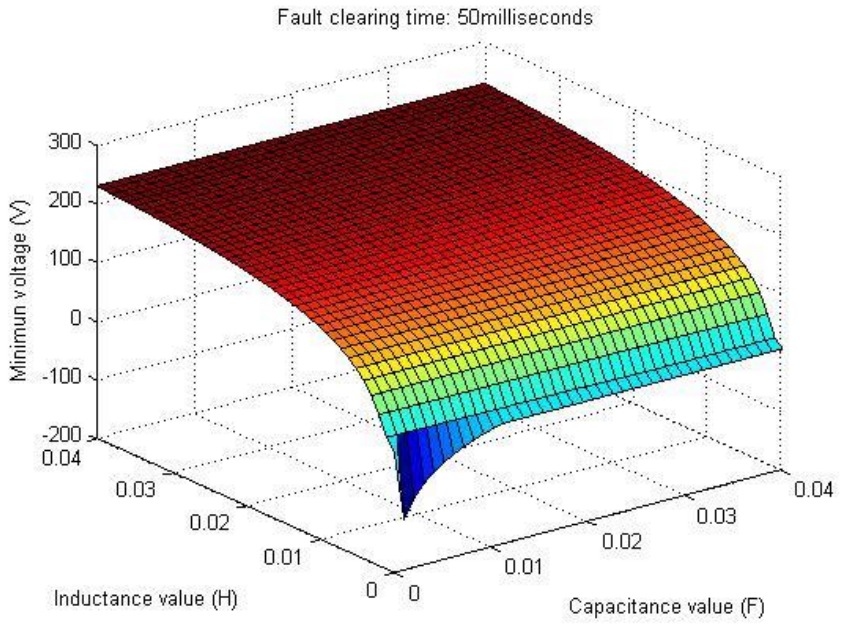

Figure 67. Minimum sensed voltage of interconnected non-faulted bus during a fault for varying filter inductance and capacitance values for a 50 ms protection operation speed.

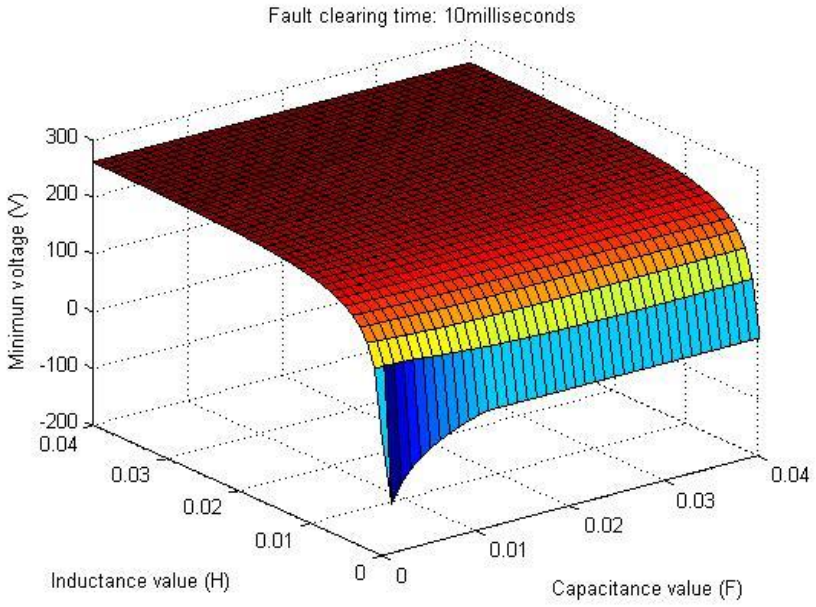

Figure 68. Minimum sensed voltage of interconnected non-faulted bus during a fault for varying filter inductance and capacitance values for a 10 ms protection operation speed.

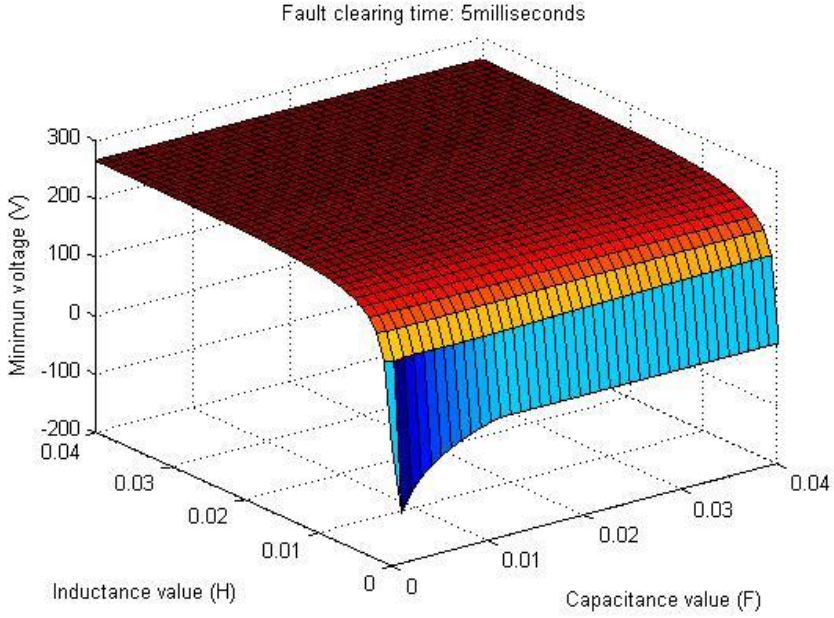

Figure 69. Minimum sensed voltage of interconnected non-faulted bus during a fault for varying filter inductance and capacitance values for a 5 ms protection operation speed.

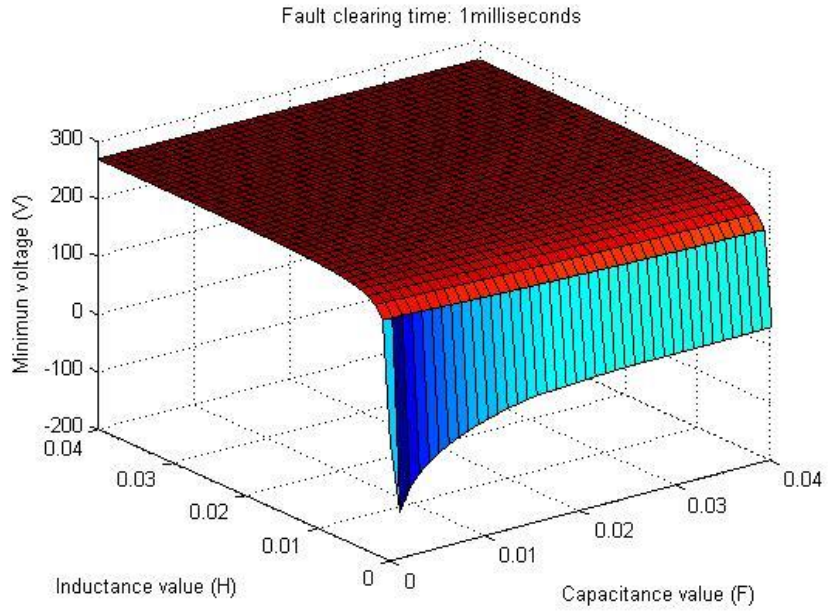

Figure 70. Minimum sensed voltage of interconnected non-faulted bus during a fault for varying filter inductance and capacitance values for a 1 ms protection operation speed.

2. Four-bus DC architecture

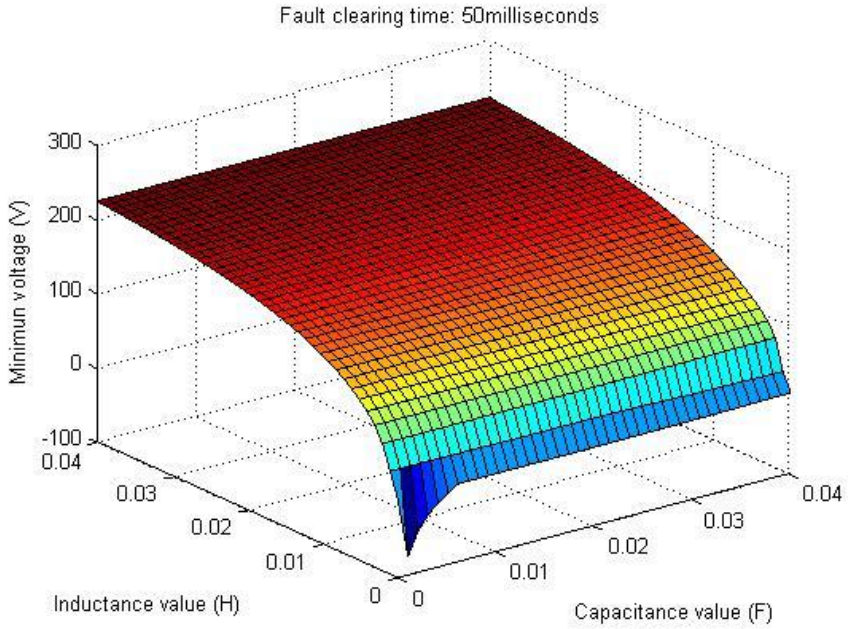

Figure 71. Minimum sensed voltage of interconnected non-faulted bus during a fault for varying filter inductance and capacitance values for a 50 ms protection operation speed.

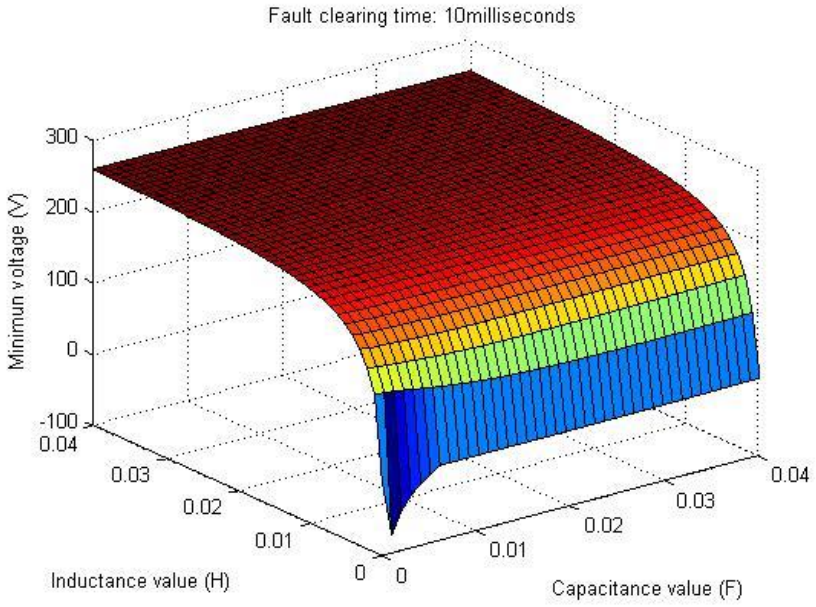

Figure 72. Minimum sensed voltage of interconnected non-faulted bus during a fault for varying filter inductance and capacitance values for a 10 ms protection operation speed.

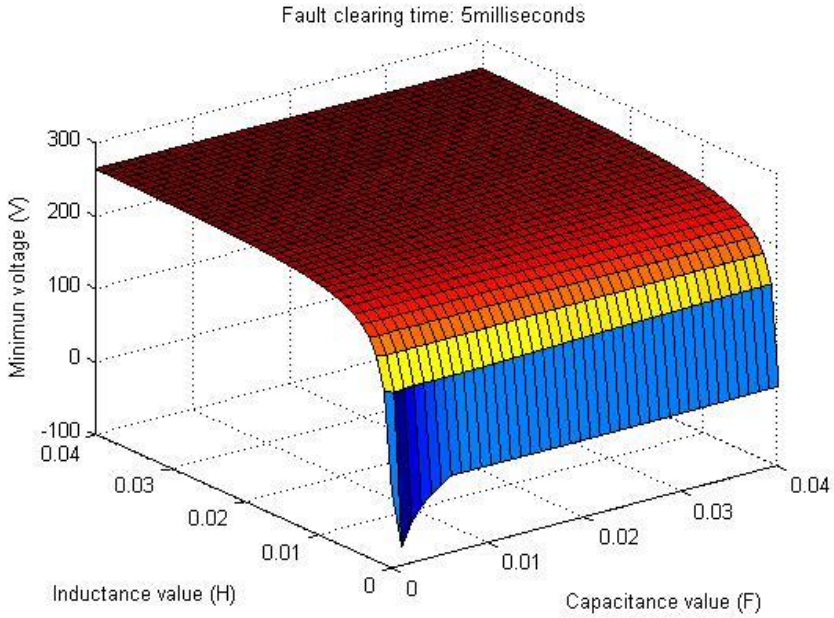

Figure 73. Minimum sensed voltage of interconnected non-faulted bus during a fault for varying filter inductance and capacitance values for a 5 ms protection operation speed.

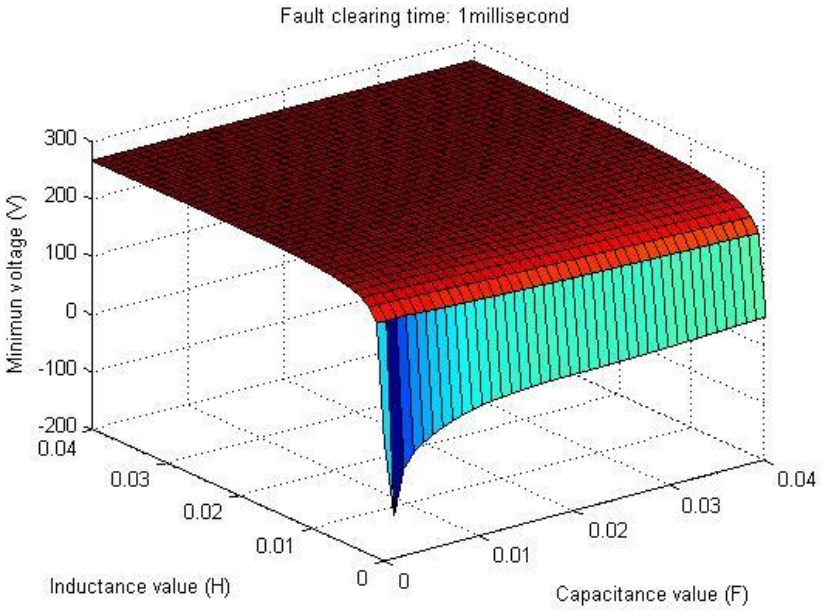

Figure 74. Minimum sensed voltage of interconnected non-faulted bus during a fault for varying filter inductance and capacitance values for a 1 ms protection operation speed.

References

[1] J. A. Romero, J. A. Ortega, E. Aldabas, and L. Romeral, "Moving towards a more electric aircraft," *IEEE Aerospace and Electronics Magazine,* vol. 22, no. 3, pp. 3-9, March 2007.

[2] C. R. Avery, S. G. Burrow, and P. H. Mellor, "Electrical generation and distribution for the more electric aircraft," presented at the 42nd International Universities Power Engineering Conference (UPEC), China, September 2007.

[3] I. Berlowitz, "All/More Electric Aircraft Engine & Airframe Systems Implementation," presented at the 9th Israeli Symposium on Jet and Gas Turbines, October 2010.

[4] P. W. Wheeler, J. C. Clare, A. Trentin, and S. Bozhko, "An overview of the more electric aircraft," *Journal of Aerospace Engineering,* vol. 227, no. 4, pp. 578-585, September 2012.

[5] T. Jomier, "More open electric technologies-final technical report," in "MOET 6th RTD Framework Programme," European Union, December 2009.

[6] R. I. Jones, "The more electric aircraft - assessing the benefits," *Journal of Aerospace Engineering,* vol. 216, no. 5, pp. 259-269, May 2002.

[7] J. A. Weiner, "The role of electric machines and drives in the more electric aircraft," presented at the Electric Machines and Drives Conference (IEMDC), USA, June 2003.

[8] The Institution of Engineering and Technology (IET), "Rolls-Royce Plc: More Electric Engines for More Electric Aircraft," IET Transportation Sector Case Study, 2007, available at http://www.theiet.org/sectors/transport/topics /energyefficiency/articles/electric-aircraft.cfm.

[9] S. Fletcher, "Protection of Physically Compact Multiterminal DC Power Systems," PhD thesis, Department of Electronic and Electrical Engineering, University of Strathclyde, May 2013.

[10] B. H. Chowdhury and S. Rahman, "A review of recent advances in economic dispatch," *IEEE Transactions on Power Systems,* vol. 5, no. 4, pp. 1248-1259, November 1990.

[11] D. Koyama, "How the More Electric Aircraft is influencing a More Electric Engine and More!," presentation, Electrical Technologies for Aviation of the Future, Rolls-Royce Japan, 2015.

[12] S. A. Long *et al.,* "Ultra-compact Intelligent Electrical Networks," presented at the 3rd SEAS DTC Techncal Conference, pp. 1-8, January 2008,

[13] P. J. Norman, S. I. Galloway, G. M. Burt, D. R. Trainer, and M. Hirst, "Transient Analysis of the More-Electric Engine Electrical Power Distribution Network," presented at the 4th IET Conference on Power Electronics, Machines and Drives, pp. 1-5, April 2008.

[14] E. Kontos, S. Rodrigues, R. Teixeira Pinto, and P. Bauer, "Optimization of limiting reactors design for DC fault protection of multi-terminal HVDC networks," presented at the 2014 IEEE Energy Conversion Congress and Exposition, pp.5347-5354, September 2014.
[15] The Boeing Company, "787 No Bleed Systems," *AERO Magazine,* vol. 4, no. 28, 2007.
[16] C. R. Spitzer and R. V. Hood, "The All Electric Airplane - Benefits and Challenges," in *Proceedings of the Aerospace Congress and Exposition*, USA, no. SAE 821434: Society of Automotive Engineers (SAE).
[17] D. A. Woodburn, "Modelling and Simulation of All-Electric Aircraft Power Generation and Actuation," PhD thesis, Department of Electrical Engineering and Computer Science, University of Central Florida, USA.
[18] S. L. Botten, C. R. Whitley, and A. D. King, "Flight Control Actuation for Next Generation All-Electric Aircraft," *Technology Review Journal*, vol. Fall/Winter, pp. 55-68, 2000.
[19] M. Sinnett, "787 No-Bleed Systems: Saving fuel and enhancing operational efficiencies," *Boeing AERO magazine,* no. 28, pp. 6-11, December 2007.
[20] S. F. Clark, "787 Propulsion System," *Boeing AERO magazine,* vol. 3, 2012.
[21] I. Moir and A. Seabridge, "Aircraft Systems: mechanical, electrical, and avionics subsystems integration," 3rd ed. John Wiley & Sons Ltd, ISBN 978-0-470-05996-8, 2008.
[22] G. Norris, "Operators Reporting Positive 787 Fuel-Burn Results," available at http://aviationweek.com/awin/operators-reporting-positive-787-fuel-burn-results ,June 2012.
[23] Design News, "Boeing's 'More Electric' 787 Dreamliner Spurs Engine Evolution," available at https://www.designnews.com/electronics-test/boeings-more-electric-787-dreamliner-spurs-engine-evolution/194899474451471?doc_id=222308 ,June 2007.
[24] K. J. Karimi, "Future Aircraft Power Systems- Integration Challenges," available at https://www.ece.cmu.edu/~electriconf/2008/PDFs/Karimi.pdf ,The Boeing Company, 2007.
[25] J. Clare, "Examples of More Electric Aircraft Research in the Aerospace Research Centre," presentation, Electrical Systems and Optics Research Division, University of Nottingham.
[26] Airbus Commercial Aircraft, "A380 Technology," available at http://www.airbus.com/aircraftfamilies/passengeraircraft/a380family/innovation/.
[27] G. Norris and M. Wagner, "Airbus A380: Superjumbo of the 21st Century," Zenith Press, June 2010, ISBN 978-0760338384.
[28] The Boeing Company, "787 Electrical System," available at http://787updates.newairplane.com/787-Electrical-Systems/787-Electrical-System#.
[29] J. S. Cloyd, "Status of the united states air force's more electric aircraft initiative," *IEEE Aerospace and Electronic Systems Magazine*, vol. 13, no. 4, pp. 17-22, April 1998.
[30] K. W. E. Cheng, "Comparative Study of AC/DC converters for More Electric Aircraft," presented at the 7th International Conference on Power Electronics and Variable Speed Drives, September 1998.

[31] A. Abdel-Hafez, "Power Generation and Distribution System for a More Electric Aircraft - A Review," InTech, 2012, ISBN 978-953-51-0150-5.
[32] T. Nelson, "787 Systems and Performance," presentation, Boeing Commercial Airplanes, 2005.
[33] S. F. Follett, "Electrical equipment in aircraft: survey of past and present practise and future trends in design," *Proceedings of the IEE-Part A: Power Engineering*, vol. 103, no. 1, p. 10, May, 1956.
[34] Flight, "Valiant..." 4 July 1958, available at https://www.flightglobal.com/FlightPDFArchive/1958/1958-1-%20-%200017.PDF.
[35] Smith, "Flight and Aircraft Engineer Magazine - Bound Issues from 4 July 1958 to 26 September 1985," Iliffe and Sons Ltd, 1958, ASIN B002D01NL0.
[36] B. Gunston and P. Gilchrist, "Jet Bombers. From the Messerschmitt Me 162 to the Stealth B-2," Osprey Publishing, 1993, ISBN 9781855322585.
[37] I. Moir, A. Seabridge, and M. Jukes, "Civil Avionics Systems," 2nd ed., Wiley, 2013, ISBN 978-1118341803.
[38] T. Blackman and A. Wright, "Valiant Boys," Grub Street Publishing, 2014, ISBN 978-1909808218.
[39] Air Ministry, "Pilot's Notes Vulcan B Mk 1 A," FlightWay, 1961, ASIN B00FWWQ4OM.
[40] T. Blackman, "Flight Testing to Win," Blackman Associates, 2007, ASIN B00SLVZ1D6.
[41] Air Ministry, "Vulcan B Mk.2 Aircrew Manual," AP101B-1902-15, 2nd edition, 1970.
[42] T. Laming, "The Vulcan Story 1952-2002," 2nd ed., Silverdale Books, 2002, ISBN 978-1856057011.
[43] AeroPrecision, "F-16 Electric Power Systems," 2006, available at http://www.aeroprecision.com/PDF/HS_F16_EPS.pdf.
[44] D. A. Day, "Computers in Aviation," U.S Centennial of Flight Commission, 2003, available at http://www.centennialofflight.net/essay/Evolution_of_Technology/Computers/Tech37.htm.
[45] M. Nielsen, "Total Immersion Fuel Tank Airborne Cable Assemblies," Glenair, 2007, available at https://www.glenair.com/interconnect_product_showcase/tiftac.htm.
[46] W. H. Thompson, "F-16 Study," Electrical Overstress-Electrostatic Discharge Symposium Proceedings, p. 23, ESD Association, 1984, ISBN 9781878303110.
[47] D. Richardson, "General Dynamics F-16 Fighting Falcon," Gallery Books, 1990, ISBN 9780831714017.
[48] U. S. Navy, "Navy Training System Plan for the F/A-18 Aircraft," N88-NTSP-A-50-7703H/A, December 2001.
[49] U. S. Navy, "F-18 NATOPS Flight Manual Navy Model F/A-18A/B/C/D," A1-F18AC-NFM-000, September 2008.
[50] ITW GSE Military, "270 VDC Power Supply," available at http://itwgse.com/int/military-lp/products/270-vdc-power-supply/.
[51] C. Kopp, "Replacing the RAAF F/A-18 Hornet Fighter: Strategic, Operational and Technical Issues," Submission to the Minister of Defence, Parliament House, Canberra, May 1998.

[52] FCX Systems, "Benefits of the 270 VDC in the aviation industry," September 2016, available at http://www.fcxinc.com/benefits-of-270-vdc-in-the-aviation-industry/.
[53] L. Dewiette, "F-35 Lighting II News: F-35 fleet grounded for generator failure and oil leak," forum article, March 2011, available at http://www.f-16.net/f-35-news-article4312.html.
[54] S. Trimble, "In-flight failure leads to F-35 grounding," FlightGlobal, March 2011, available at https://www.flightglobal.com/news/articles/in-flight-failure-leads-to-f-35-grounding-354281/.
[55] M. Traskos, "F-22 crash and aircraft electrical arcing," Lectromechanical Design Company, November 2013, available at http://www.lectromec.com/f-22-crash-and-aircraft-electrical-arcing/.
[56] Airbus SAS, "A380-800: Flight Deck and Systems Briefing for Pilots," STL945.1380/05, issue 2, p, 103, Customer Services Directore, France, March 2006.
[57] M. Hacker, D. Burghardt, L. Fletcher, A. Gordon, and W. Peruzzi, "Engineering and Technology," Cengage Learning, p. 319, March 2009, ISBN 978-1-285-95643-5.
[58] N. Hall, "Turbofan Engine," Glenn Research Center, NASA, May 2015.
[59] P. Spittle, "Gas Turbine Technology," *Physics Education*, vol. 38, no. 6, pp. 504-511, November 2003.
[60] K. Hunecke, "Jet Engines: Fundamentals of Theory, Design and Operation," 1st ed., The Crowood Press Ltd, October 1997, ISBN 978-1853108341.
[61] J. M. Owen, "Developments in Aeroengines," *Pertanika Journal of Science & Technology*, vol. 9, no. 2, pp. 127-138, 2001.
[62] Rolls-Royce plc, "Trent 1000: Technology," Civil Aerospace, 2007, available at https://www.rolls-royce.com/products-and-services/civil-aerospace/products/civil-large-engines/trent-1000/technology.aspx#technology.
[63] UTC Aerospace Systems, "FADEC Electronic Engine Control," Engine Control Systems Products, 2007, available at http://utcaerospacesystems.com/cap/products/Pages/fadec-engine-electronic-controller.aspx.
[64] S. J. Cutts, "A collaborative approach to the More Electric Aircraft," presented at the International Conference on Power Electronics, Machines and Drives, June 2002.
[65] K. Emadi and M. Ehsani, "Aircraft power systems: technology, state of the art, and future trends," *IEEE Aerospace and Electronic Systems Magazine*, vol. 15, no. 1, January 2000.
[66] R. K. Agarwal, "Recent Advances in Aircraft Technology," InTech, February 2002, ISBN 953-51-0150-5.
[67] M. Hirst, A. McLoughlin, P. J. Norman, and S. J. Galloway, "Demonstrating the more electric engine: a step towards the power optimized aircraft," *IET Electric Power Applications*, vol. 5, no. 1, pp. 3-13, January 2011.
[68] A. Boglietti, A. Cavagnino, A. Tenconi, and S. Vaschetto, "The safety critical electric machines and drives in the more electric aircraft: A survey," presented at the 35th Annual of IEEE industrial Electronics (IECON), November 2009.

[69] W. Camilleri, "An assessment of high overall pressure ratio intercooled engines for civil aviation," PhD thesis, p. 19, School of Engineering, Cranfield University, January 2014.
[70] N. Cumpsty and A. Heyes, "Jet Propulsion: A simple guide to the aerodynamics and thermodynamic design and performance of jet engines," 3rd ed., Cambridge University Press, 2015, ISBN 978-1-107-51122-4.
[71] P. P. Walsh and P. Fletcher, "Gas Turbine Performance," 2nd ed., Blackwell Publishing, 2004, ISBN 0-632-06434-X.
[72] H. D. Helfrich and J. C. Dierffenderfer, "Aircraft Electrical Systems," Report of the American Electrical Advisory Staff for Aircraft Electrical Systems, 16th April-15th June, 1951.
[73] V. A. Higgs, "Applications of electricity of aircraft. A review of progress," *Proceeding of the IEE- Part A: Power Engineering*, vol. 107, no. 32, p. 5, April 1960.
[74] K. Darling, "De Havilland Comet," vol. 7, Specialty Press, November 2001, ISBN 978-1580070362.
[75] P. L. Cronbach, "Rectified-alternating-current generating systems in aircraft," *Proceedings of the IEE - Part A: Power Engineering*, vol. 103, no. 1, p. 11, April 1956.
[76] R. S. Saul and F. M. Wilson, "Category II Landing Approach System for Turbojet Aircraft," presented at the 2nd International Aviation Research and Development Symposium, September 1963.
[77] Federal Aviation Administration, "de Havilland DH-106 Comet 1, Accident Overview," U.S Department of Transport, Washington DC, available at http://lessonslearned.faa.gov/ll_main.cfm?TabID=1&LLID=28& LLTypeID=2.
[78] A. Drewett, "de Havilland 106 Comet," forum article, Gloucestershire Transport, July 2004, available at http://www.visit-gloucestershire.co.uk/ boards/topic/62-de-havilland-106-comet/.
[79] Federal Aviation Administration, "Master Minimum Equipment List: B-707 and B-720," U.S. Department of Transport, Washington D.C., November 1990.
[80] Qantas Airways, "Boeing 707-138B Operations Manual," vol. 1, part II, April 1968.
[81] Boeing-727.com, "System Descriptions," p. 18, available at https://www.boeing-727.com/Data/systems/System%20Descriptions.pdf.
[82] Smartcockpit, "Boeing 727 - Electrical," p. 9, Aircraft Systems, available at http://www.smartcockpit.com/docs/B727-Electrical.pdf.
[83] Boeing-727.com, "Electrical System," Aircraft Systems Described, February 2001, available at http://www.boeing-727.com/Data/systems/infoelect.html.
[84] Air Accidents Investigation Branch, "AAIB Bulletin: 8/2014," Boeing 737-377 (G-CELF), Commercial Air Transport-Fixed Wing, AAIB Field Investigations, August 2014.
[85] Smartcockpit, "Boeing 737 NG Electrical," Boeing 737 NG - Systems Summary, p.1, available at http://www.737ng.co.uk/B_NG-Electrical.pdf.
[86] IXO Aviation, "ATA 24 Electrical Power: B737NG-Systems Course," presentation, 2017, available at http://ixo-aviation.com/boeing-737-ata-24-electrical-power-for-b737-pilot-training-self-study/.

[87] B737.com, "Electrical," Aircraft systems, available at http://www.b737.org.uk/electrics.htm.
[88] Air Accidents Investigation Branch, "AAIB Bulletin: 4/2014," Boeing 747-4H6 (9M-MPL), p. 21, Bulletin-Field Investigation, Commercial-fixed wing, April 2014.
[89] B747classic.co.uk, "Electrical," Systems, available at http://www.b747classic.co.uk/electrical.
[90] C. Tenning, "Unplanned Characteristics of the 747-400 Electrical Power Generation System," available at http://www.angelfire.com/ct3/ctenning/electrical_essays/747dash400elec/747dash400elec.html.
[91] The Boeing Company, "747 Flight Crew Operations Manual: Virgin Atlantic Airways," Document no. D6-30151438, Revision no. 20, Electrical, ch. 6, section 20, p. 6, October 2006.
[92] Federal Aviation Administration, "Master Minimum Equipment List: Boeing B-757 200/300," revision 30, U.S. Department of Transport, Washington D.C., May 2012.
[93] Federal Aviation Administration, "Master Minimum Equipment List: Boeing 767," revision 37, U.S. Department of Transport, Washington D.C., March 2015.
[94] Federal Aviation Administration, "Master Minimum Equipment List: Boeing 777," revision 18, U.S. Department of Transport, Washington D.C., October 2011.
[95] Federal Aviation Administration, "Master Minimum Equipment List: Boeing 787," revision 12, U.S. Department of Transport, Washington D.C., September 2015.
[96] Federal Aviation Administration, "Master Minimum Equipment List:Boeing B-747-8, B-747-8F," revision 2, U.S. Department of Transport, Washington D.C., December 2012.
[97] D. Briere and P. Traverse, "Airbus A320/A330/A340 Electrical Flight Controls: A Family of Fault-Tolerant Systems," presented at the IEEE 23rd International Symposium on Fault-Tolerant Computing, pp.616-623, June 1993.
[98] Airbus, "Airbus A340 Flight Deck and Systems Briefing for Pilots," Smartcockpit, January 2000, available at http://www.smartcockpit.com/aircraft-ressources/A340_Flight_Deck_and_Systems_Briefing_For_Pilots.html.
[99] Airbus, "ATA 24 Electrical Power," A380 Technical Training Manual, Training & Flight Operations Support and Services, pp. 60, March 2006.
[100] J. Chang and A. Wang, "New VF-power system architecture and evaluation for future aircraft," *IEEE Transactions on Aerospace and Electronic Systems*, vol. 42, no. 2, pp. 527-539, April 2016.
[101] P. W. Wheeler, J. Rodriguez, J. C. Clare, L. Empringham, and A. Weistein, "Matrix converters: a technology review," *IEEE Transactions on Industrial Electronics*, vol. 49, no. 2, pp. 276-288, August 2002.
[102] P. Wheeler *et al.*, "A Reliability Comparison of a Matrix Converter and an 18-Pulse Rectifier for Aerospace Applications," 12th International Power Electronics and Motion Control Conference, pp. 496-500, September 2006.

[103] G. Norris and M. Wagner, "Douglas Jetliners," p. 85, MBI Publishing Company, 1999, ISBN 0-7603-0676-1.
[104] Flight International, "McDonnell Douglas MD-90-30," Flightglobal, June 1993, available at https://www.flightglobal.com/FlightPDFArchive/1993/1993%20-%201319.PDF.
[105] The Boeing 737 Technical Site, "Generators - VSCF " 1999, available at http://www.b737.org.uk/generators.htm.
[106] L. Andrade and C. Tenning, "Design of the Boeing 777 Electric System," *IEEE Aerospace and Electronic Systems Magazine*, vol. 7, no. 7, pp. 4-11, July 1992.
[107] C. Adams, "A380: 'More Electric' Aircraft," Avionics, Commercial, October 2001, available at http://www.aviationtoday.com/2001/10/01/a380-more-electric-aircraft/.
[108] I. Purellku, A. Lucken, J. Brombach, B. Nya, and D. Schulz, "Optimization of the Energy-Supply-Structure of Modern Aircraft by using Conventional Power System Technologies," presented at the 21st International Conference on Electricity Distribution CIRED, Germany, June 2011.
[109] T. Kostakis, "Implementation of Interconnected Generation in More Electric Aircraft (MEA)," MSc dissertation, Department of Electronic and Electrical Engineering, University of Strathclyde, August 2013.
[110] U.S. Government, "Part 23-Airworthiness Standards: Normal, utility, acrobatic and commuter category planes," chapter I, Title 14 in *Aeronautics and Space*, U.S. Government Publishing Office, March 2015.
[111] European Aviation Safety Agency, "Certification Specifications for Large Aeroplanes CS-25," September 2007.
[112] G. MacKenzie-Leigh, P. Norman, S. Galloway, G. Burt, and E. Orr, "Defining Requirements for the Implementation of Interconnected Generation in Future Civil Aircraft," presented at the SAE 2013 AeroTech Congress & Exhibition, 2013.
[113] Airbus, "A320 Flight Deck," Aircraft Families/A320 Family, 2008, available at https://web.archive.org/web/20080822221052/http://www.airbus.com/en/aircraftfamilies/a320/flight_deck.html.
[114] U.S. Navy, "Aircraft Electrical Power Characteristics MIL-STD-704F," Rev. F-CHG_1, Department of Defense Interface Standard, U.S. Government, December 2016.
[115] L. Austrin, M. Torabzadeh-Tari, and G. Engdahl, "A New High Power Density Generation System," presented at the 25th Congress of International Council of the Aeronautical Sciences, ICAS 2006-7.1.1, Germany, September 2006.
[116] S. Chandrasekaran, D. K. Linder, K. Louganski, and D. Boroyevich, "Subsystem Interaction Analysis in Power Distribution Systems of Next Generation Airlifters," presented at the European Power Electronics Conference, Switzerland, September 1999.
[117] D. Izquierdo, A. Barrado, C. Raga, M. Sanz, and A. Lazaro, "Protection Devices for Aircraft Electrical Power Distribution Systems: State of the Art," *IEEE Transactions on Aerospace and Electronic Systems*, vol. 47, no. 3, pp. 1538-1550, July 2011.

[118] C. Furce, "Finding Fault: Locating Hidden Hazards on Aircraft Wiring," College of Engineering, University of Utah, February 2004.
[119] S. Krstic, E. L. Wellner, A. R. Bendre, and B. Semenov, "Circuit Breaker Technologies for Advanced Ship Power Systems," presented at the IEEE Electric Ship Technologies Symposium, pp. 201-208, May 2007.
[120] W. Liu and A. Q. Huang, "A novel high current solid state power controller," presented at the 31st Annual Conference of IEEE Industrial Electronics Society IECON 2005, p. 5, November 2005.
[121] M. A. Rezaei and A. Huang, "Ultra fast protection of radial and looped electric power grid using a novel solid-state protection device," presented at the 2012 IEEE Energy Conversion Congress and Exposition (ECCE), pp. 610-614, September 2012.
[122] Data Device Corporation, "Solid-state power controllers (SSPCs), Series 91000," p. 4, available at http://www.nationalhybrid.com/downloads/sspc% 209100%20seriesdscomp01-4.pdf.
[123] T. Nguyen, "System and method utilizing a solid state power controller (SSPC) for controlling an electrical load of variable frequency three-phase power source," U.S Patent US7193337 B2, March 2007.
[124] E. A. Henderson, "Power Control Interrupt Management," U.S.Patent US20060044721 A1, March 2006.
[125] Z. Xu, B. Zhang, S. Sirisukpraset, X. Zhou, and A. Huang, "The emitter turn-off thyristor-based DC circuit breaker," *IEEE Power Engineering Society Winter Meeting*, vol. 1, pp. 288-293, January 2002.
[126] D. Sheridan, J. Casady, M. Mazzola, R. Schrader, and V. Bondarenko, "Silicon Carbide Power Electronics for High-Temperature Power Conversion and Solid-State Circuit Protection in Aircraft Applications," SAE technical paper 2011-01-2625, p. 6, Aerospace Technology Conference and Exposition, SAE International, October 2011.
[127] C. Gan, R. Todd, and J. Apsley, "HIL emulation for future aerospace propulsion systems," presented at the 7th IET Conference on Power Electronics, Machines and Drives, pp. 1-6, April 2014.
[128] P. J. Norman, S. J. Galloway, G. M. Burt, J. E. Hill, and D. R. Trainer, "Evaluation of the dynamic interactions between aircraft gas turbine engine and electrical system," presented at the 4th IET Conference on Power Electronics, Machines and Drives, pp. 6 71-675, April 2008.
[129] D. Rensch, "Turbofan engine with at least one apparatus for driving at least one generator," U.S. Patent US20100000226 A 107, January 2010.
[130] J. M. Kern and H. L. N. Wiegman, "Integrated electrical power extraction for aircraft engines," U.S.Patent US7468561 B223, December 2008.
[131] E. Papandreas, "Multi spool gas turbine system," U.S.Patent US8220245 B1, July 2012.
[132] D. B. Sidelkovskiy, "Multi-shaft gas turbine engine," U.S. Patent US20140250860 A1, September 2014.
[133] R. J. Hoppe, "Multi-shaft power extraction from gas turbine engine," European Patent EP2644866 A2, October 2013.
[134] K. A. Dooley, "Gas turbine engine including apparatus to transfer power between multiple shafts," U.S. Patent 8631655, January 2014.

[135] J. Derouineau, "Engine power extraction control system," U.S. Patent US7285871, October 2007.
[136] A. O. F. Colin, A. Lebrun, and G. Barjon, "Device for producing electrical power in a two-spool gas turbine engine," U.S. Patent US7973422 B2, July 2011.
[137] A. C. Newton and J. Sharp, "Gas turbine engine system," U.S. Patent US5867979 A09, February 1999.
[138] M. J. Provost, "The More Electric Aero-engine: a general overview from an engine manufacturer," presented at the International Conference on Power Electronics, Machines and Drives, pp. 246-251, 2002.
[139] A. J. Mitcham and J. J. A. Cullen, "Permanent magnet generator options for the More Electric Aircraft," presented at the 2002 International Conference on Power Electronics, Machines and Drives, pp. 241-245, June 2002.
[140] P. H. Mellor, S. G. Burrow, T. Sawata, and M. Holme, "A wide-speed-range hybrid variable-reluctance/permanent-magnet generator for future embedded aircraft generation systems," *IEEE Transactions on Industry Applications*, vol. 41, no. 2, pp. 551-556, April 2005.
[141] A. Linden, "RAH-66 Comanche," Sikorsky Product History, August 2014, available at http://www.sikorskyarchives.com/RAH-66%20COMANCHE.php.
[142] D. Pfahler, "Air Force Power Requirements," U.S. Air Force Research Laboratory, OMB No. 0704-0188, p. 22, January 2006.
[143] B. Bullerdick, "How To Supply Power and Air For The F-35," e-Military P roduct News for Aviation, Cygnus Business Media, p. 6, Summer 2013.
[144] PRNeswire, "Unique Integrated System Starts F-35 Engine in Joint Test by Lockheed Martin, Pratt & Whitney," Lockheed Martin press release, April 2005, available at http://www.prnewswire.com/news-releases/unique-integrated-system-starts-f-35-engine-in-joint-test-by-lockheed-martin-pratt--whitney-54447287.html.
[145] defenceWeb, "F-35 fleet grounded due to electrical failure," August 2011, available at http://www.defenceweb.co.za/index.php?option=com_content&view=article&id=17790.
[146] B. Cox, "All F-35 fighter jets grounded due to power system problems," McClatchy DC Bureau, August 2011, available at http://www.mcclatchydc.com/news/nation-world/national/article24689125.html.
[147] R. V. Petrescu and F. I. Petrescu, "Lockheed Martin," p. 94, Books on Demand GmbH, February 2013, ISBN 978-3-8482-6053-9.
[148] P1 Business Aviation Magazine, "Full on Falcon," Flight Test Dassault Falcon 7X, p. 40, July-August 2009.
[149] F. George, "Flying the Falcon 7X," Business & Commercial Aviation Magazine, p. 32, The McGraw-Hill Companies, August 2006.
[150] Dassault Aviation, "ATA 24 - Electrical Power," Falcon 7X Electrical Power, Smartcockpit, available at http://www.smartcockpit.com/docs/Falcon_7X-Electrical_Power.pdf.
[151] K. Muehlbauer and D. Gerling, "Two-Generator-Concepts for Electric Power Generation in More Electric Aircraft Engine," presented at the XIX International Conference on Electrical Machines, pp. 1-5, September 2010.

[152] Y. Jia, "Induction Generator Based More Electric Architectures For Commercial Transport Aircraft," PhD thesis, Power Electronics and Drives Laboratory, The University of Texas at Dallas, December 2016.
[153] A. Lucken, J. Brombach, and D. Schulz, "Design and protection of a high voltage DC onboard grid with integrated fuel cell system on more electric aircraft," presented at the Electrical Systems for Aircraft, Railway and Ship Propulsion (ESARS), October 2010.
[154] K. Rajashekara, J. Grieve, and D. Daggett, "Hybrid fuel cell power in aircraft," *IEEE Industry Applications Magazine*, vol. 14, no. 4, pp. 54-60, 2008.
[155] J. A. Oliver *et al.*, "High level decision methodology for the selection of a fuel cell based power distribution architecture for an aircraft application," presented at the 2009 IEEE Energy Conversion Congress and Exposition, pp. 459-464, September 2009.
[156] D. S. Parker and C. G. Hodge, "The Electric Warship II," *Transactions IMarE*, vol. 109, no. 2, pp. 127-137, 1997.
[157] J. Haire, "F-22 Program Delivers Power System Breakthrough," U.S. Air Force News Release, July 2000, available at http://connection.ebscohost.com /c/articles/3500526/f-22-program-delivers-power-system-breakthrough.
[158] O. Langlois, L. Prisse, E. Foch, and D. Alejo, "Power supply system and method on board an aircraft," U.S. Patent US2008100136 A1, May 2008.
[159] R. G. Michalko, "Electric power distribution system and method with active load control," U.S.Patent US7400065, July 2008.
[160] E. Yue, J. L. Derouineau, and W. T. Pearson, "Paralleled HVDC bus electrical power system architecture," U.S. Patent US7936086 B2, May 2011.
[161] K. J. Karimi, S. Liu, M. E. Liffring, S. B. Helton, and S.-W. Fu, "Vehicle electrical power management and distribution," U.S. Patent US8738268 B2, May 2014.
[162] G. I. Rozman and J. C. Swenson, "Bus-tie SSPCS for DC power distribution system," U.S. Patent US8344544 B2, January 2013.
[163] P. M. Hield, J. M. Cundy, R. A. Midgley, and A. C. Newton, "Shaft power transfer in gas turbine engines with machines operable as generators or motors," U.S. Patent US5694765, December 1997.
[164] C. D. Eick *et al.*, "More electric aircraft power transfer systems and methods," U.S. Patent US7552582 B2, June 2009.
[165] A. Trentin, P. Zanchetta, P. Wheeler, and J. Clare, "Power conversion for a novel AC/DC aircraft electrical distribution system," *IET Electrical Systems in Transportation*, vol. 4, no. 2, pp. 29-37, June 2014.
[166] F. Gao, "Decentralised Control and Stability Analysis of a Multi-Generator Based Electrical Power System for More Electric Aircraft," PhD thesis, University of Nottingham, August 2016.
[167] S. D. A. Fletcher, P. J. Norman, S. J. Galloway, P. Crolla, and G. M. Burt, "Optimizing the Roles of Unit and Non-unit Protection Methods Within DC Microgrids," *IEEE Transactions on Smart Grid*, vol. 3, no. 4, pp. 2079-2087, December 2012.
[168] D. Salomonsson, L. Soder, and A. Sannino, "Protection of low-voltage DC microgrids," *IEEE Transactions on Power Delivery*, vol. 24, no. 3, pp. 1045-1053, July 2009.

[169] R. Schmerda, R. Cuzner, R. Clark, D. Nowak, and S. Bunzel, "Shipboard Solid-Stare Protection: Overview and Applications," *IEEE Electrification Magazine,* vol. 1, no. 1, pp. 32-39, October 2013.
[170] A. A. Elserougi, A. S. Abdel-Khalik, A. M. Massoud, and S. Ahmed, "A new protection scheme for HVDC converters against DC-side faults with current suppression capability," *IEEE Transactions on Power Delivery,* vol. 29, no. 4, pp. 1569-1577, June 2014.
[171] P. Cairoli and R. A. Dougal, "New Horizons in DC Shipboard Power Systems: New fault protection strategies are essential to the adoption of dc power systems," *IEEE Electrification Magazine,* vol. 1, no. 2, pp. 38-45, December 2013.
[172] D. Jovcic, M. Taherbaneh, J. P. Taisne, and S. Nguefeu, "Offshore DC grids as an Interconnection of Radial Systems: Protection and Control Aspects," *IEEE Transactions on Smart Grid,* vol. 6, no. 2, pp. 903-910, March 2015.
[173] K. Jia, E. Christopher, D. Thomas, M. Sumner, and T. Bi, "Advanced DC zonal marine power system protection," *IET Generation, Transmission & Distribution,* vol. 8, no. 2, pp. 301-309, February 2014.
[174] M. E. Baran and N. R. Mahajan, "Overcurrent protection on voltage-source-converter-based multiterminal DC distribution systems," *IEEE Transactions on Power Delivery,* vol. 22, no. 1, pp. 406-412, December 2006.
[175] G. A. Whaytt and L. A. Chick, "Electrical Generation for More-Electric Aircraft using Solid Oxide Fuel Cells," Pacific Northwest National Laboratory, U.S. Department of Energy, Washington, April 2012.
[176] R. Abdel-Fadil, A. Eid, and M. Abdel-Salam, "Electrical Distribution Power Systems of Modern Civil Aircrafts," presented at the 2nd International Conference on Energy Systems and Technologies, pp. 201-210, Egypt, February 2013.
[177] D. C. Yu and S. H. Khan, "An adaptive high and low impedance fault detection method," *IEEE Transactions on Power Delivery,* vol. 9, no. 4, pp. 1812-1821, October 1994.
[178] E. Rappaport, "Myths of Equipment Grounding and Bonding," *IEEE Transactions on Industry Applications,* vol. 51, no. 6, pp. 5212-5217, April 2015.
[179] J. I. Marvik, S. D'Arco, and J. A. Suul, "A two-layer detection strategy for protecting multi-terminal HVDC systems against faults within a wide range of impedances," presented at the 13th IET International Conference on Development in Power System Protection, pp. 1-6, March 2016.
[180] P. P. Das, S. Chattopadhayay, and M. Palmal, "A d-q Voltage Droop Control Method With Dynamically Phase-Shifted Phase-Locked Loop for Inverter Paralleling Without Any Communication Between Individual Inverters," *IEEE Transactions on Industrial Electronics,* vol. 64, no. 6, pp. 4591-4600, June 2017.
[181] M. Ramezani, S. Li, and Y. Sun, "Combining droop and direct current vector control for control of paralleled inverters in microgrid," *IET Renewable Power Generation,* vol. 11, no. 1, pp. 107-114, August 2016.
[182] S. D. A. Fletcher, P. J. Norman, S. G. Galloway, and G. M. Burt, "Determination of protection system requirements for dc unmanned aerial vehicle electrical power networks for enhanced capability and survivability,"

IET Electrical Systems in Transportation, vol. 1, no. 4, pp. 137-147, December 2011.
[183] L. Lupelli, "A study on the integration of the IP Power Offtake system within the Trent 1000 turbofan engine," technical report, pp. 123, Faculty of Engineering, University of Pisa, Italy 2012.
[184] D. P. Brown, "Ten interesting facts about the Rolls-Royce Trent 1000 engine used on the Boeing 787 Dreamliner," AirlineReporter.com, March 2010, available at http://www.airlinereporter.com/2010/03/ten-interesting-facts-about-the-rolls-royce-trent-1000-engines-used-on-the-boeing-787-dreamliner/.
[185] European Aviation Safety Agency, "Type-Certificate Data Sheet for Trent XWB series engines," TCDS no. E-111, is. 3, pp. 1-13, April 2016.
[186] R. D. Flack, "Fundamentals of Jet Propulsion with Applications," p. 315, Cambridge Aerospace Series, Cambridge University Press, January 2005, ISBN 978-0-521-15417-8.
[187] A. J. Mitcham and N. Grum, "An integrated LP shaft generator for the more electric aircraft," presented at the IEE Colloquium on All Electric Aircraft, June 1998.
[188] P. Ohja and K. Raghava, "Rolls Royce Trent 1000 Aircraft engine," presentation, Indian Institute of Space Science and Technology, available at https://www.slideshare.net/egajunior/trent-1000-presentation.
[189] Rolls Royce plc, "The Jet Engine," 5th ed., p. 137, John Wiley & Sons Ltd, August 2005, ISBN 978-1119065999.
[190] M. Sztykiel, S. Fletcher, P. Norman, S. Galloway, and G. Burt, "Modular and Reconfigurable Transient Modeling and Simulation Design Support Tool for MEE/MEA Power Systems," presented at the SAE 2016 Aerospace Systems and Technology Conference, pp.12, September 2016.
[191] F. Whittle, "Gas Turbine Aero-Thermodynamics: With Special Reference to Aircraft Propulsion," p. 207, Pergamon Press, 1981, ISBN 978-0080267180.
[192] H. Han, X. Hou, J. Yang, J. Wu, M. Su, and J. M. Guerrero, "Review of Power Sharing Control Strategies for Islanding Operation of AC Microgrids," *IEEE Transactions on Smart Grid*, vol. 7, no. 1, pp. 200-215, June 2015.
[193] O. R. Adefajo *et al.*, "Voltage control on an uninhabited autonomous vehicle electrical distribution system," presented at the 4th IET Conference on Power Electronics, Machines and Drives, pp. 676-680, April 2008.
[194] S. Bayhan and H. Abu-Rub, "Model predictive droop control of distributed generation inverters in islanded AC microgrids," presented at the 11th IEEE Conference on Compatibility, Power Electronics and Power Engineering, pp. 247-252, April 2017.
[195] Z. Zhao, J. Hu, and H. Chen, "Bus Voltage Control Strategy for Low Voltage DC Microgrid Based on AC Power Grid and Battery," presented at the IEEE International Conference on Energy Internet (ICEI), pp. 349-354, April 2017.
[196] M. Roche, W. Shabbir, and S. A. Evangelou, "Voltage Control for Enhanced Power Electronic Efficiency in Series Hybrid Electric Vehicles," *IEEE Transactions on Vehicular Technology*, vol. 66, no. 5, pp. 3645-3658, August 2016.
[197] A. Engler and A. Soultanis, "Droop control in LV-grids," presented at the International Conference on Future Power Systems, pp. 1-6, November 2005.

[198] Z. Shuai, D. He, J. Fang, J. Shen, C. Tu, and J. Wang, "Robust droop control of DC distribution networks," *IET Renewable Power Generation,* vol. 10, no. 6, pp. 807-814, June 2016.
[199] J. Hu, J. Duan, H. Ma, and M. Chow, "Distributed Adaptive Droop Control for Optimal Power Dispatch in DC-Microgrid," *IEEE Transactions on Industrial Electronics,* no. 99, pp. 1-12, April 2017.
[200] W. Tang and R. H. Lasseter, "An LVDC industrial power distribution system without central control unit," presented at the IEEE 31st Annual Power Electronics Specialists Conference, pp. 979-984, June 2000.
[201] M. S. Mahmoud, "Microgrids: Advanced Control Methods and Renewable Energy System Integration," Butterworth-Heinemann, p. 338, October 2016, ISBN 978-0-08-101753-1.
[202] Q. C. Zhong and Y. Zeng, "Universal Droop Control of Inverters With Different Types of Output Impedance," *IEEE Access,* vol. 4, pp. 702-712, February 2016.
[203] M. Hajian, L. Zhang, and D. Jovcic, "DC Transmission Grid With Low-Speed Protection Using Mechanical DC Circuit Breakers," *IEEE Transactions on Power Delivery,* vol. 30, no. 3, pp. 1383-1391, November 2014.
[204] M. K. Bucher and C. M. Franck, "Contribution of Fault Current Sources in Multiterminal HVDC Cable Networks," *IEEE Transaction on Power Delivery,* vol. 28, no. 3, pp. 1796-1803, May 2013.
[205] H.-J. Choi and J.-H. Jung, "Practical Design of Dual Active Bridge Converter as Isolated Bi-directional Power Interface for Solid State Transformer Applications," *Journal of Electrical Engineering and Technology,* vol. 11, no. 5, pp. 1265-1273, April 2016.
[206] B. Zhao, Q. Song, W. Liu, and Y. Sun, "Overview of Dual-Active-Bridge Isolated Bidirectional DC-DC Converter for High-Frequency-Link Power-Conversion System," *IEEE Transactions on Power Electronics,* vol. 29, no. 8, pp. 4091-4106, August 2014.
[207] S. R. Goldman and M. Glass, "SSPC Advancements Enhance Vehicle Power System Design," The Journal of Military Electronics and Computing, available at http://archive.cotsjournalonline.com/articles/view/101085, November 2009.
[208] Z. Ziyue, Q. Haihong, N. Xin, F. Dafeng, and X. Huajuan, "Status and development of overcurrent protection devices for more electric aircraft applications," presented at the 8th IEEE International Power Electronics and Motion Control Conference, pp. 1-7, May 2016.
[209] D. Izquierdo, A. Barrado, C. Fernandez, M. Sanz, and A. Lazaro, "SSPC Active Control Strategy by Optimal Trajectory of the Current for Onboard System Applications," *IEEE Transactions on Industrial Electroncics,* vol. 60, no. 11, pp. 5195-5205, September 2012.
[210] D. A. Molligoda, P. Chatterjee, C. J. Gajanayake, A. K. Gupta, and K. J. Tseng, "Review of design and challenges of DC SSPC in more electric aircraft," presented at the IEEE Annual Southern Power Electronics Conference, pp. 1-5, December 2016,
[211] M. M. R. Ahmed and P. A. Mawby, "Design Specifications of a 270 V 100 A Solid-State Power Controller Suitable for Aerospace Applications," presented

at the 13th European Conference on Power Electronics and Applications, pp. 1-8, October 2009.
[212] Sinfonia Technology CO, "SSPC (Solid State Power Controller)," presentation, Power Control Equipment Group, p. 10, April 2016, available at https://sunjet-project.eu/sites/default/files/Product_Sinfonia_SSPC(2016 04)r.pdf.
[213] G. H. Zhao, K. Tone, X. Li, P. Alexandrov, L. Fursin, and M. Weiner, "3.6 mΩcm 2 , 1726 V 4H-SiC normally-off trenched-and-implanted vertical JFETs and circuit applications," *IEE Proceedings - Circuits, Devices and Systems*, vol. 151, no. 3, pp. 231-237, June 2004.
[214] Y. Li, P. Alexandrov, and J. H. Zhao, "1.88-mΩcm^2 1650-V Normally on 4H-SiC TI-VJFET," *IEEE Transactions on Electron Devices*, vol. 55, no. 8, pp. 1880-1886, August 2008.
[215] J. Cao, T. Chen , Z. Jiang, X. Wen, and M. Zhang, "Coupling calculation of temperature field for dry-type smoothing reactor," presented at the 17th International Conference on Electrical Machines and Systems, pp. 1-5, October 2014.
[216] T. Chen , J. Cao, G. Zhou, J. Zhipeng, Y. Wang, and X. Wen, "Electric field research of 800kV dry-type smoothing reactor," presented at the 17th International Conference on Electrical Machines and Systems. pp. 1-4, October 2014.
[217] D. F. Peelo, "Effect of series reactors on circuit breaker transient recovery voltages," presented at the 2014 IEEE Power and Energy Engineering Conference, pp. 1-3, December 2014.
[218] H. Abdollahzadeh, B. Mozafari, A. Tavighi, and J. Marti, "Impact of shunt capacitance of a SSSC-compensated transmission line on performance of distance relays," presented at the 2013 IEEE Power and Energy Society General Meeting, pp. 1-5, July 2013.
[219] L. Menghe, P. Shenghui, Z. Fan, and L. Chuan, "Protection against Reactor Inter-Turn Fault with Shunt Capacitance Compensator Based on Voltage Ratio," presented at the 3rd International Conference on Measuring Technology and Mechatronics Automation, pp. 1-3, January 2011.
[220] S. Ruppert, "State of the art megawatt drive train applications," Siemens presentation, pp. 1-18, March 2016.
[221] M. M. Jalla, A. Emadi, G. A. Williamson, and B. Fahimi, "Modeling of multiconverter more electric ship power systems using the generalized state space averaging method," presented at the 30th Annual Conference of IEEE Industrial Electronics Society, pp. 508-513, November 2004.
[222] E. Haugan, H. Rygg, A. Skjellnes, and L. Barstad, "Discrimination in offshore and marine dc distribution Systems," presented at the 17th IEEE Workshop on Control and Modeling for Power Electronics, pp. 1-7, June 2016.
[223] O. Settemsdal, E. Haugan, K. Aagesen, and B. Zahedi, "New enhanced safety power plant solution for DP vessels operated in closed ring configuration," presented at the Marine Technology Society Dynamic Positioning Conference, pp. 1-22, October 2014.
[224] Vishay, "Low profile, high current power inductor IHLP-5050CE-L1," commercial product source,March 2015, available at http://www.vishay.com

/ppg?34183.
[225] Hammond Manufacturing, "Heavy Current Chassis Mount 195C100," commercial product source, March 2015, available at https://www.hammfg.com/electronics/transformers/choke/195-196.
[226] S. Saridakis *et al.*, "Reliability analysis for a waste heat recovery power electronic interface applied at all-electric aircrafts," published at the 2015 International Conference on Electrical Systems for Aircraft, Railway, Ship Propulsion and Road Vehicles, pp. 1-6, Germany, March 2015.
[227] K. Naishadham, "Closed-Form Design Formulas for the Equivalent Circuit Characterization of Ferrite Inductors," *IEEE Transactions on Electromagnetic Compatibility*, vol. 53, no. 4, pp. 923-932, November 2011.
[228] Civil Aviation Safety Authority, "Aircraft electrical load analysis and power source capacity," Advisory Circular 21-38(0), pp. 22, Australian Government, March 2005.
[229] D. Carbaugh, M. Carriker, D. Huber, and A. Ryneveld, "In-Flight Aircraft Vibrations and Flight Crew Response," Aero Magazine, no. 16, is. 4, p. 5, The Boeing Company, October 2001.
[230] B737.org.uk, "Turbofan Engine Malfunction Recognition and Response," Pilot Notes,1999, available at http://www.b737.org.uk/enginemalfunctions.htm.
[231] M. Sztykiel, S. Fletcher, P. Norman, S. Galloway, and G. Burt, "Modular and Reconfigurable Transient Modeling and Simulation Design Support Tool for MEE/MEA Power Systems," presented at the SAE 2016 Aerospace Systems and Technology Conference, pp.12, September 2016.
[232] E. Kontos and P. Bauer, "Reactor design for DC fault ride-through in MMC-based multi-terminal HVDC grids," presented at the IEEE Annual Southern Power Electronics Conference, pp. 1-6, December 2016.
[233] A. D. Paquette, M. J. Reno, R. G. Harley, and D. M. Divan, "Transient load sharing between inverters and synchronous generators in islanded microgrids," presented at the 2012 IEEE Energy Conversion Congress and Exposition, pp. 2735-2742, September 2012.
[234] W. U. N. Fernando, M. Barnes, and O. Marjanovic, "Modelling and control of variable frequency multiphase multi-machine AC-DC power conversion systems," presented at the 5th IET International Conference on Power Electronics, Machines and Drives, pp. 1-6, April 2010.
[235] A. Gkountaras, S. Dieckerhoff, and T. Sezi, "Real time simulation and stability evaluation of a medium voltage hybrid microgrid," presented at the 7th IET International Conference on Power Electronics, Machines and Drives, pp. 1-6, April 2014.
[236] S. Luo, X. Dong, S. Shi, and B. Wang, "A non-unit protection principle based on travelling wave for HVDC transmission lines," presented at the 50th International Universities Power Engineering Conference, pp. 1-6, September 2015.
[237] P. Rakhra, P. J. Norman, and S. J. Galloway, "Experimental validation of protection blinding on DC aircraft electrical power systems with power-dense energy storage," presented at the 8th IET International Conference on Power Electronics, Machines and Drives, pp. 1-6, April 2016.

[238] K. Lai, M. S. Illindala, and M. A. Haj-ahmed, "Comprehensive Protection Strategy for an Islanded Microgrid Using Intelligent Relays," *IEEE Transactions on Industry Applications,* vol. 53, no. 1, pp. 47-55, August 2016.
[239] G. L. Johnson, "Tesla Coil Impedance," chapter 6, pp.1-16, Electrical and Computer Engineering Department, Kansas State University, October 2006.
[240] B. Le, C. A. Canizares, and K. Bhattacharya, "Incentive Design for Voltage Optimization Programs for Industrial Loads," *IEEE Transactions on Smart Grid*, vol. 6, no. 4, pp. 1865-1873, July 2015.
[241] E. Gallestey, A. Stothert, M. Antoine, and S. Morton, "Model predictive control and the optimization of power plant load while considering lifetime consumption," *IEEE Transactions on Power Systems,* vol. 17, no. 1, pp. 186-191, February 2002.
[242] A. H. Habib, E. L. Ratnam, V. R. Disfani, J. Kleissl, and R. A. de Callafon, "Optimization-based residential load scheduling to improve reliability in the distribution grid," presented at the 55th IEEE Conference on Decision and Control, pp. 2419-2424, December 2016.
[243] A. Boveri, F. Silvestro, and P. Gualeni, "Ship electrical load analysis and power generation optimisation to reduce operational costs," presented at the International Conference on Electrical Systems for Aircraft, Railway, Ship Propulsion and Road Vehicles, pp. 1-6, November 2016.
[244] European Aviation Safety Agency, "Certification Specifications for Normal, Utility, Aerobatic and Commuter Category Aeroplanes CS-23," pp. 429, November 2003.
[245] European Aviation Safety Agency, "Certification Specifications for Normal-Category Aeroplanes CS-23, Ammendment 5," pp. 33, March 2017.
[246] U.S. Department of Defense, "Electric Power, Aircraft, Characteristics and Utilization Of Military Standard MIL-STD-704," pp. 25, U.S. Department of Defense, U.S. Government, October 1959.
[247] U.S. Department of Defense, "Aircraft Electrical Power Characteristics MIL-STD-704B," pp. 29, U.S. Department of Defense, U.S. Government, November 1975.
[248] U.S. Department of Defense, "Military Specification MIL-E-7016F Electric load and power source capacity, Aircraft, Analysis of," pp. 48, U.S. Government, July 1976.
[249] U.S. Navy, "MIL-E-7016F Notice 1," pp. 1, U.S. Department of Defense, U.S. Government, April 1988.
[250] J. Hasson and D. Crotty, "Boeing's safety assessment processes for commercial airplane designs," *16th IEEE Digital Avionics Systems Conference,* vol. 1, pp. 1-7, October 1997.
[251] I. Chakraborty, "Subsystem architecture sizing and analysis for aircraft conceptual design," PhD thesis, p. 12, Daniel Guggenheim School of Aerospace Engineering, Georgia Institute of Technology, December 2015.
[252] Airlines Electronic Engineering Committee, "Guidance for aircraft electrical power utilization and transient protection," pp. 141, ARINC report 143A, Aeronautical Radio Inc., October 1989.

[253] J. J. Treacy, "Flight Safety Issues of an All-Electric Aircraft," *IEEE Transactions on Aerospace and Electronic Systems,* vol. 20, no. 3, pp. 227-233, May 1984.
[254] J. P. Potocti de Montalk, "Computer software in civil aircraft," presented at the 10th IEEE Digital Avionics Systems Conference, pp. 1-7, October 1991.
[255] M. Howse, "All Electric Aircraft," *IET Power Engineer Magazine,* vol. 17, no. 4, pp. 35-37, Aug.-Sept. 2003.
[256] C. M. Ananda, "General aviation aircraft avionics: Integration and system tests," *IEEE Aerospace and Electronic Systems Magazine,* vol. 24, no. 5, pp. 19-25, May 2009.
[257] B. A. Kish, J. Deems, D. Dunlop, and E. Fitz, "Lessons learned on the T-38 avionics upgrade program," *2000 IEEE Aerospace Conference Proceedings*, vol. 2, pp. 49-54, March 2000.
[258] "Today...tomorrow [of multidisciplinary systems of systems]," *IEEE Aerospace and Electronic Systems Magazine*, vol. 15, no. 10, pp. 137-144, October 2000.
[259] S. Burger, O. Hummel, and M. Heinisch, "Airbus Cabin Software," *IEEE Software,* vol. 30, no. 1, pp. 21-25, January 2013.
[260] K. Keller *et al.*, "Aircraft electrical power systems prognostics and health management," presented at the 2006 IEEE Aerospace Conference, pp. 1-12, March 2006.
[261] G. Ramohalli, "The Honeywell on-board diagnostic and maintenance system for the Boeing 777," presented at the 11th IEEE Digital Avionics Systems Conference, pp. 1-6, October 1992.
[262] M. Frank, "Design of transient voltage suppressors for digital inputs of avionics devices in indirect lightning tests according to ED-14/DO-160," presented at the 2013 International Symposium on Electromagnetic Compatibility, pp. 833-836, September 2013.
[263] J. S. Frichtel, "Influence of power quality on avionic design and weapon system effectiveness," presented at the 1971 IEEE Power Electronics Specialists Conference, April 1971.
[264] B. B. Choi, "Propulsion Powertrain Simulator: Future turboelectric distributed-propulsion aircraft," *IEEE Electrification Magazine*, vol. 2, no. 4, pp. 23-34, December 2014.
[265] P. J. Masson and C. A. Luongo, "High power density superconducting motor for all-electric aircraft propulsion," *IEEE Transactions on Applied Superconductivity*, vol. 15, no. 2, pp. 2226-2229, June 2005.
[266] P. J. Masson and C. A. Luongo, "HTS Machines for Applications in All-Electric Aircraft," presented at the 2007 IEEE Power Engineering Society General Meeting, pp. 1-6, June 2007.
[267] The Boeing Company, "ETOPS - Extended Operations," presentation, pp. 1-7, August 2009.
[268] European Aviation Safety Agency, "EASA certifies Airbus 350 XWB for up to 370 minute ETOPS," press release, October 2014.
[269] C. Ekstrand, M. Pandey, and J. Spencer, "The New FAA ETOPS Rule," AERO Magazine, quarter 2, is. 26, pp. 6-13, 2007.

[270] R. Hammett, "Design by Extrapolation: An Evaluation of Fault Tolerant Avionics," *IEEE Aerospace and Electronic Systems Magazine*, vol. 17, no. 4, pp. 17-25, April 2002.
[271] R. Hammett, "Rapid Start-Up/Restart Avionics Provide Robust Fault Tolerance with Reduced Size, Weight and Power," presented at the 2011 IEEE Aerospace Conference, pp. 1-7, March 2011.
[272] Y. Shi and H. Li, "A novel modular dual-active-bridge (MDAB) dc-dc converter with dc fault ride-through capability for battery energy storage systems," presented at the 2016 IEEE Energy Conversion Congress and Exposition, pp. 1-6, September 2016.
[273] B. Sarlioglu and C. T. Morris, "More Electric Aircraft: Review, Challenges, and Opportunities for Commercial Transport Aircraft," *IEEE Transactions on Transportation Electrification*, vol. 1, no. 1, pp. 54-64, June 2015.
[274] International Air Transport Association, "IATA Forecasts Passenger Demand to Double Over 20 Years," press release, no. 59, October 2016, available at http://www.iata.org/pressroom/pr/Pages/2016-10-18-02.aspx.